

NISTIR 6096

Post-Installed Anchors - A Literature Review

Building and Fire Research Laboratory
Gaithersburg, Maryland 20899



United States Department of Commerce
Technology Administration
National Institute of Standards and Technology

NISTIR 6096

Post-Installed Anchors - A Literature Review

Geraldine S. Cheok
Long T. Phan

January 1998

Building and Fire Research Laboratory
National Institute of Standards and Technology
Gaithersburg, MD 20899



U.S. Department of Commerce
William M. Daley, *Secretary*
Technology Administration
Gary R. Bachula, *Acting Under Secretary for Technology*
National Institute of Standards and Technology
Raymond Kammer, *Director*

ABSTRACT

A literature review of studies on the behavior of post-installed concrete anchors is presented. The survey covers several types of anchors that are subjected to tension loads, shear loads, and to combined shear and tension loads. Brief summaries of the studies or investigations and their findings are presented. More detailed information may be found in the cited references. There are quite a number of studies on the behavior of these anchors subjected to shear or tension loads, but only a few studies on the behavior of anchors subjected to combined shear and tension loads, especially adhesive anchors. An experimental program to study the behavior of anchors subjected to combined shear and tension loads needs to be conducted to add to the existing database.

Keywords: Anchors; adhesive anchors; building technology; concrete; expansion anchors; grouted anchors; post-installed anchors; undercut anchors.

TABLE OF CONTENTS

ABSTRACT	i
TABLE OF CONTENTS	iii
LIST OF TABLES	vii
LIST OF FIGURES	ix
NOTATION	xi
1.0 INTRODUCTION	1
1.1 Background	1
1.2 Scope	1
2.0 ANCHOR TYPES AND FAILURE MODES	3
2.1 Anchor Types	3
2.2 Anchor Failure Modes	5
3.0 ANCHORS SUBJECTED TO TENSION ONLY	7
3.1 Studies at the University of Texas at Austin	7
3.2 Study by Eligehausen, Mallée, and Rehm	11
3.3 Study by Fuchs, Eligehausen, and Breen	13
3.4 Study by Farrow and Klingner	16
3.5 Studies Reported in the CEB Bulletin D'Information and Design of Fastenings in Concrete: Design Guide	18
3.5.1 Static Loading	18
3.5.2 Seismic Loading	24
3.6 Study by Ammann	24
3.7 Study by McMackin, Slutter, and Fisher	24
3.8 Study by Hosokawa	25
3.9 Study by Burdette, Perry, and Funk	26
3.10 Discussion	26
4.0 ANCHORS SUBJECTED TO SHEAR	35
4.1 Study by Eligehausen and Fuchs	35
4.2 Study by Fuchs, Eligehausen and Breen	36
4.3 Study by Ammann	38
4.4 Studies Reported in the CEB Bulletin D'Information and Design of Fastenings in Concrete: Design Guide	38
4.4.1 Static Loading	39

4.4.2	Seismic Loading	42
4.5	Study by McMackin, Slutter and Fisher	44
4.6	Study by Klingner, Mendonca, and Malik	44
4.7	Study by Bass, Carrasquillo, and Jirsa	45
4.8	Study by Akiyama, Yamamoto, Hirose, Matsuzaki, and Imai	46
4.9	Study by Swirsky, Dusel, Crozier, Stoker, and Nordlin	47
4.10	Study by Burdette, Perry, and Funk	48
4.11	Discussion	48
5.0	ANCHORS SUBJECTED TO COMBINED TENSION AND SHEAR LOADS	55
5.1	Study by the Cannon, Burdette, and Funk	55
5.2	Study by Eligehausen and Fuchs	55
5.3	Study by McMackin, Slutter, and Fisher	56
5.4	Study by Johnson and Lew	57
5.5	Study by Lindquist	58
5.6	Studies Reported in the CEB Bulletin D'Information	59
5.6.1	Static Load	59
5.6.2	Seismic Load	61
5.7	Report by the ASCE Nuclear Structures and Materials Committee	61
5.9	Discussion	62
6.0	SUMMARY AND CONCLUSIONS	67
6.1	General	67
6.2	Summary of Findings	68
6.2.1	Concrete Compressive Strength	68
6.2.2	Anchor Preload	68
6.2.3	Cyclic Loading	68
6.2.4	Embedment Depth	69
6.2.5	Cracked Concrete	69
6.2.6	Anchor Capacity	69
6.2.6.1	Tension Loading	70
6.2.6.2	Shear Loading	70
6.2.6.3	Combined Loading	70
6.2.7	Transverse Reinforcement	70
6.3	Conclusions	71
REFERENCES		73
APPENDIX A - TENSILE CAPACITY		79
A.1	CONCRETE FAILURE - EXPANSION ANCHOR	79
A.2	CONCRETE FAILURE - UNDERCUT ANCHOR	81
A.3	CONCRETE FAILURE - CIP ANCHOR BOLT	83
A.3.1	No Edge Distance Effect	83

A.3.2 Edge Distance Effect	85
APPENDIX B - SHEAR CAPACITY	89
B.1 STEEL FAILURE - EXPANSION ANCHOR	89
B.2 CONCRETE FAILURE - EXPANSION ANCHORS	89
B.3 CONCRETE FAILURE - HEADED STUDS	92
B.3.1 254 mm (10 in.) Edge Distance	92
B.3.2 51 mm (2 in.) Edge Distance	96

BLANK PAGE

LIST OF TABLES

2.1 Post-Installed Anchors	3
3.1 Comparison of ACI 349-85 and CCD Methods	13
3.2 Predicted Tensile Capacities	27
4.1 Predicted Shear Capacities	47

BLANK PAGE

LIST OF FIGURES

2.1	Failure Modes	6
3.1	Typical Load-Displacement Curves for Bonded Anchors	30
3.2	Projected Areas for ACI 349-85 Method	30
3.3	Projected Areas for CCD Method	31
3.4	Area Calculations for Blow-out Failure Mode	32
3.5	Influence of Cracks on Anchor Behavior	34
4.1	Projected Areas for ACI 349-85 Method	51
4.2	Projected Areas for CCD Method	52
4.3	Loading Sequences for Cyclic Tests	53
5.1	Load-Deflection Under Combined Loading	64
5.2	Load-Deflection for Various Anchor Types	64
5.3	Comparison of Eqs. 5-2 and 5-6 with Experimental Data	65
A.1	Projected Area Calculation for ACI 349-85 Method	88

1.0 INTRODUCTION

1.1 Background

Strengthening and rehabilitation of existing or older structures have become more prevalent as the awareness for the need of these structures to resist lateral loads has increased. This awareness is reflected in the development of provisions for strengthening methodologies [e.g. FEMA (1992)] and in changes to the building code.

A workshop was conducted by the National Institute of Standards and Technology (NIST) in 1995 on the strengthening of lightly reinforced concrete (LRC) frames to determine the research needs in this area [Cheok (1995)]. The workshop was part of an ongoing program at NIST on the strengthening of existing buildings. The objective of the program is to develop guidelines for strengthening LRC frames.

One of the issues identified as critical in the workshop was the connections between the existing LRC frame and the new strengthening element. Based on the recommendations of the workshop and on the need to focus the research, connections between LRC frames and concrete infill walls were singled out for further study. In particular, the load-deformation behavior of post-installed anchors was selected for further investigation as this knowledge is basic to the understanding of connection behavior.

Therefore, a literature survey of the available research in this area was conducted to determine the state-of-the-knowledge and to determine if there is sufficient data available to develop a load-deformation relationship for post-installed anchors. Since the focus of the program was on anchors used for infill walls, studies on the behavior of post-installed anchors subjected to combined shear and tension loads and to cyclic loads were of interest. From these studies, a load-deformation relationship could then be developed and incorporated into existing analysis programs which are used to determine the effectiveness of a strengthening methodology. The ability to accurately model the behavior of the connection (anchors) would in turn increase the accuracy of the predicted results. Parametric studies could then be conducted using these analysis programs, followed by experimental verification.

1.2 Scope

A literature survey of post-installed anchors is presented in this report. Studies of cast-in-place (CIP), headed, adhesive/chemical/bonded, grouted, and expansion type anchors are covered. Studies of CIP and headed anchors were included if they were considered relevant. The report attempts to cover research not reported in, or published since the NIST report by Johnson, Lew, and Phan (1988).

Chapter 2 of this report gives a brief overview of the different anchor types and anchor failure modes, Chapter 3 presents studies of anchors subjected to tension loads only, Chapter 4 covers studies of anchors subjected to shear loads only, Chapter 5 covers studies of anchors

subjected to combined shear and tension loads, and Chapter 6 presents a summary of the findings based on the literature survey and conclusions.

2.0 ANCHOR TYPES AND FAILURE MODES

2.1 Anchor Types

As mentioned in Chapter 1, the types of anchors that are of interest in this report are post-installed anchors. These anchors are typically used to hold down machinery and equipment and to connect new elements such as braces or infill walls used for strengthening purposes. Post-installed anchors are placed in holes that are drilled into an existing concrete member. These anchors can be either mechanical anchors or bonded anchors.

Mechanical anchors such as expansion anchors rely on the friction developed between the sides of the hole and the anchor wedges or sleeve to transfer loads. The expansion force is usually provided by tightening of nuts or by driving the anchor to expand the wedges or sleeves. Undercut anchors, another type of mechanical anchor, depend on bearing of the anchor against the concrete to transfer the loads - similar to cast-in-place headed anchors or studs. Usually, a special drill bit is required to make the undercut hole.

Bonded anchors rely on the adhesion between the anchor and the adhesive or between the adhesive and the concrete to transfer the loads. These anchors fall into two categories - grouted or chemical. The adhesives used in chemical anchors are either epoxy, polyester, or vinyl ester [Ward (1993)]. The different types of post-installed anchors are given in Table 2.1 [taken from ACI Committee 355 (1993)].

Table 2.1 Post-Installed Anchors [ACI Committee 355 (1993)]

<p>BONDED ANCHORS</p> <p>Grouted anchors Headed bolts or anchor</p> <p>Chemical anchors With threaded rod With reinforcing steel</p>
<p>EXPANSION ANCHORS</p> <p>Torque-controlled Heavy-duty sleeve anchor Sleeve anchor Shell expansion anchor Wedge anchor Rock/concrete expansion anchor</p> <p>Deformation controlled Drop-in anchor Self-drilling anchor Stud anchor</p> <p>Undercut With predrilled under-cut hole Self undercutting</p>

Advantages of mechanical anchors are that they may be loaded immediately after installation and no mixing of an adhesive is required. However, the expansion forces from the mechanical anchors could result in spalling of the concrete near edges.

Unlike mechanical anchors, the adhesives used for bonded anchors require time to cure and gain strength. Also, overhead installations of the bonded anchors may be difficult, care in hole preparation and cleaning is important to ensure good bond between the concrete and the adhesive, and care must be taken to ensure proper proportioning and mixing of the resin and the hardening agent. However, these drawbacks have been minimized or eliminated with the introduction of fast-curing adhesives and adhesives with high viscosities and pre-measured mix components in cartridges. Chemical anchors could be used when edge distance is a factor as they do not introduce an expansion force which would cause concrete spalling. More detailed descriptions of the different anchor types are given in the report prepared by ACI Committee 355 (1993) and the CEB Bulletin d'Information (1991).

2.2 Anchor Failure Modes

Typical failure modes for anchors are steel failure, concrete cone failure (for single or multiple anchors) or edge breakout, bursting failure, splitting failure, pull-out failure, bond failure between anchor and bonding agent or between concrete and bonding agent, or combinations of two or more of the failure modes. Some of these failure modes are shown in Fig. 2.1. Brief descriptions of these failure modes are presented in the following paragraphs. More detailed discussions of the various failure modes may be found in the report by ACI Committee 355 (1993) and the CEB Bulletin d'Information (1991).

Steel failure generally occurs when sufficient embedment length and edge distance are provided to develop the ultimate strength of the steel and to prevent concrete failure. Steel failure would generally be considered a ductile failure mode. The anchor capacity is affected by the steel strength and the anchor size.

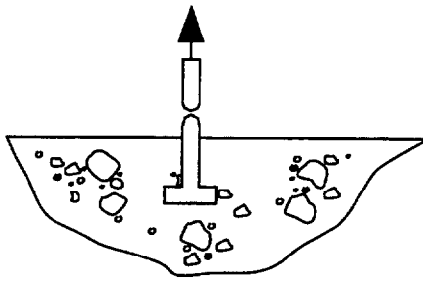
Concrete cone failure usually occurs for short embedment depths and low concrete strength. The capacity of the anchor is affected by concrete strength, proximity to other anchors and edges, and the presence of cracks.

Bursting failure occurs when the anchors are located close to the edge of a member. The capacity of an anchor experiencing this type of failure mode is mainly a function of edge distance and concrete strength. This failure mode may be avoided by providing sufficient edge distance and transverse reinforcement.

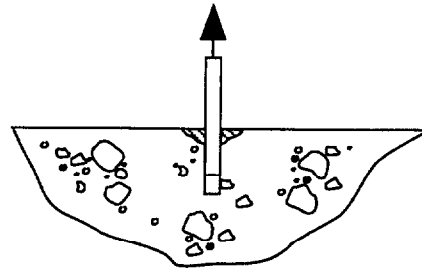
Splitting failure occurs "only if the concrete member dimensions are small relative to the anchor size and embedment or the anchor is close to a free edge" [CEB Bulletin d'Information (1991)]. Insufficient spacing between expansion anchors could also result in this type of failure mode. The anchor capacity is affected by member size, edge distance, anchor spacing and concrete strength.

Pull-out (slip) failure occurs for expansion anchors with "moderate to deep embedments in lower strength concrete" or anchors in oversized holes [ACI Committee 355 (1993)]. Increasing the coefficient of friction between the slip surfaces and the expansion force increases the anchor capacity.

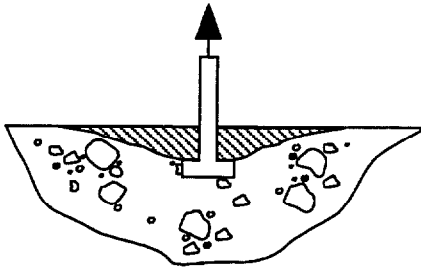
Pull-out failure for adhesive or chemical anchors results from bond failure. Bond failure between the bonding agent and the concrete occurs when the embedment depth is insufficient or when the hole is improperly cleaned. The anchor capacity is increased for increased embedment depth and hole roughness and cleanliness.



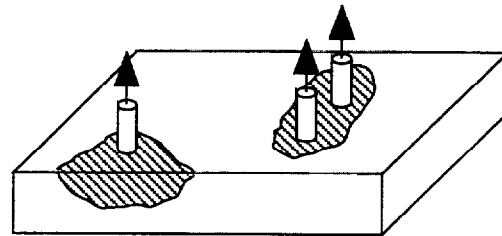
a. Steel Failure



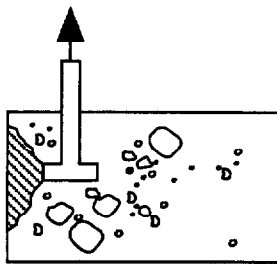
b. Pull-out Failure



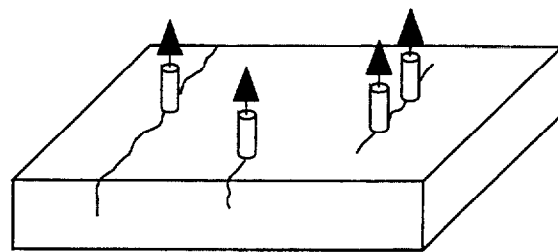
c. Concrete Cone Failure



d. Edge Break-out and Group Cone Failure



e. Bursting Failure



f. Splitting Failure

Figure 2.1 Failure Modes.

3.0 ANCHORS SUBJECTED TO TENSION ONLY

3.1 Studies at the University of Texas at Austin

A body of work on anchors has been conducted at the University of Texas, Austin and at the University of Florida at Gainesville [Doerr and Klingner (1989), Collins et al. (1989), Cook et al. (1991), and Cook et al. (1993)]. Most of the work was on chemically bonded or adhesive anchors.

Bonded anchors have four types of failure modes: anchor steel failure, concrete cone failure, bond failure, and combined cone-bond failure [Cook (1993)]. The tensile strength of the anchor must be less than the strength of the embedded portion of the anchor for the first type of failure to occur. For the second type of failure, the anchors have shallow embedment depths. For embedment depths of 50 mm - 100 mm (2 in. - 4 in.), the combined cone-bond failure mode is observed. Improper hole preparation or curing of the adhesive can result in bond failure. Bond failure can also occur if the top part of the anchor is debonded.

Based on the results obtained by Collins et al. (1989) and Cook et al. (1991), the following observations were made for the combined cone-bond failure mode: 1) The load-displacement relationship for bonded anchors is linear up to an elastic limit. 2.) Cone failure occurs simultaneously with bond failure. 3.) The behavior of bonded anchors is unpredictable after the elastic limit is reached.

Doerr and Klingner (1989) and Cook [1993] tested 97 chemically bonded anchors which used two-component polyester, vinyl ester, and epoxy systems. The anchors were made of 16 mm (5/8 in.) diameter high strength threaded rod. Of the 97 anchors, 25 were fully bonded, 36 were partially bonded, and 35 were paired, fully bonded anchors. Partially bonded anchors were similar to the fully bonded anchors except that the top 51 mm (2 in.) of the anchor was debonded from the hole. The hole diameter was 19 mm [3/4 in., anchor diameter + 3 mm (1/8 in.)] unless specified otherwise by manufacturers. The variables included bonding, embedment depth [102 mm, 152 mm, 203 mm (4 in., 6 in., 8 in.)], adhesive type, and anchor spacing [102 mm, 152 mm, 203 mm (4 in., 6 in., 8 in.)].

Some conclusions drawn from the tests were that fully bonded anchors failed by forming a concrete cone and an adhesive core below the concrete cone. The depth of the cone averaged between 25 mm (1 in.) and 51 mm (2 in.). Half of the anchors with an embedment depth of 152 mm (6 in. or $9.6d$ where d = diameter of anchor) yielded. Bond failure occurred for the partially bonded anchors with no formation of concrete cones. The capacity of the partially bonded anchors was approximately equal to that of the fully bonded anchors for the same embedment depth indicating that the concrete cone formed prior to bond failure or the contribution of the cone to the total strength of the anchor was not significant. The load capacity was not significantly affected by the close spacing of the paired anchors. For spacings of 102 mm (4 in. or $6.4d$), the ultimate loads of the paired anchors were 95% of that expected for two single anchors. For spacings of greater than or equal to 203 mm (8 in. or $12.8d$), there was no effect on the ultimate load.

The following design recommendations were developed for adhesive anchors subjected to tension loads [Cook (1993)]:

1. The cone depth, h_{cone} , for combined cone-bond failure may be predicted by:

$$h_{cone} = \frac{\tau_o \pi d_o}{1.84 \sqrt{f'_c}} \quad [mm, MPa] \quad (3-1)$$

where d_o is the hole diameter and τ_o is the uniform bond stress.

2. For shallow embeddings, $h_e < h_{cone}$, the following equation for concrete cone failure model proposed by Eligehausen et al.(1984a, 1984b) to predict the tension load is appropriate:

$$N_{u,m} = 0.92 h_e^2 \sqrt{f'_c} \quad [N, mm, MPa] \quad (3-2)$$

3. For $h_{cone} < h_e < 40 d_o^{1/2} + h_{cone}$, the tensile load may be predicted using the following equation based on uniform bond-stress distribution:

$$N_{u,m} = \tau_o \pi d_o (h_e - h_{cone}) + 0.92 h_{cone}^2 \sqrt{f'_c} \left[\frac{40 \sqrt{d_o} - (h_e - h_{cone})}{40 \sqrt{d_o}} \right] \quad [N, mm] \quad (3-3)$$

4. For $h_e > 40 d_o^{1/2} + h_{cone}$, the tensile load capacity may be predicted using the following equation based on elastic bond-stress formulation:

$$N_{u,m} = \tau_{max} \pi d_o \left[\frac{\sqrt{d_o}}{\lambda'} \tanh \frac{\lambda' (h_e - h_{cone})}{\sqrt{d_o}} \right] \quad [N, mm] \quad (3-4)$$

The strength contribution from the concrete cone for anchors with this embedment depth was found to be minimal and was thus not included in Eq. 3-4. The variables τ_o , τ_{max} , and λ' are properties of the adhesive system: τ_o is the uniform bond stress and is defined as the load at the elastic limit divided by the bonded surface of the anchor, τ_{max} is the maximum bond stress at the surface at the elastic limit and λ' , and λ' is the stiffness of the system and is determined from the slope of the load-displacement plot.

The above recommendations are for chemical anchors subject to the following conditions: embedment failure mode, clean and dry holes, normal laboratory temperatures, loading after a 24 hour cure period, monotonically applied tension load, and uncracked concrete.

The differences in the load-deflection behavior of cast-in-place (CIP), undercut, adhesive, grouted, and expansion anchors under a tension load were studied by Cook et al. (1992). A total of 48 tests were conducted. Test variables included type of anchor, type of loading - static, fatigue, impact, and embedment length. Edge distance was not a variable in these tests. All anchors were 16 mm (5/8 in.) diameter and were either low strength, f_u of about 414 MPa (60 ksi), or high strength, f_u of about 690 MPa - 862 MPa (100 ksi - 125 ksi). The embedment lengths of the anchors were specified [ACI (1989)] so that a ductile failure occurred whereby the anchor steel yielded prior to concrete failure or anchor pullout.

For the fatigue tests, the anchors were loaded statically to 60% of the minimum specified yield load. They were then cycled 1 million times between 48 MPa (7 ksi) and 60% of yield strength. After the fatigue cycles, the anchors were tested statically to failure. Impact loads were applied using a triangular loading pulse with an approximate duration of 0.25 s. Three pulses each at 60%, 80%, and 100% of yield load were applied.

A brief summary of the results follows:

Static tests:

1. All CIP anchors experienced steel failure with no anchor slippage. The load-deflection behavior depends on the embedment depth - the larger the embedment depth, the lower the anchor stiffness as there is little or no bond between the anchor shank and concrete. For adhesive and grouted anchors, steel failure occurred for high strength anchors with 203 mm (8 in. or 12.8d) embedment lengths and for low strength anchors with 127 mm - 152 mm (5 in. - 6 in. or $8d$ - $8.6d$) embedment lengths. Adhesive and grouted anchors were stiffer than CIP anchors.
2. For adhesive, expansion and undercut anchors with steel failure and anchor slippage, the typical slip of anchors were about 3.6 mm (0.14 in.). For adhesive anchors, some spalling of the concrete, 19 mm (3/4 in.) deep, formed around the anchor when slip occurred. For expansion anchors, slip initiated when the applied load equaled the anchor preload. No concrete spalling was noted for the expansion and undercut anchors.
3. Expansion and undercut anchors experiencing anchor pullout reached and maintained 2/3 of the fracture load at which point slip occurred. This failure mode was considered to be a non-ductile failure mode. It was suggested that the pullout failure was caused by inadequate frictional resistance rather than inadequate embedment length. This type of failure can not be predicted by testing and static tensile tests in the field will have to be conducted to determine the behavior of these anchors.

4. The maximum failure loads varied widely for anchors experiencing bond failure between the anchor and the concrete [44.5 kN - 138 kN = fracture load (10 k - 31 k)]. The anchors showed little or no slip before bond failure. Concrete spalling of about 25 mm - 51 mm (1 in. - 2 in.) deep formed around the anchors when bond failure occurred.
5. For adhesive and grouted anchors experiencing bond failure between the steel and the bonding material, failure was attained suddenly without any anchor slip. Spalls in concrete were 25 mm - 63 mm (1 in. - 2.5 in.) deep.

Fatigue tests:

No failure occurred during the first static loading or during the fatigue loading stages. All failures occurred in the second static loading which was static loading until failure occurred and which followed the fatigue loading stage.

1. The behavior of grouted and adhesive anchors experiencing steel fracture with no slippage of the anchor nor loss of anchor stiffness was similar to that for the anchors with the same failure mode subjected to the static test. No spalling of the concrete occurred but slight cracking of concrete was observed.
2. CIP anchors which failed in the steel with no anchor slippage experienced some loss of anchor stiffness due to the fatigue cycles. The failure mode was steel fracture and was considered a ductile type of failure.
3. The stiffnesses of adhesive anchors were basically unchanged before and after the fatigue tests. Although slip occurred in the second stage of the static test (load to failure), the anchors carried additional load until fracture. For the same adhesive and embedment length, the load level at which slip occurred and the spall depth were similar to those for the adhesive anchors subjected to static load only.

Expansion anchors lost stiffness as a result of the fatigue cycles with steel fracture occurring in the second phase of the static loading. As in the static tests, slip occurred when the applied load exceeded the bolt preload. Slips in the fatigue tests were slightly greater than those observed for the static tests.

Undercut anchors were not affected by the fatigue loading.

4. For grouted anchors experiencing failure at the grout-steel interface and loss of anchor stiffness, failure was sudden and occurred in the second static test stage. No slip occurred before bond failure. Spalling of the concrete, 51 mm (2 in.) deep, occurred. Fatigue loading did not seem to affect the behavior of grouted anchors.

Impact test:

All anchors underwent the three levels of impact load without steel fracture or anchor pullout.

1. For CIP, adhesive, and grouted anchors with no loss of anchor stiffness nor anchor slip, the anchors were not affected by the impact load at all three levels. The embedment was sufficient to develop the anchor strength for impact loading.
2. Adhesive anchors, which exhibited loss of anchor stiffness and some slip, typically slipped during the second load level (80% of yield). This load level corresponded to the load in the static and fatigue tests at which slip occurred. Expansion and undercut anchors did not slip nor lose stiffness below the anchor preload. Slip and loss of stiffness occurred when the load level was above the anchor preload. This behavior was similar to that for anchors subjected to static load.

Conclusions:

1. Embedment length requirement for CIP anchors per ACI 349-85 may be used for CIP bolts, expansion, and undercut anchors to insure a ductile failure.
2. Embedment length requirement for high strength adhesive and grouted anchors per ACI 349-85 appears to be insufficient to insure ductile failure. Embedment lengths should be based on manufacturer's recommendations.
3. Strength of expansion anchors was a function of the frictional force between the anchor sleeve and the concrete. This frictional force was affected by several factors. The performance of expansion and undercut anchors should be verified by field tests.
4. High cycle fatigue had no effect on anchor strength for anchors with sufficient embedment to insure ductile failure.
5. Expansion anchors subjected to fatigue loads had more slip at failure than those subjected to static load only. This additional slip did not impact the anchor strength.
6. Fully embedded undercut, adhesive, and grouted anchors showed no reduction in stiffness and undercut anchors showed no increase in slip due to fatigue loading.
7. Impact loading had no effect on anchor strength when the anchors have sufficient embedment to insure ductile failure.
8. Fully embedded CIP, adhesive, and grouted anchors showed no loss in stiffness up to yield load due to impact loads.

3.2 Study by Eligehausen, Mallée, and Rehm

Extensive work on resin anchors has also been conducted by Eligehausen et al. (1984a, 1984b). The anchors consisted of a threaded rod, washer, nut, and a cartridge with a cold-curing resin. Typical load-displacement relationships for tension and shear are shown in Fig. 3.1. Both tension and shear loadings were studied. The results for the shear tests are reported in Chapter 3. Possible failure modes for these anchors are: 1) Pull-out of anchor - bond failure between the wall of the hole and the resin 2) Conical breakout of concrete 3) Splitting of concrete with crack extending towards the edge or between adjacent anchors 4) Fracture of the anchor rod. Variables

in the test program included distance to edge, single or multiple anchors, cracked or uncracked concrete, anchor diameters 8 mm [M8 (0.3 in.)] to 24 mm [M24 (0.9 in.)], and the effects of creep. Some of the findings obtained are briefly summarized below:

1. Failure loads in uncracked concrete:

- a. For single anchors with large edge distances, splitting of the concrete was not observed. The average bond stress developed was 8 MPa (1.2 ksi) for anchor pull-out and an embedment depth of $9d$. The bond stress increased for increased concrete strength and it decreased for embedment depths greater than $9d$. The fracture load of the anchor can be computed by multiplying the nominal area of the anchor and the tensile strength of the anchor.

Conical concrete failure was greatly influenced by the concrete strength and the embedment depth. The failure load may be computed using:

$$N_{uo} = 0.85 h_e^2 \sqrt{f_{cc}} \quad [N, mm, MPa] \quad (3-5)$$

where f_{cc} is the concrete compressive strength obtained from tests of 20 cm x 20 cm x 20 cm cubes and is valid for $h_e \leq 9d$. For $h_e > 9d$, the load is more proportional to h_e^2 than to h_e .

- b. For anchor groups (2 or 4) with large edge distances and for the concrete breakout mode, the load capacity was reduced if the concrete failure cones overlapped. The load capacity was not affected if the failure mode was anchor pullout or anchor fracture. The failure load for two anchors was reduced linearly by a factor that accounts of the distance between adjacent anchors. The upper bound of the failure load equals $2 N_{uo}$ (N_{uo} = load capacity of one anchor) and the lower bound equals the load capacity of one anchor, N_{uo} . Similarly, for groups of four anchors, the failure load is further reduced linearly by a second factor accounting for the orthogonal distance between the anchors.
 - c. For single anchors close to edge, the failure load is linearly reduced by the factor, $c_1 / c_{crit} \leq 1$, where c_1 is the distance to the edge and c_{crit} is the critical edge distance equal to h_e . The failure load varies from N_{uo} to zero.
 - d. For anchor groups close to an edge, the influence of adjacent anchors and edge distance are multiplicatively superimposed as a means of simplification. In essence, the failure capacity of the anchors, $2 N_{uo}$ or $4 N_{uo}$ for two and four anchors, respectively, are multiplied by four factors - two factors accounting for spacing (one in each direction) and two factors accounting for edge distance (one in each direction).
2. The failure capacity for anchors in cracked concrete subjected to a tension load is approximately 0.2 to 0.6 times the load in uncracked concrete. The capacity is further reduced under cyclic loading.

3. Long term behavior: The displacement vs. time data show that the slope of the curve is higher for increased higher initial temperature and that the curve achieves a definite plateau. The bond strength decreases for increased temperature. The strengths at 50° C and 80° C are about 0.85 and 0.80 times, respectively, that at 20° C. Other factors, such as variation in humidity and temperature fluctuations have not been examined and need to be.

3.3 Study by Fuchs, Eligehausen, and Breen

A comparison of the load capacities obtained using the design recommendation of ACI 349-85 and the concrete capacity design (CCD) method was made by Fuchs et al. (1995) for expansion and undercut anchors subjected to tension and to shear loads in uncracked concrete. The CCD method is based on the κ - or ψ -method [as used in the CEB Bulletin d'Information (1991)] and was developed at the University of Stuttgart for 1.) single and multiple anchors, close to and far from the edge, subjected to tension load and 2.) single and double anchors subjected to a force directed toward the edge - members vary from wide to narrow and thin to thick. A rigid base plate is assumed and no plastic action of the anchors is considered. The capacity reduction factor ϕ used in ACI 349-85 and the partial material safety factor, γ_m , are taken as 1.

The main differences between the ACI 349-85 method and the CCD method are summarized in the following table:

Table 3.1 Comparison of ACI 349-85 and CCD Methods
[Taken from Fuchs et al. (1995)]

		ACI 349-85	CCD Method
Anchorage depth, tension load		$N_{uo} \propto h_e^2$	$N_{uo} \propto h_e^{1.5}$
Edge distance, shear load		$V_{uo} \propto c_1^2$	$V_{uo} \propto c_1^{1.5}$
Slope of failure cone		$\alpha = 45 \text{ deg.}$	$\alpha = 35 \text{ deg.}$
Req'd spacing to develop full anchor capacity		2 h_e , tension 2 c_1 , shear	3 h_e , tension 3 c_1 , shear
Req'd edge distance to develop full anchor capacity		1 h_e , tension 1 c_1 , shear	1.5 h_e , tension 1.5 c_1 , shear
Small spacing or close to edge	1 direction	Nonlinear (area proportional) reduction	Linear reduction
	2 directions		Nonlinear reduction
Eccentricity of load		----	Taken into account

Comparisons of the tension and shear load capacities predicted using the two methods were made with 1955 experimental tension tests and 218 experimental shear tests. These experimental

tests were conducted by various researchers from various affiliations. The experimental tests embodied various concrete strengths, embedment depths, edge distances, and spacing between anchors.

ACI 349-85 Tension Capacity.

This method assumes a tensile stress, f_p equal to $\phi 10.5 \sqrt{f'_c}$ (MPa) [$\phi 4 \sqrt{f'_c}$ (ksi)] acting on the failure plane and a 45° inclination between the failure plane and the concrete surface. ϕ is a capacity reduction factor and was taken in this case as 1.0. For single anchors not influenced by edge distance, the tensile capacity, N_{uo} , is:

$$N_{uo} = 4 \sqrt{f'_c} \pi h_e^2 \left(1 + \frac{d_h}{h_e} \right) \quad [lb, in, psi] \quad (3-6a)$$

$$N_{uo} = 0.96 \sqrt{f_{cc}} h_e^2 \left(1 + \frac{d_h}{h_e} \right) \quad [N, mm, MPa] \quad (3-6b)$$

where

- A_N = Actual projected area of stress cones. For single anchors not influenced by edge distance or overlapping cones, $A_N = A_{NO} = \pi h_e^2 (1 + d/h_e)$
- f'_c = Concrete compressive strength of 6 in. x 12 in. cylinders, psi.
- f_{cc} = $1.18 f'_c$. Concrete compressive strength of 200 mm x 200 mm x 200 mm cubes, MPa.

For anchors influenced by edge effects ($c_1 < h_e$, c_1 = distance to the edge) and/or concrete breakout cones ($s < 2 h_e$, s = spacing between anchors), the tensile capacity is:

$$N_u = \frac{A_N}{A_{NO}} N_{uo} \quad (3-7)$$

where N_{uo} is defined in Eq. 3-6 and A_N is as defined in Fig. 3.2.

CCD Method

A 35° inclination of the failure plane from the concrete surface is assumed in this method. The concrete cone failure load of a single anchor without influence of edge distance and overlapping cones in uncracked concrete is:

$$N_{uo} = k_{nc} \sqrt{f'_c} h_e^{1.5} \quad (3-8)$$

where

- $k_{nc} = 35$ for post-installed anchors (Eng. units).
- $= 40$ for cast-in-place anchors (Eng. units).
- $= 13.5$ for post-installed anchors (SI units).
- $= 15.5$ for cast-in-place anchors (SI units).

The cube strength, f_{cc} , should be used instead of the cylinder strength, f'_c , for the value for the concrete strength in Eq. 3-8.

To account for edge distance, spacing, and different anchor arrangements, the capacity is calculated using:

$$N_u = \frac{A_N}{A_{NO}} \Psi_2 N_{uo} \quad (3-9)$$

where

- $A_{NO} =$ Projected area of one anchor at the concrete surface without the influence of edge distance or other anchors.
 $= 9 h_e^2$
- $A_N =$ Actual projected area at the concrete surface assuming the failure surface of individual anchors as a pyramid with base length $s_{cr} = 3 h_e$. See Fig. 3.3.
- $\Psi_2 =$ Factor to account for influence of edge distance.
 $= 1$ if $c_1 \geq 1.5 h_e$
 $= 0.7 + 0.3 (c_1 / 1.5 h_e)$ if $c_1 \leq 1.5 h_e$
- $h_e =$ Effective depth. For fastenings with 3 or 4 edges and $c_{max} \leq 1.5 h_e$ ($c_{max} =$ largest edge distance), $h_e = c_{max}/1.5$.
- $N_{uo} =$ Capacity of one anchor not influenced by edge distance or other anchors.

For eccentrically loaded anchor groups, the capacity is computed as follows:

$$N_u = \frac{A_N}{A_{No}} \Psi_1 \Psi_2 N_{uo} \quad (3-10)$$

where

ψ_1 = Factor to account for eccentric tensile load on anchors. If the load is eccentric about two axes, ψ_1 is equal to the product of the two individual factors.

$$= \frac{1}{1 + 2 e_N / (3 h_e)} \leq 1$$

e_N = Distance between the resultant tensile force and the centroid of the fasteners.

The CCD method predicted loads that compared well with the average loads of the test data for all embedment depths except for two anchors with the largest embedment depths. The ACI 349-85 method however was conservative for anchors with small embedment depths and unconservative for anchors with large embedment depths [transition point at $h_e \approx 175$ mm (6.9 in.)]. The coefficient of variation of the ratio of experimental to predicted loads using the CCD method was 15% - 20% which is similar to the coefficient of variation of concrete tensile strength as obtained from various batches. For multiple anchors, agreement of the experimental data with the CCD predicted loads was better than with those predicted using the ACI method. Also, the calculations of the projected area is easier with the CCD method than with the ACI method making it easier to use.

3.4 Study by Farrow and Klingner

A similar comparison of three approaches to determine the tensile capacity of anchors was performed by Farrow and Klingner (1995). The three methods of prediction used in the comparison were the concrete capacity (CC) [same as CCD method discussed by Fuchs et al. (1995)], ACI 349-90, and the variable angle cone (VAC) methods. The failure mode of the anchors were either steel fracture or concrete cone failure. The predicted capacities were compared to experimental data obtained from tests by other researchers. The data was for anchor bolts, headed studs, undercut and expansion anchors subjected to "concentrated" static loads. Adhesive anchors were not included. In addition, the probability of steel fracture or concrete cone failure was calculated. The anchors were single anchors close to an edge or multiple anchors far from an edge. The tensile capacities were computed based on the following equations (units in N, mm):

$$N_u = \frac{A_N}{A_{NO}} 0.96 \sqrt{f_{cc}} h_e [h_e + d] \quad \text{ACI 349-90} \quad (3-11)$$

$$= \frac{A_N}{A_{NO}} 0.96 \sqrt{f_{cc}} \left(\frac{h_e}{\tan \theta} \right) \left(\frac{h_e}{\tan \theta} + d \right) \quad \text{VAC} \quad (3-12)$$

$$= \frac{A_N}{A_{NO}} \Psi_2 \Psi_1 15.5 \sqrt{f_{cc}} h_e^{1.5} \quad \text{CC for headed anchors} \quad (3-13)$$

$$= \frac{A_N}{A_{NO}} \Psi_2 \Psi_1 13.5 \sqrt{f_{cc}} h_e^{1.5} \quad \text{CC for undercut and expansion anchors} \quad (3-14)$$

where

$$\begin{aligned} \theta &= \text{Cone angle measured from failure surface to longitudinal axis of anchor} \\ &= 45^\circ \quad \text{for } h_e \geq 127 \text{ mm (5 in.)} \\ &= 28^\circ + (0.13386 h_e)^\circ \quad \text{for } h_e < 127 \text{ mm (5 in.)} \\ \psi_2 &= 1 \quad \text{if } c_1 / h_e \geq 1.5 \\ &= 0.25 (2.5 + c_1 / h_e) \quad \text{if } c_1 / h_e < 1.5 \\ \psi_1 &= 1 / [1 + 2e / (3 h_e)] \leq 1 \\ e &= \text{Eccentricity} \leq s/2 \end{aligned}$$

In Eqs. 3-11 to 3-14, A_N is the actual projected area of the anchor group, A_{NO} is the projected area of the anchor group not affected by edge distance or anchor spacing, and f_{cc} is the actual concrete compressive strength. In this study, the eccentricity was set equal to 1.

Loads and resistances based on load and resistance factor design (LRFD) were used to determine the probabilities of steel failure and concrete cone failure for the three methods. Probabilities of failure were calculated for known loads (design loads incorporating load and understrength factors) and unlimited loads (loads that exceed the design loads). Details on the procedure to compute the probabilities may be found in Farrow and Klingner (1995).

Of the three methods, the CC method had the lowest squared error for both single and multiple anchors. All three methods yielded low probabilities of failure under known loads for single anchors far from an edge and for closely spaced multiple anchors. For unlimited loads and

single anchors near an edge, the probability of concrete cone failure associated with the CC method was in general lower than that for the other two methods.

3.5 Studies Reported in the CEB Bulletin D'Information and Design of Fastenings in Concrete: Design Guide

3.5.1 Static Loading

A comprehensive discussion of the behavior of headed, expansion, undercut and bonded anchors in cracked and uncracked concrete may be found in the CEB (Comité Euro-International Du Béton) Bulletin D'Information (1991). The discussions are based on work by various researchers. The Design of Fastenings in Concrete: Design Guide (1997) by the CEB is a recent issue of the CEB Bulletin D'Information (1991). In the CEB Design Guide (1997), two design approaches are presented: elastic and plastic. The elastic design approach is presented in this report and more details on the plastic design approach may be found in the CEB Design Guide (1997). Unless specified otherwise, the information in this section was summarized from the CEB Bulletin (1991).

The discussion in the CEB Bulletin (1991) covers anchors subjected to tension, shear, and combined shear and tension loads. However, discussion in this section will focus on anchors subjected to tension loads.

For headed anchors in uncracked concrete, the failure capacity for steel failure may be predicted by:

$$N_n = A_s f_t \quad (3-15)$$

The CEB Design Guide (1997) uses the yield instead of the tensile strength of the anchor in Eq. 3-15 for computing the tensile capacity of expansion, undercut, and CIP headed anchors.

For anchors located in cracked concrete and experiencing steel failure, the capacity of the anchor may be calculated using Eq. 3-15. However, it was recommended (CEB, 1991) that this capacity be reduced due to the variability of the anchor behavior in cracked concrete.

For headed anchors with concrete cone failure, three predictive equations are presented: ACI 349-85 method, Bode and Hanenkamp (1985) and Bode and Roik (1988) method, and Eligehausen, Fuchs, Mayer (1987/1988) and Rehm, Eligehausen, Mallée - ψ -method or κ -method (1988). The equations for the ACI 349-85 and the κ -methods have already been presented in Section 3.3 [Fuchs, Eligehausen, and Breen (1995)] and will therefore not be presented again. The equations by Bode and Hanenkamp (1985) and Bode and Roik (1988) were:

For single anchors:

$$N_{uo} = a h_e^{1.5} \left(1 + \frac{d_h}{h_e} \right) \sqrt{f_{cc}} \quad [N, mm, MPa] \quad (3-16)$$

$$\begin{aligned} a &= 10.96 \text{ for cube strength} \\ &= 11.89 \text{ for cylinder strength} \end{aligned}$$

For multiple anchors:

$$N_{u, group} = N_{uo} \left[1 + \frac{s(n-1)}{4h_e} \right] \quad [N, mm] \quad (3-17)$$

n = Number of studs in group

For anchors located near edges:

$$N_{u, edge} = \frac{c_1}{c_{crit}} N_{uo} \leq N_{uo} \quad (3-18)$$

$$\begin{aligned} c_{crit} &= 1.5 h_e && \text{for one free edge} \\ &= 2.0 h_e && \text{for } > 1 \text{ free edge} \end{aligned}$$

For headed anchors in cracked concrete and failing in concrete cone failure mode, ACI 349-85 recommended the cracked capacity be 85% of the capacity in uncracked concrete for anchors located in the compression zone of a member and 65% of uncracked capacity for all other types of embedment. Rehm, et al. (1988) recommended that the capacity of anchors in cracked concrete be equal to 60% the capacity in uncracked concrete and to 50% of the uncracked capacity if two cracks crossed the anchor. A further reduction was recommended for short embedments with the reduction varying linearly from 30% to 0% for embedment depths of 40 mm (1.6 in.) to 100 mm (3.9 in.), respectively. This cracked capacity would be multiplied by this additional reduction.

The tensile capacity calculation for expansion and undercut anchors with concrete cone failures as proposed by the CEB Design Guide (1997) is given in Eq. 3-19 which is very similar to the CC method. The influence of cracks is quantified and included in the equation.

$$N_u = N_{uo} \psi_{A, N} \psi_{s, N} \psi_{ec, N} \psi_{re, N} \psi_{ucr, N} \quad [N] \quad (3-19)$$

where

- N_{uo} = Tensile capacity of one anchor in cracked concrete not influenced by edge distance or other anchors.
 = $k_1 (f'_c)^{0.5} (h_e)^{1.5}$
 k_1 = 7.5 [N/mm]^{0.5} for expansion and undercut anchors
 = 9.0 [N/mm]^{0.5} for CIP headed anchors
 $\Psi_{A,N}$ = Factor to account for geometric effects of spacing and edge distance.
 = $A_{c,N} / A_{c,NO}$
 $A_{c,NO}$ = $9 h_e^2$
 $A_{c,N}$ = Actual area of concrete cone anchorage at the concrete surface (see Fig. 3.3 for examples).
 $\Psi_{s,N}$ = Factor to account for influence of edge distance on stress distribution (see definition for ψ_2 , Eq. 3-9).
 $\Psi_{ec,N}$ = Factor to account for group effect (see definition for ψ_1 , Eq. 3-10).
 $\Psi_{re,N}$ = Shell spalling factor for small embedment depths ($h_e < 100$ mm).
 = $0.5 + h_e / 200 \leq 1$ for $s < 150$ mm for any reinforcement diameter
 or $s < 100$ mm for $d_s \leq 10$ mm
 = 1 for $s \geq 150$ mm for any reinforcement diameter
 or $s \geq 100$ mm for $d_s \leq 10$ mm
 $\Psi_{ucr,N}$ = Factor for uncracked or cracked concrete.
 = 1.0 for anchors in cracked concrete.
 = 1.4 for anchors in uncracked concrete.

For pull-out failure of CIP headed anchors, the proposed capacity equation in the CEB Design Guide (1997) is as follows:

$$N_u = p_k A_h \quad [N, MPa, mm^2] \quad (3-20)$$

where

- p_k = 7.5 f'_c for cracked concrete
 = 11 f'_c for uncracked concrete
 A_h = Bearing area of the head.
 = $\pi (d_h^2 - d^2) / 4$

Equations predicting the tensile capacity of headed anchors with a bursting failure mode proposed in ACI 349-85 were reported to be conservative. Equations based on Furche and Eligehausen's (1990) work were:

$$N_{u,t} = 17 c_1 \sqrt{A_h f_c} \quad (3-21)$$

where A_h is defined in Eq. 3-20.

For groups of anchors where overlapping concrete cones may reduce the failure capacity, a factor ψ_s is applied to Eq. 3-21 where

$$\begin{aligned}\psi_s &= 1 + s_r/s_c < n \\ s_r &= \text{Spacing of the outer anchors in the group.} \\ s_c &= 6 c_1\end{aligned}$$

The tensile capacity equation recommended by the CEB Design Guide (1997) for CIP headed anchors is:

$$N_u = N_{uo} \psi_{A, Nb} \psi_{s, Nb} \psi_{ec, Nb} \psi_{ucr, Nb} \quad (3-22)$$

where

$$\begin{aligned}N_{uo} &= \text{Single anchor capacity in cracked concrete at the edge not influenced by other anchors, a corner, member thickness.} \\ &= k_5 c_1 d (f'_c)^{0.5} \\ k_5 &= 8 \text{ [N}^{0.5} \text{ / mm]} \quad \text{for } d_h / d = 1.5 \\ &= 8 \text{ [0.9 (} d_h^2 / d^2 - 1 \text{) }^{0.5} \text{]} \quad \text{for } d_h / d \neq 1.5 \\ \psi_{A, Nb} &= \text{Factor to account for geometric effects of spacing, edge distance and member thickness.} \\ &= A_{c, Nb} / A_{c, NbO} \\ A_{c, Nb} &= \text{Actual area of concrete cone of anchorage on the side of concrete member. See Fig. 3.4 for examples.} \\ A_{c, NbO} &= 36 c_1^2. \text{ See Fig. 3.4.} \\ \psi_{s, Nb} &= \text{Factor to account for the corner.} \\ &= 0.7 + 0.3 [c_2 / (3 c_1)] \leq 1 \\ \psi_{ec, Nb} &= \text{Factor to account for group effect.} \\ &= 1 / [1 + 2 e_N / (6 c_1)] \leq 1 \\ \psi_{ucr, Nb} &= \text{Factor to account for cracked or uncracked concrete (same as for } \psi_{ucr, N}\text{).}\end{aligned}$$

A brief discussion on splitting failure is included in the CEB Bulletin (1991). This failure mode is not well understood and an equation to predict the splitting load for unreinforced concrete based on Spieth's (1961) and Lieberum's (1985) work was presented:

$$N_u = f_c \sqrt{A A_1} \quad (3-23)$$

$$\begin{aligned}A_1 &= \text{Loaded area} = \pi d_h^2 / 4 \\ A &= \text{Concrete surface area, undefined.}\end{aligned}$$

Due to the uncertainties associated with splitting failures, avoidance of this type of failure mode may be prudent. Splitting failures in unreinforced concrete may be avoided if the following conditions are met (CEB, 1997):

edge distance, c_1	$\geq 1.0 h_e$	for undercut anchors
	$\geq 1.5 h_e$	for torque-controlled expansion anchors with one cone
	$\geq 3.0 h_e$	for torque-controlled expansion anchors with two cones and deformation-controlled anchors
spacing, s	$\geq 1.0 h_e$	for undercut and torque-controlled expansion anchors
	$\geq 3.0 h_e$	for deformation-controlled anchors
member thickness, h	$\geq 2.0 h_e$	for all anchor types

The behavior of undercut anchors was found to be very similar to that of headed anchors [Furche (1988)] and the equations to predict the capacity of headed anchors may be used for undercut anchors. Splitting failures during anchor installation due to edge distance and spacing may be avoided if the following conditions are met and assuming a concrete strength of 20 MPa (2.9 ksi):

c_1	$\geq 1.0 h_e$	for crack prevention during installation.
c_1	$\geq 1.5 h_e$	to ensure concrete cone failure.
s	$\geq 1.0 h_e$	for crack prevention during installation.
h	$\geq 2.0 h_e$	

Similarly, capacity reductions for undercut anchors in cracked concrete were the same for headed anchors in cracked concrete.

The capacity of expansion anchors under tensile loads did not change significantly with different anchor types but the displacement and stiffness were affected by the type of anchor. Again, the capacity of expansion anchors with steel failures can be calculated using Eq. 3-15. For concrete failures, the equation per ACI 349-85 is similar to Eq. 3-6 without the term in parentheses. The capacity equation suggested by the ψ -method [Eligehausen et al. (1987)] was:

$$N_u = 13.5 h_e^{1.5} \sqrt{f_{cc}} \quad [N, mm, MPa] \quad (3-24a)$$

$$N_u = 15 h_e^{1.5} \sqrt{f_c} \quad [N, mm, MPa] \quad (3-24b)$$

The effects of edge distance, spacing and eccentricity may be accounted for with the use of the different ψ factors discussed earlier. Other prediction methods were also discussed in the CEB Bulletin (1991).

Another failure mode for expansion anchors is anchor pull-out under tension load. The capacity for this type of failure mode is given by:

$$N_u = \mu_{sw} F_{exp} \quad (3-25)$$

Values of μ_{sw} ranged from 0.2 to 0.3 for torque-controlled anchors and 0.35 for displacement-controlled anchors [Wagner-Grey (1977)] and 0.4 to 0.6 for all types of expansion anchors [Faoro (1988)]. Equation 3-25 does not yield accurate results as a reliable procedure to compute the expansion force, F_{exp} , has yet to be developed.

The prediction of the capacity of expansion anchors failing by splitting and bursting is difficult as the capacity is dependent on edge distance, member thickness, spacing, and the installation procedures. The prediction would only be valid for a given set of conditions and would differ for each type of anchor. However, for members with thicknesses greater than $2 h_e$ and concrete with minimum compressive strengths of 20 MPa (2.9 ksi), the splitting and bursting failure mode could be prevented if minimum edge distances ($1.5 h_e$ to $3 h_e$, depending on anchor type) are provided.

Under tension loads, the observed behavior of expansion anchors in cracked concrete indicate that these anchors have the same failure modes as those in uncracked concrete. However, the failure mode for anchors which experienced concrete cone failure may alter to anchor pull-out. As with headed anchors, the tensile capacity of anchors in cracked concrete [crack widths of 0.3 mm - 0.4 mm (0.011 in. - 0.016 in.)] was reduced by 30% to 50% of that for anchors in uncracked concrete. Figure 3.5 [Eligehausen (1988b)] shows the effect of cracks on the load-displacement behavior of expansion anchors. Greater reduction in anchor capacity as compared with the uncracked capacity was noted for:

- a. Larger crack widths [> 0.4 mm (0.016 in.)]
- b. Anchors failing by pull-out in uncracked concrete
- c. Anchors which do not expand further under load

The capacity of bonded anchors with steel failure and located in uncracked concrete subjected to tensile loads may be calculated using Eq. 3-15. For concrete cone failure of bonded anchors in uncracked concrete, Eq. 3-4 as proposed by Doerr and Klingner (1989) or Eq. 3-5 as proposed by Eligehausen et al. (1984a) may be used to calculate of the capacity of bonded anchors in uncracked concrete. The pull-out capacity of bonded anchors may be predicted using:

$$N_u = \tau_m h_e \pi d_o \quad [N, mm] \quad (3-26)$$

$$\tau_m = \text{mean bond strength} \quad [N/mm^2]$$

$$= 8 \text{ N/mm}^2$$

The capacity of bonded anchors is significantly affected by the condition of the hole. Environmental effects such as freeze thaw will also reduce the capacity of bonded anchors.

More scatter in the experimental results was noted for bonded anchors located in the cracked concrete as compared to those in uncracked concrete. The results also indicate that the presence of cracks affected the capacity of smaller diameter anchors more significantly and that the anchor capacity decreases with increasing crack width, as expected. The anchor capacity is reduced by as much as 40%-80% for anchors in cracked concrete for crack widths of 0.3 mm - 0.4 mm (0.012 in. - 0.016 in.).

3.5.2 Seismic Loading

Discussions of undercut anchors in cracked concrete subjected to cyclic tension tests based on work by Usami [1981] and Keintzel [1990] are presented in the CEB Bulletin [1991]. For concrete failure, the load capacity for an anchor subjected to cyclic loads was approximately 80% of that for anchors subjected to static loads. For identical failure modes, the effects of cyclic loads were higher stiffness and lower energy dissipation capacity. The maximum axial deformation under cyclic tension loads cannot exceed that obtained under monotonic loads unless the concrete surrounding the anchor is sufficiently reinforced to prevent the concrete cone from pulling out. Load degradations were observed for anchors when they were cycled to deformations less than the maximum obtained under monotonic loading. If the anchor did not fail during the cyclic test, the peak load and deformation at peak load were not influenced by the previous loading history. For anchors experiencing steel failure, the behavior was similar to that for anchors experiencing concrete failure. However, the strength and stiffness degradations would be less than that for anchors experiencing concrete failure. The behavior of anchors subjected to tension/compression cyclic loading (a more realistic case) is expected to be worse than that for anchors subjected to cyclic tension loading only.

3.6 Study by Ammann

Ammann (1992) investigated "medium and heavy-duty" mechanical and chemical anchors. Expansion anchors were subjected to cyclic tensile loads (10 cycles at each displacement level). It was found that a loss of about 30%-40% in the pre-tension load may result due to creep and relaxation. Results showed that the pre-tension force in the anchors was reduced by about 33% due to the cyclic loading. Also, the force-deformation curves showed little energy dissipation and a pronounced change in its slope when the test load exceeds the pre-tension load. As a result, it was concluded that the positive pre-tension load should not be relied upon in the event of an earthquake. Also, formation of cracks in the concrete due to an earthquake would reduce the load capacity of the expansion anchors.

3.7 Study by McMackin, Slutter, and Fisher

Tension tests of 19 mm (3/4 in.) diameter anchor studs with embedment depths of 178 mm (7 in. or 9.3*d*) and 102 mm (4 in. or 5.3*d*) were conducted by McMackin et al. (1973). For the given conditions, it was found that a minimum edge distance of 102 mm (4 in.) was required to

develop the full tensile capacity of the anchor stud with an embedment depth of 178 mm (7 in.). An equation to determine the anchor capacity was proposed by McMackin et al. [1973]:

$$N_u = \frac{2 c_1}{9 d} N_{uo} \leq 0.85 f_u A_s \quad (3-27)$$

$$N_{uo} = 0.475 C (h_e + d_h) h_e (f'_c)^{1/2} \leq 0.85 f_u A_s$$

$C = 0.75$ for "all lightweight concrete".
 $C = 0.85$ for sanded lightweight concrete.
 $C = 1.0$ for normal weight concrete.
 $A_s =$ Area of stud.

3.8 Study by Hosokawa

The behavior of expansion, undercut, and adhesive anchors subjected to cyclic tension loads was studied by Hosokawa (1993). The variables in the study included embedment length, type of anchor, and method of hole cleaning. The yield strength of the expansion, undercut, and bonded anchors were 630 MPa (91.4 ksi), 580 MPa (84.1 ksi), and 370 MPa (53.7 ksi), respectively.

Some findings from Hosokawa's study for expansion and undercut anchors were that the displacements for expansion anchors were greater than that for undercut anchors and there was a large reduction in strength of the expansion anchors after reaching maximum capacity whereas this drop-off in strength was more gradual for undercut anchors. The initial stiffnesses and strength capacities of the undercut anchors were higher than those for the expansion anchors. The embedment length required to yield the anchor was less for undercut anchors ($5d$) than for expansion anchors ($7d$). The pull-out capacity of expansion and undercut anchors with a bearing failure (crushing of concrete around the top of the anchor) could be calculated using:

$$N_u = F_b \sin (\alpha + \phi) / \cos \phi \quad (3-28)$$

where

$F_b =$ Bearing strength of concrete $= 12 f'_c$
 $\alpha =$ Angle of plug as measured from the vertical axis.
 $\phi =$ Angle of friction. $\tan \phi = \mu = 0.4$

For concrete cone failure, the capacity may be computed as follows:

$$N_u = A_c \sqrt{f'_c} \quad [kN, cm, kN/cm^2] \quad (3-29)$$

where

$$A_c = \text{Projected area of concrete cone} = \pi h_e (h_e - d)$$

Some of the findings for bonded anchors were that the hole cleaning method affected the bond strength of the anchor with the method of cleaning the hole with a wire brush yielding the highest bond strength of 14 MPa (2 ksi). The pull-out capacity of bonded anchors with concrete cone failure and bond failure could be predicted by:

$$N_u = \pi h_{cone} (h_{cone} + d) f_t + \pi d h_e \tau_a \quad (3-30)$$

$$\begin{aligned} h_{cone} &= d (\tau_a - f_t) / (2 f_t) \\ \tau_a &= \text{Bond stress.} \end{aligned}$$

3.9 Study by Burdette, Perry, and Funk

The main objective of a study by Burdette et al. (1988) was to determine the effects of dynamic loading on the tensile and shear capacities of undercut anchors. The study was conducted at the University of Tennessee and at the Tennessee Valley Authority and consisted of 122 tests. The variables studied included anchor size - 13 mm (1/2 in., $h_e = 12d$), 16 mm (5/8 in., $h_e = 12d$), 19 mm (3/4 in., $h_e = 12.3d$), 25 mm (1 in., $h_e = 12.5d$), 32 mm (1 1/4 in., $h_e = 12.8d$), and type of loading (static tension, static shear, dynamic tension, dynamic shear). The number of cycles in the dynamic tests were in the thousands.

All the anchors failed by steel fracture indicating that an embedment length of $12d$ was sufficient to ensure a ductile failure and the full tensile capacity of the undercut anchors. The tensile capacity of the anchor was reduced as a result of the dynamic loading. This reduction ranged from about 10%-20%. The variability of the results for the dynamic tests was greater than that for the static tests. The variability between dynamic shear tests was less than that for the dynamic tension tests, and the reverse was true for the static tests.

3.10 Discussion

As seen in the previous sections, there are several methods available to predict the tensile capacity of anchors. The prediction of the tensile capacity of anchors failing by steel fracture is straightforward. However, the prediction of the tensile capacity of anchors with concrete cone failures is more complex as witnessed by the various capacity equations presented in this chapter. These equations were developed for a given set of conditions to best fit the experimental data and/or other relevant test data. As a result, the equations may not yield reliable capacities for anchors under different sets of conditions.

As a means to compare the different equations, some sample calculations (Appendix A) were made for an expansion anchor from the study by Johnson and Lew (1990), for an undercut

anchor from a study by Rodriguez (1995), and for a CIP anchor bolt from the Cannon et al. (1975) study. The reason for the selection of these anchors was that all necessary data was available in the cited references. For the expansion and undercut anchors, the behavior of the anchors were not influenced by edge distance or the presence of other anchors. For the CIP anchor, two cases were examined: 1.) no edge or other anchor influence 2.) edge distance influence.

As seen in Table 3.2, the different equations yielded a wide spread in the predicted anchor tensile capacity for concrete cone failure. However, all of the equations underpredicted the anchor capacity. As mentioned in Section 3.3, the CCD and the CEB methods are very similar since they are both based on the ψ -method. However, as seen in Appendix A, the main differences for the sample cases were the empirically derived constants of 13.5 and 15.5 for the CCD equation as compared to 7.5 and 9.0 for the CEB equation and the use of the cube strength, f_{cc} , in the CCD equation as opposed to the cylinder strength, f'_c , in the CEB equation. Also, the ACI 349-85 and VAC equations do not differentiate between the different types of anchor - expansion, undercut, and CIP while the CCD and CEB equations do. As seen in Table 3.2, the standard deviations for the N_u / N_{exp} ratios using the CCD and CEB equations for the three different types of anchors were 0.039 and 0.070, respectively, whereas the standard deviations for the ratios as obtained using the ACI 349-85 and VAC equations were 0.082 and 0.096, respectively. It is obviously easier to have one equation to predict the anchor capacity for all types of anchors but the different anchor behaviors do not allow this simplification.

Table 3.2 Predicted Tensile Capacities

Predictive Equation	Expansion Anchor		Undercut Anchor		CIP Anchor			
	No Edge Distance Effect		No Edge Distance Effect		No Edge Distance Effect		Edge Distance Effect	
	Predicted Tensile Capacity, N_u kN (k)	N_u / N_{exp}^\dagger	Predicted Tensile Capacity, N_u kN (k)	N_u / N_{exp}^*	Predicted Tensile Capacity, N_u kN (k)	N_u / N_{exp}^\ddagger	Predicted Tensile Capacity, N_u kN (k)	$N_u / N_{exp}^{\dagger\dagger}$
1. CEB Design Guide (Eq. 3-19)	61.7 (13.7)	0.55	58.1 (13.1)	0.60	59.9 (13.5)	0.53	41.2 (9.3)	0.51
2. ACI 349-85 (Eq. 3-6a)	76.4 (17.2)	0.69	69.2 (15.5)	0.71	59.4 (13.4)	0.53	54.8 (12.3)	0.67
3. CCD (Eq. 3-8)	85.2 (19.2)	0.77	81.1 (18.2)	0.83	80.1 (18.0)	0.71	54.7 (12.3)	0.67
4. VAC (Eq. 3-12)	94.7 (21.3)	0.86	86.0 (19.3)	0.89	79.8 (18.0)	0.71	NA ^{##}	--

[†] Experimental tensile capacity = 110.8 kN (24.9 k) from Johnson and Lew (1990).

^{*} Experimental tensile capacity = 97.1 kN (21.8 k) from Rodriguez (1995).

[‡] Experimental tensile capacity = 113.0 kN (25.4 k) from Cannon et al. (1975).

^{††} Experimental tensile capacity = 81.4 kN (18.3 k) from Cannon et al. (1975).

^{##} Not available. See Appendix A.2.2.

There has been an ongoing effort to synthesize the available research data to develop more robust equations to predict the capacity of anchors in tension and in shear. This has been reflected in the publication of the CEB Design Guide (1997) in Europe and by the efforts of ACI Committee 355 to develop a similar guide, based on the CCD method, in the United States.

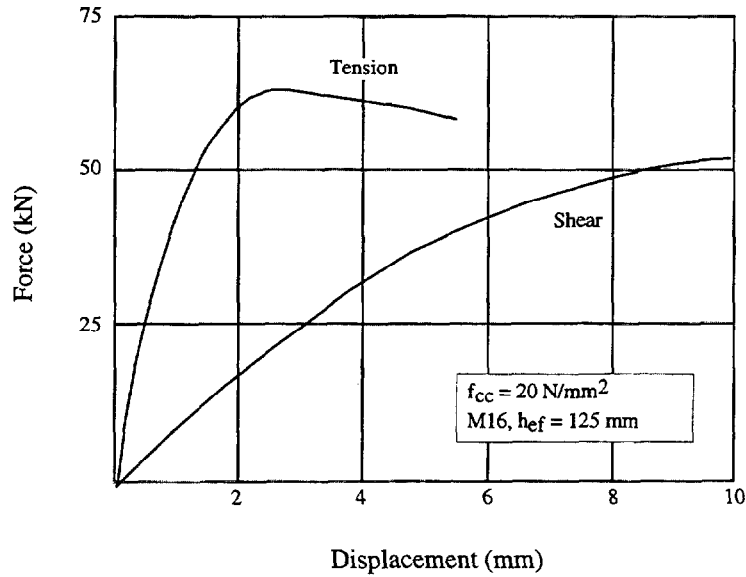


Figure 3.1 Typical Load-Displacement Curves for Bonded Anchors. Taken from Eligehausen et al. (1984a).

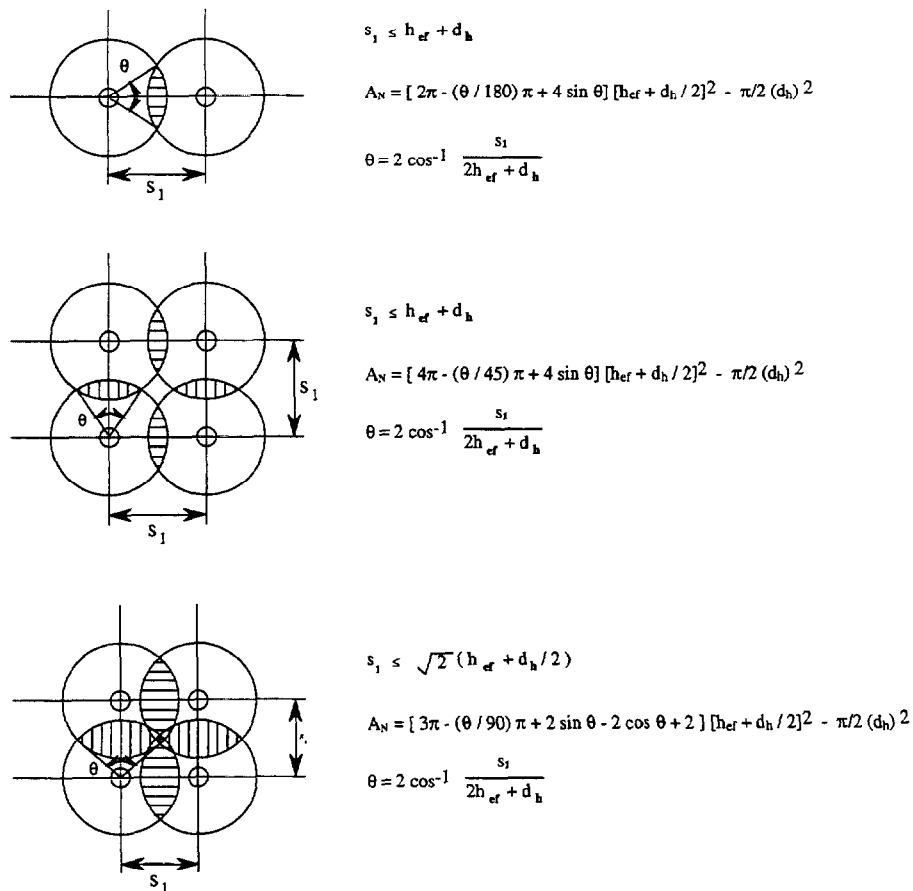


Figure 3.2 Projected Areas for ACI 349-85 Method. Taken from Fuchs et al. (1995).

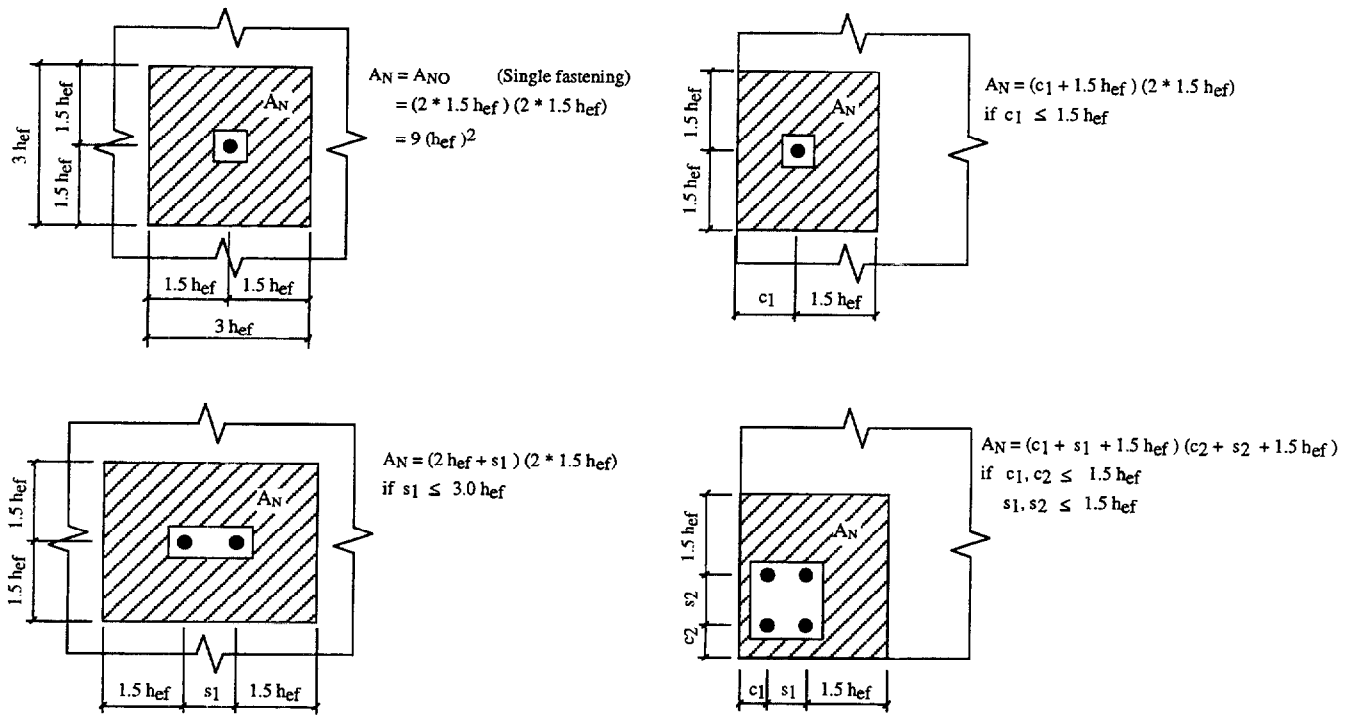
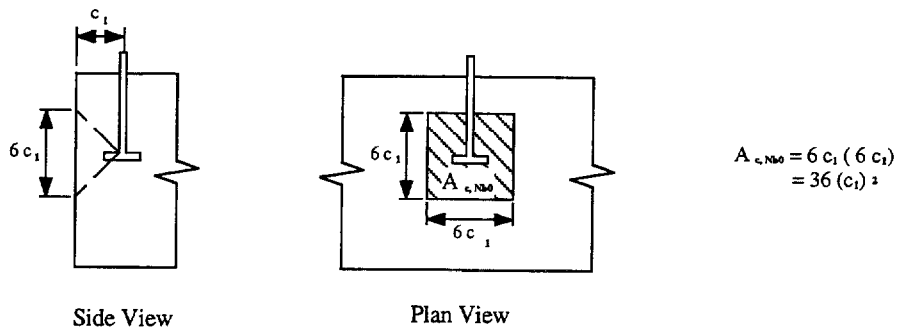
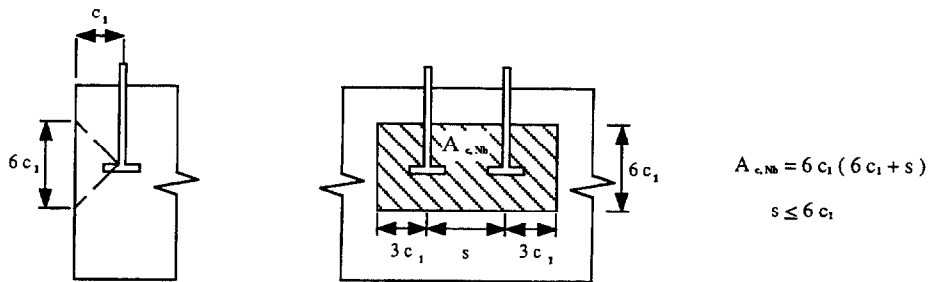


Figure 3.3 Projected Areas for CCD Method.
 Taken from Fuchs et al. (1995).



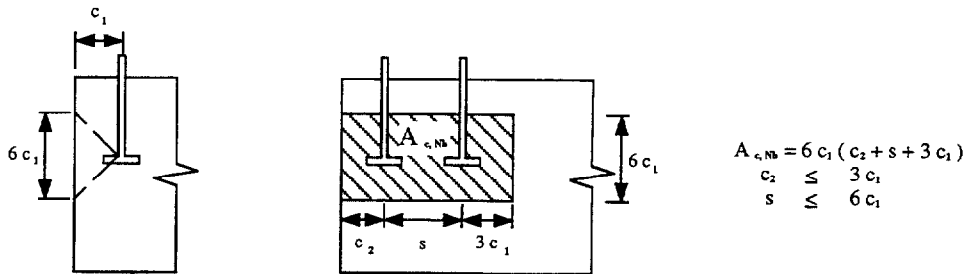
$$A_{c,NS0} = 6c_1 (6c_1) = 36(c_1)^2$$

a. Idealized Concrete Area for One Anchor



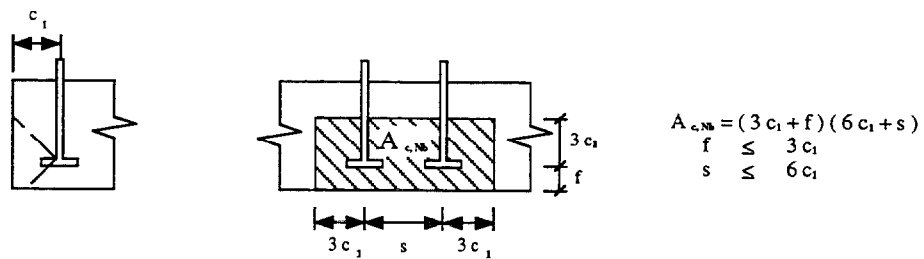
$$A_{c,NS} = 6c_1 (6c_1 + s) \\ s \leq 6c_1$$

b. Actual Projected Area for Two Anchors at Edge



$$A_{c,NS} = 6c_1 (c_2 + s + 3c_1) \\ c_2 \leq 3c_1 \\ s \leq 6c_1$$

c. Actual Projected Area for Two Anchors at Corner



$$A_{c,NS} = (3c_1 + f)(6c_1 + s) \\ f \leq 3c_1 \\ s \leq 6c_1$$

d. Actual Projected Area for Two Anchors in Thin Member

Figure 3.4. Area Calculations for Blow-out Failure Mode.
Taken from CEB Design Guide (1997).

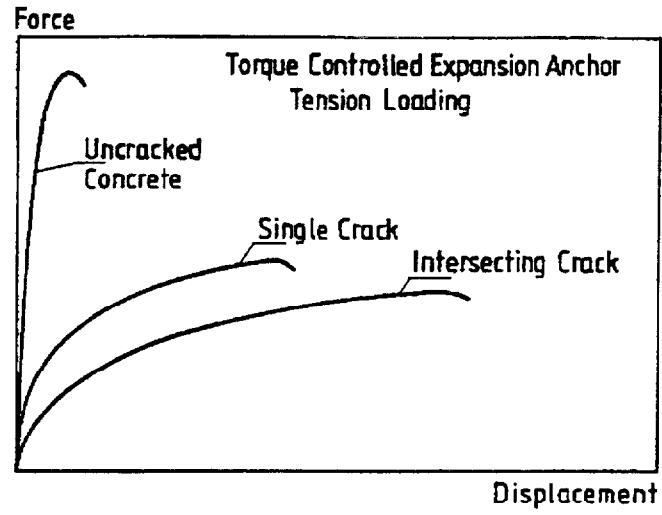


Figure 3.5 Influence of Cracks on Anchor Behavior.
Taken from Eligehausen (1988).

BLANK PAGE

4.0 ANCHORS SUBJECTED TO SHEAR

4.1 Study by Eligehausen and Fuchs

Eligehausen and Fuchs (1988) found that for expansion and undercut anchors in uncracked concrete with anchor embedment depths greater than $4d_o$ (d_o = hole diameter), the failure occurs in the steel. Based on 230 tests, the maximum load for steel failure may be computed using:

$$V_{no} = \alpha A_s f_u \quad (4-1)$$

where

$$\begin{aligned} A_s &= \text{Tensile area of threaded bolt or anchor sleeve} \\ f_u &= \text{Tensile strength of steel} \\ \alpha &= 0.60 \end{aligned}$$

Equation 4-1 is valid for single anchors. For multiple anchors, the total load would be equal to the number of anchors times the load for a single anchor. This is true if there is no clearance between the bolts and the anchor plate. The maximum load is reduced if there is a clearance between the bolt and anchor plate or if two or more bolts are directly in line with the line of loading.

For anchors experiencing concrete failure:

1. For individual anchors at the edge of the member. Based on 31 tests, the predicted breakout concrete strength is:

$$V_{uo} = 1.3 \sqrt{d_o} \sqrt{f_{cc}} c_1^{1.5} \quad [N, mm, MPa] \quad (4-2)$$

The failure load is mainly influenced by the edge distance as seen in the above equation. For members whose thickness are less than $1.4 c_1$, the breakout load, V_{uo} is reduced by χ_d as shown in the following equation:

$$V_{u,h} = \chi_d V_{uo} \quad (4-3)$$

where

$$\chi_d \approx h/(1.4 c_1) \leq 1$$

2. For groups of anchors at the edge of the member. Based on overlapping breakout concrete cones and a 30° angle between the surface and the breakout mass, the load capacity for a group of anchors parallel to the edge with the loading direction toward the edge is:

$$V_{u, group} = \chi_a V_{u, h} \quad (4-4)$$

where

$$\begin{aligned} \chi_a &= 1 + s_{ges}/s_{crit} \leq n_p \\ s_{ges} &= \text{Center-to-center distance between the extreme anchors.} \\ s_{crit} &= \text{Critical anchor spacing.} \\ &= 3.5 c_1 \\ n_p &= \text{Number of adjacent anchors in a line.} \end{aligned}$$

Equation 4-4 was developed for a maximum of two anchors in a row. For grouped anchors subjected to eccentric loading, the maximum load is:

$$V_{u, group, e} = \chi_a \chi_{ex} V_{u, h} \quad (4-5)$$

where

$$\begin{aligned} \chi_{ex} &= 1/(1 + 2 e/s_{crit}) \leq 1 \\ e &= \text{Eccentricity of load} \\ &\leq s_{ges}/2 \\ s_{crit} &= 3.5 c_1 \end{aligned}$$

More details may be found in the Eligehausen and Fuchs (1988) for anchors located in a corner or in a narrow member.

For cracked concrete, the maximum load was not reduced for large edge distances. For members without edge reinforcement and for crack widths less than 0.4 mm (0.02 in.), the maximum load was 60% of the corresponding value for uncracked concrete for close edge distances.

4.2 Study by Fuchs, Eligehausen and Breen

Fuchs et al. (1995) made comparisons between the ACI 349-85 and Concrete Capacity Design (CCD) methods to calculate the shear capacity of an anchor in uncracked concrete with the direction of the load towards the free edge. The main differences between the two methods are shown in Table 3.1.

ACI 349-85 Shear Load Capacity

For an individual anchor, the capacity an anchor is:

$$\begin{aligned}
V_{uo} &= \phi 2 \sqrt{f'_c} \pi c_1^2 && [\text{lb, psi, in}] \\
&= 0.48 \sqrt{f_{cc}} c_1^2 && [N, MPa, mm]
\end{aligned}
\tag{4-6}$$

where

$$\phi = 1 \text{ assumed by Fuchs et al. (1995)}$$

For anchors influenced by member thickness, h , ($h < c_1$), and/or spacing, s , ($s < 2 c_1$) and/or edge distance perpendicular to load, c_2 , ($c_2 < c_1$), the capacity is reduced as follows:

$$V_u = \frac{A_v}{A_{vo}} V_{uo} \tag{4-7}$$

where

A_v = Actual projected area. See Fig. 4.1.

A_{vo} = Projected area of one anchor not influenced by edge distance, other anchors, and member thickness. See Fig. 4.1.

$$= (\pi/2) c_1^2$$

CCD Method

The capacity of an anchor not influenced by member thickness is:

$$\begin{aligned}
V_{uo} &= 13 \left(\frac{1}{d} \right)^{0.2} \sqrt{d f'_c} c_1^{1.5} && [\text{lb, in, psi}] \\
&= \left(\frac{1}{d} \right)^{0.2} \sqrt{d f_{cc}} c_1^{1.5} && [N, mm MPa]
\end{aligned}
\tag{4-8}$$

For single and multiple anchors, the capacity, taking into account eccentric load and corner effects, may be calculated as follows:

$$V_u = \frac{A_v}{A_{vo}} \psi_4 \psi_5 V_{uo} \tag{4-9}$$

where

- A_v = Actual projected area at side of concrete member with the fracture area idealized as a half pyramid with sides $1.5 c_1$ and $3 c_1$. See Fig. 4.2.
- A_{v0} = Projected area of one anchor not influenced by edge distances, spacing, or member thickness, idealized as a half pyramid with sides $1.5 c_1$ and $3 c_1$. See Fig. 4.2.
 = $4.5 c_1^2$
- ψ_4 = Factor to account for effect of eccentric shear load.
 = $\frac{1}{1 + 2 e_v' / (3 c_1)}$
- ψ_5 = Factor to account for symmetric stress distribution caused by a corner.
 = 1 if $c_2 \geq 1.5 c_1$
 = $0.7 + 0.3 (c_2 / 1.5c_1)$ if $c_2 \leq 1.5 c_1$
- c_1 = Edge distance in direction of loading; this value is limited for narrow, thin members.
- c_2 = Edge distance perpendicular to direction of loading.

For single anchors, the CCD method resulted in predictions of the shear loads that matched the average of the experimental failure loads well. The ACI 349-85 method was conservative for small edge distances and unconservative for large edge distances. For multiple anchors, the loads predicted by the CCD method compared better with the experimental loads than did those predicted by the ACI 349-85 method. For both single and multiple anchors, the coefficient of variation for the ratio of the predicted loads to the experimental data was lower for the CCD method than that for the ACI 349-85 method. The calculations of the projected area is simpler in the CCD method making it easier to use than the ACI 349-85 method.

4.3 Study by Ammann

Ammann (1992) subjected expansion (mechanical) anchors to a series of pulsating loads (shown in Fig. 4.3). F_p and F_a in Fig. 4.3 are load levels determined from static tests. The pre-tension load in the anchors was set at 30% of the initial pre-tension load to simulate the load loss due to creep and relaxation. The results showed that the envelope of the load-deflection cycles for the pulsating test followed the curve for the static curve for pure shear. No results were reported for the reversed cyclic shear loading, but this type of loading would be a more severe loading condition than the pulsating load condition.

4.4 Studies Reported in the CEB Bulletin D'Information and Design of Fastenings in Concrete: Design Guide

As stated in Section 3.5, the information in the CEB Design Guide (1997) is based mainly on the CEB Bulletin (1991) with revisions reflecting more recent information. Unless specifically mentioned, the information in this section was summarized from the CEB Bulletin (1991).

4.4.1 Static Loading

The capacity of headed anchors subjected to shear loads with failure occurring in the steel may be calculated based on shear friction theory per ACI 349-85:

$$V_n = \phi A_s f_y \mu \quad (4-10)$$

ϕ	=	0.55	for structural steel shapes, fabricated sections, and shear lugs
	=	0.85	for bolts, studs, bars.
μ	=	Coefficient of friction.	
	=	0.9	for concrete/grout against as-rolled steel with the contact plate one baseplate thickness below concrete surface.
	=	0.7	for concrete/grout against as-rolled steel with the contact plate coincidental with the concrete surface.
	=	0.55	for grouted conditions with contact plate between grout and as-rolled steel exterior to concrete surface.
f_y	≤	827 MPa (120 ksi)	

The equation proposed by the CEB Design Guide (1997) is the same as that proposed by Eligehausen and Fuchs (1988), Eq. 4-1 except that the yield strength rather than the tensile strength of steel is used. An additional factor of 0.8 was proposed to account for steel with low ductility and for anchor groups.

For the calculation of anchor capacities not based on shear friction theory, the equation has the form of Eq. 4-1. Based on test results obtained by various researchers, α , in Eq. 4-1, ranged from 0.53 to 1.0 and f_u was taken as either the yield or tensile strength of the anchor.

For anchors loaded towards an edge and experiencing lateral concrete-cone failures, several methods for predicting the anchor capacity were represented. Among them were the ACI 349-85 and the ψ -methods which were presented in Section 4.2. Other empirical equations for predicting anchor capacities for concrete failures were:

by Shaik and Whayong (1985):

$$\begin{aligned}
 V_u &= 12.5 \sqrt{f'_c} c_1^{1.5} && [\text{lbs, psi, in}] \\
 &= 5.23 \sqrt{f'_c} c_1^{1.5} && [N, MPa, mm]
 \end{aligned}
 \quad (4-11)$$

by Paschen and Schönhoff (1983):

for $c_2/c_1 < 1.73$

$$V_u = (190 + 0.23 c_1^2) (f_{cc})^{0.67} \sin (0.91 c_2 / c_1) \quad (4-12a)$$

$$V_u = (212 + 0.26 c_1^2) (f_c')^{0.67} \sin (0.91 c_2 / c_1) \quad (4-12b)$$

for $c_2/c_1 \geq 1.73$

$$V_u = (190 + 0.23 c_1^2) (f_{cc})^{0.67} \quad [N, mm, MPa] \quad (4-12c)$$

$$V_u = (212 + 0.26 c_1^2) (f_c')^{0.67} \quad [N, mm, MPa] \quad (4-12d)$$

where

c_1 = Distance to free edge parallel to shear load.

c_2 = Distance to free edge perpendicular to shear load.

For headed anchors with failures resulting in the formation of concrete spalls, an equation proposed by AISC (1978) to predict the shear capacity was:

$$V_u = 0.5 A_s \sqrt{f_c' E_c} \quad [kips, in, psi] \quad (4-13)$$

where E_c is in units of ksi. The capacity is reduced for $(c_1 - 1) < 8d$. The following equation was proposed by Hawkins (1987):

$$V_u = 18.2 d^{0.33} \sqrt{f_c'} (15 + 1.1 h_e + d_w) \quad [lbs, psi, in] \quad (4-14)$$

$$V_u = 13.1 d^{0.33} \sqrt{f_c'} (381 + 1.1 h_e + d_w) \quad [N, MPa, mm]$$

where

d_w = washer diameter $< h_e$
= 0 if no washer present.

Hawkins (1987) found that the increased embedment depth corresponded to increased stiffness of the stud and to a significant increase in the slip at failure. Also, increased concrete strength corresponded to increased stud capacity.

The shear capacity for headed anchors in cracked concrete may be taken as 70% of the shear capacity of anchors in uncracked concrete [Eligehausen and Fuchs (1988)].

As stated in Chapter 2, the behavior of undercut anchors, in uncracked and cracked concrete, is very similar to that of headed anchors, and the capacity prediction equations for headed anchors may be used for undercut anchors. Undercut anchors may exhibit greater displacements under shear loads than headed anchors as a result of the clearance between the anchor sleeve and the hole which does not exist for CIP anchors.

The failure behavior of expansion anchors is similar to that of headed anchors. The capacity of expansion anchors with steel failure under shear loading was found to be about 50% of the tensile capacity of the anchor. However, for expansion anchors, concrete cone failures are more typical due to the practice of using high strength steel for the anchor material and short embedment depths. The calculation of the shear capacity of expansion anchors was similar to that for headed anchors with a modification to account for the possible inclusion of the anchor sleeve in resisting the shear load.

Expansion anchors loaded in shear and located in cracked concrete had a reduced capacity as compared to similar anchors in uncracked concrete if their failure mode under tension load was concrete cone failure in uncracked concrete. Reductions of the shear capacity of up to 20% were noted for anchors which failed by anchor pull-out under tension load in uncracked concrete.

The equations for headed anchors subjected to shear loads and experiencing steel failure in uncracked concrete may be used for bonded anchors for the same conditions. For concrete failure of bonded anchors in uncracked concrete, the prediction of the shear capacity based on Fuchs's (1984) work was:

$$V_{u,m} = 20 \pi \sqrt{f_{cc}} \sqrt{d_o} c_1 \quad [N, MPa, mm] \quad (4-15a)$$

$$V_{u,m} = 21.7 \pi \sqrt{f'_c} \sqrt{d_o} c_1 \quad [N, MPa, mm] \quad (4-15b)$$

Dieterle et al. (1989) found that cracks did not affect the capacity of bonded anchors which failed by steel failures. However, for concrete cone failures, it was found that in cracked concrete the reduction in the anchor capacity was larger and the drop-off in the capacity was steeper for bonded anchors than for other types of anchors.

For concrete edge failures, the equation for predicting the shear capacity for expansion, undercut, and CIP headed anchors in cracked or uncracked concrete presented in the CEB Design Guide (1997) is similar to the CC method and is as follows:

$$V_u = V_{uo} \psi_{A,v} \psi_{h,v} \psi_{s,v} \psi_{ec,v} \psi_{\alpha,v} \psi_{ucr,v} \quad [N] \quad (4-16)$$

where

$$V_{uo} = \text{Shear capacity of one anchor in cracked concrete not influenced by edge}$$

		distances, other anchors, or member thickness and loaded in direction of edge.
k_4	$= k_4 \sqrt{d} (\ell_f / d)^{0.2} \sqrt{f'_c} c_1^{1.5}$	
	$= 0.5 \text{ [N}^{0.5} / \text{mm]}$	
ℓ_f	$=$	Effective length of anchor under shear loading.
$\Psi_{A, v}$	$=$	Factor to account for geometric effects of spacing, edge distance parallel to the direction of loading and member thickness.
	$= A_v / A_{v0}$	where A_v and A_{v0} are defined in Section 4.2 for Eq. 4-9.
$\Psi_{h, v}$	$=$	Factor to account for the fact that resistance does not decrease linearly with member thickness as assumed in the factor $\Psi_{A, v}$.
	$= (1.5 c_1 / h)^{1/3} \geq 1$	
$\Psi_{s, v}$	$=$	Factor to account for edges parallel to the loading direction (see definition for ψ_5 for Eq. 4-9).
$\Psi_{ec, v}$	$=$	Factor to account for anchor groups (see definition for ψ_4 for Eq. 4-9).
$\Psi_{\alpha, v}$	$=$	Factor to account for angle between the direction of loading and the direction perpendicular to the free edge.
	$= 1.0$	for $0^\circ \leq \alpha_v \leq 55^\circ$
	$= 1 / (\cos \alpha_v + 0.5 \sin \alpha_v)$	for $55^\circ < \alpha_v \leq 90^\circ$
	$= 2.0$	for $90^\circ < \alpha_v \leq 180^\circ$
$\Psi_{ucr, v}$	$= 1.0$	for cracked concrete without edge reinforcement or stirrups.
	$= 1.2$	for cracked concrete with straight edge reinforcement ($d_s \geq 12 \text{ mm}$).
	$= 1.4$	for cracked concrete with edge reinforcement and closely spaced stirrups ($\leq 100 \text{ mm}$) or welded wire mesh ($d_s \geq 8 \text{ mm}$ and $s \leq 100 \text{ mm}$) or uncracked concrete.

Also, an equation for the capacity for the pry-out failure mode for expansion, undercut and CIP headed anchors was presented in the CEB Design Guide (1997):

$$V_u = k_3 N_u \quad (4-17)$$

where

$$\begin{aligned} k_3 &= 1.0 \text{ for } h_e < 60 \text{ mm} \\ &= 2.0 \text{ for } h_e \geq 60 \text{ mm} \\ N_u &= \text{As defined in Eq. 3-19} \end{aligned}$$

4.4.2 Seismic Loading

Information from various research studies on anchors subjected to shear loads was summarized and presented in the CEB Bulletin (1991). Work based on Usami and others' [1981] study of headed anchors with a strength, f_u , of 480 MPa (70 ksi) was presented. The variables included embedment depth which ranged from $5.3d$ to $8.4d$, number of anchors (2 or 4), anchor spacing, type of loading (cyclic shear in one direction or reversed cyclic shear), test specimen in

single or double shear planes (the latter situation is more common in the field). The study found that failure was due to the fracture of the bolt except in two cases where the bolts pulled out of the concrete ($h_e = 5.3d$). The failure loads for specimens with the double shear planes were much higher than those with a single shear plane. The type of loading significantly affected the failure displacement - the displacement was much lower when the loading was reversed cyclic shear as opposed to shear in one direction only. The failure load of anchors subjected to reversed cyclic shear was approximately 70-80% of that for anchors subjected to cyclic shear in one direction. Pinching of the hysteresis loops and severe load degradation were observed for specimens subjected to reversed cyclic shear. Also, anchors with longer embedment depths dissipated more energy than those with shorter embedment depths, and load degradation was greater for anchors with shorter embedments.

The discussion for expansion anchors in uncracked concrete was based on work performed by Higashi et al. [1983] and Endo et al. [1985]. Three loading sequences were studied: monotonic displacement, cyclic shear loads, cyclic shear displacements. The following results were observed:

1. Pinched hysteresis loops - low hysteretic damping.
2. Stiffness and strength degradation due to cyclic loading. Strength degradation was more pronounced in the earlier cycles and the degradation was independent of the maximum displacement imposed. The shear capacity, V_u , at any cycle may be computed based on:

$$V_u = V_1 \left[1 - 0.25 \sqrt{n - 1} \right] \quad (4-18)$$

where

$$\begin{aligned} V_1 &= \text{Shear capacity in the first cycle} \\ n &= \text{Cycle number.} \end{aligned}$$

Also included in the CEB Bulletin (1991) were tests by Eligehausen (1988a) and Vintzeleou (1990) on expansion, undercut, and bonded anchors in cracked concrete, under reversed cyclic shear loads. The cracks were parallel to the direction of loading and the crack widths ranged from 0.1 mm to 0.8 mm (0.004 in. to 0.031 in.). Edge distance varied between 80 mm and 150 mm (3.1 in. and 5.9 in.). The tests were conducted under imposed displacements. Based on these tests, Eq. 4-18 was modified so that the shear capacity, $V_{u,n}$, for cycle n ($n < 10$), was equal to:

$$V_{u,n} = V_1 \left[1 - \delta \sqrt{n - 1} \right] \quad (4-19)$$

$$\begin{aligned} \delta &= 0.11 \text{ for undercut anchors} \\ &= 0.13 \text{ for expansion anchors} \\ &= 0.17 \text{ for bonded anchors} \\ V_1 &= \text{Shear capacity for cycle 1} \end{aligned}$$

The results are summarized as follows :

- Behavior of anchors under monotonic and reversed cyclic shear was similar unlike that for anchors subjected to tension.
- Anchor capacity dropped off drastically after achieving peak load as obtained under monotonic loading. For cyclic displacements less than or equal to $\pm 0.75 \Delta_u$ (Δ_u is the maximum displacement under monotonic load) there was a significant load degradation and pinching. This was independent of failure mode. Torque controlled expansion and bonded anchors were affected more by the cyclic loads than undercut anchors.
- Cyclic displacements less than or equal to $0.75 \Delta_u$ did not affect the peak shear load and displacement.
- For cracked concrete (crack width ≥ 0.3 mm), the failure load for concrete cone pull out was 70% of that for uncracked concrete. For steel failure, the values for cracked and uncracked concrete were similar.
- The maximum anchor displacement increased with increased edge distance and was greater for steel failure than for concrete cone failure.

4.5 Study by McMackin, Slutter and Fisher

McMackin, et al. (1973) found that 19 mm (3/4 in.) diameter, 102 mm (4 in.) long anchor studs with embedment depths of 102 mm (4 in.) in normal weight concrete required a minimum edge distance of 203 mm (8 in.) to develop their full shear capacity. An equation to determine the anchor capacity was proposed:

$$V_u = V_{uo} \left(\frac{c_1 - 1}{8d} \right) \leq 0.85 f_u A_s \quad [kips, in] \quad (4-20)$$

$$V_{uo} = 0.94 A_s f_c'^{0.3} E_c^{0.44} \leq 0.85 f_u A_s$$

E_c = Modulus of elasticity of concrete, ksi.
 A_s = Area of anchor stud, in².

4.6 Study by Klingner, Mendonca, and Malik

The objectives of the research by Klingner et al. (1984) were to develop reinforcing details for anchor bolts located close to the edges that would allow the bolts to develop their full shear capacity and to determine the behavior of short anchor bolts subjected to reversed cyclic shear. This study involves CIP anchors but is included because the reinforcing details were considered relevant to the strengthening methodology involving infill walls.

The work consisted of 56 tests of 19 mm (3/4 in.), ASTM 307 anchor bolts. The anchor bolts were 305 mm (12 in.) long and were embedded to 203 mm (8 in. or $10.7d$). This

embedment depth was determined to be sufficient to develop the full tensile capacity of the bolt. The reinforcement details consisted of 180° hairpins made of #5 [$\phi = 16 \text{ mm (0.625 in.)}$], Grade 60 [$f_y = 414 \text{ MPa (60 ksi)}$] deformed bars.

Four different hairpin placements were used: Type 1 hairpins were used for bolts with 102 mm (4 in.) edge distances. The hairpins were placed near the surface and edge of the concrete and with the bolt placed away from the hairpin. Type 2 hairpins were used with bolts with 102 mm (4 in.) edge distances and were placed against the bolt and close to the concrete surface. Type 3 hairpins were used with bolts with 51 mm (2 in.) edge distances and were placed against the bolt and close to the concrete surface. Type 4 hairpins were used with bolts with 51 mm (2 in.) edge distances and were placed against the bolt but relatively far from the concrete surface.

Results from the study for anchors subjected to monotonic loading indicate similar behavior for all bolts until spalling of the concrete occurred. Except for those bolts with the Type 4 hairpin, all the other bolts achieved loads similar to those for the bolts in unreinforced concrete with large edge distances. Therefore, Types 1 to 3 hairpins could be used for anchor bolts placed close to the edge and subjected to monotonic loading.

Some anchors were subjected to cyclic loads. For the cyclic loading, there were two load sequences used: 1) Series of reversed cycles with increasing maximum loads 2) One reversed cycle at high maximum load followed by a series of cycles with increasing maximum loads. The results show that the shear behavior of the bolts appear to be independent of the load sequences. The performances of the bolts in plain concrete and with large edge distance were satisfactory. The bolts failed in the steel due to low-cycle fatigue. Also, bolts placed close to the edge performed adequately if the concrete was reinforced with hairpins (Type 2 and 3) that were placed against the bolt and close to the top of the concrete. Under reversed loading, the maximum loads were 50% less than those obtained for monotonic loading in both plain and reinforced concrete.

The predicted capacities using Eq. 4-6 (ACI 349-85 method) for concrete failure and Eq. 4-1 for steel failure with $\alpha = 0.75$ matched the experimental values well. For purposes of design, a strength reduction factor of 0.65 and 0.90 was recommended for the concrete failure and steel failure modes, respectively.

4.7 Study by Bass, Carrasquillo, and Jirsa

The objective of the test program conducted by Bass et al. (1989) was to examine the strength and load-deflection behavior of the interface between new concrete cast on existing concrete. The variables included the amount of interface reinforcement (#6 dowels) - 2, 3, 6; the embedment depth of the dowels - 76 mm (3 in. or $4d$), 152 mm (6 in. or $8d$), 305 mm (12 in. or $16d$); concrete strength of the new and existing concretes; preparation of the interface surfaces - no treatment, sandblasting, chipping, shear keys; reinforcement detailing of the new and old concrete elements; casting procedures for the new element - vertical, horizontal, overhead [cast to within 51 mm (2 in.)] of base block and the gap was later drypacked; and the concrete interface area - width of new wall 254 mm (10 in.) vs. 152 mm (6 in.). The test specimens were subjected

to repeated load cycles based on load levels or displacement of the new walls. Most of the specimens were subjected to 10 cycles.

The results indicate that dowels with embedment depths of 76 mm (3 in. or $4d$), exhibited lower residual shear stress and a reduction of about 30% of the peak shear stresses as compared with those for dowels with 152 mm (6 in. or $8d$) and 305 mm (12 in. or $16d$) embedments. A deeper embedment depth resulted in higher shear capacities at higher slip levels. The results also showed that a sandblasted surface performed as well as the other surface preparations. Also, better confinement of the concrete in the base block resulted in higher peak stresses and residual shear capacities. The maximum shear stress and residual shear capacity increased with increased number of dowels. The width of the new wall did not affect the peak shear stresses but the thinner wall slipped more before reaching the peak capacity. The thinner wall also had a higher residual shear capacity at larger slip levels, but the wall split along the dowel line at larger slip levels.

The horizontal and vertical casting positions showed no difference in performance. This finding was contrary to that reported by the ASCE Nuclear Structures and Materials Committee (1984) which reported that the capacity of horizontal anchors was slightly less than that of vertical anchors. It was recommended [ASCE (1984)] that the capacity of horizontal anchors be set at 80% of that of vertical anchors. The overhead procedure with drypack had a lower peak shear stress and a higher slip level than the other two positions but the residual shear capacity was the same for all three positions. The residual capacities were higher for cast-in-place new walls than for shotcreted walls.

The experimental capacities were compared with those obtained using the shear-friction procedures of ACI 318. The ACI procedure specified embedment lengths of 457 mm (18 in.) on either side of the interface. The results indicated that the ACI procedures were conservative. All the specimens achieved peak shear capacities higher than that predicted by ACI even for the 76 mm (3 in.) embedment depths. However, the strength of the specimens with 76 mm (3 in.) and 152 mm (6 in.) embedments dropped below the ACI value after a slip of about 2.5 mm (0.1 in.). The specimens with 305 mm (12 in.) embedment depths maintained strengths above the ACI value for all slip values.

Based on their findings, Bass et al. (1989) recommended that the strength of the concrete used in repair should be at least as strong as that of the existing concrete. Details to prevent the concrete from splitting around the interface reinforcement should be included in the new element. If using the ACI shear friction design strengths, the embedment of the interface reinforcement may be less than required.

4.8 Study by Akiyama, Yamamoto, Hirose, Matsuzaki, and Imai

Akiyama et al. (1992) conducted a study to determine the effect of steel fibers added to the polyester resin and undercut on the shear capacity of bonded anchors. The effects of embedment length, loading sequence, and the number of anchors loaded simultaneously were also studied. A total of 60 anchors, single and grouped were tested. The loading sequences used in the test

program were monotonic loading and reversed cyclic loading.

For monotonic loading, the yield load and the post-yield stiffness were affected by the embedment length while the elastic stiffness was not. The maximum shear capacity was influenced by:

1. Type of loading - the capacity is reduced when the anchor was subjected to cyclic loading.
2. The interface between the concrete surfaces - when the surface was roughened, the load increased. There was a steep increase in the load until the bond between the two surfaces broke.
3. For short embedment lengths ($5d$), the addition of steel fibers to the resin increased the maximum shear capacity by about 10%.
4. The effect of the undercut was not clear.
5. There was an almost linear relationship between the maximum shear capacity and the embedment length.

4.9 Study by Swirsky, Dusel, Crozier, Stoker, and Nordlin

Swirsky et al. (1977) reported on the lateral resistance of 92 anchor bolt tests. The test parameters included bolt size [25 mm (1 in.) and 51 mm (2 in.)], single bolt or pairs of bolts, loading sequence (static shear, cyclic shear, static combined shear and bending, cyclic combined shear and bending), strength of bolt [mild (ASTM A307) and high strength (ASTM A449)], bolt installation [cast-in-place, canister and mortar (bolt in sleeve filled with mortar), epoxied threaded bar], edge distance [102 mm (4 in.), 152 mm (6 in.), 203 mm (8 in.), 305 mm (12 in.)], and lateral reinforcement (none or with hairpin tie-back).

The findings from the study are summarized below:

1. For CIP bolts with sufficient edge distance to develop full anchor shear capacity, both the yield load [load required to obtain 1.3 mm (0.05 in.) deflection] and the ultimate load are proportional to the edge distance. For 25 mm (1 in.) bolts, the edge distance required to develop ultimate shear capacity was 203 mm (8 in.) and the required edge distance was 610 mm (24 in.) for 51 mm (2 in.) bolts.
2. Epoxied bolts were not as stiff as CIP bolts.
3. Canister and mortar bolts had lower resistance than CIP bolts at deflections less than 5 mm (0.2 in.). The lateral resistance was better for canister and mortar bolts than CIP bolts for deflections greater than 5 mm (0.2 in.).
4. The use of hairpin reinforcement significantly increased the ductility and ultimate load for CIP bolts regardless of bolt diameter or edge distance. The bolt should be placed against the bend of the hairpin reinforcement.

5. Of the 3 bolt installations, the canister and mortar installation performed best in terms of ultimate load and ductility.
6. The combined resistance of paired bolts was less than the sum of the individual bolt capacities for bolt spacing less than 4 times the minimum edge distance.
7. Combined shear and bending reduced the lateral resistance, and increased the anchor displacements as compared to displacements of anchors subjected to shear only. This was more apparent for the smaller anchor size.
8. Low level cyclic loading at loads less than that required to obtain 1.3 mm [0.05 in. (yield load)] deformation did not significantly affect the lateral resistance. Cyclic loads at higher load levels reduced the ultimate load and the ductility.

4.10 Study by Burdette, Perry, and Funk

The main objective of a study by Burdette et al. (1988) was to determine the effects of dynamic loading on the tensile and shear capacities of undercut anchors. The test parameters are given in Section 3.9.

The results from the study was similar for the shear tests as for the tension tests. All the anchors failed by steel fracture indicating that an embedment length of $12d$ was sufficient to ensure a ductile failure and the full shear capacity of the undercut anchors. The shear capacity of the anchor was reduced as a result of the dynamic loading. This reduction ranged from about 10%-20%. The variability of the results for the dynamic tests was slightly higher than that for the static tests.

4.11 Discussion

Several methods to predict the shear capacity of an anchor were presented in the previous sections. As with the anchors subjected to a tensile load, the capacity prediction of anchors subjected to a shear load and failing by steel fracture is straightforward and there is a general consensus on the form of the equation. Sample calculations for an expansion anchor from Johnson and Lew's (1990) study were made as shown in Appendix B. As seen in Appendix B, Section B.1, the predicted capacity was 128.9 kN (29.0 k) compared with the experimental value of 109.9 kN (24.7 k). As discussed in Appendix B, the anchor fractured at the reduced section and if the area of the reduced section were used, the predicted anchor capacity would be 109.9 kN (24.7 k) which matches the experimental capacity.

However, for anchors with concrete failure mode, several equations are proposed for predicting the shear capacity. Sample calculations are made using the results from one test of an expansion anchor in Hallowell's study (1996) and from two tests of headed studs from McMackin's (1973) study. The selection of headed studs was made because all the necessary data was available in McMackin's (1973) report and the behavior of undercut anchors is similar to that

of headed studs. The two headed studs chosen were similar except for the edge distance.

As seen in Table 4.1, the predicted values vary widely. Unlike the equations predicting the tensile capacity which underpredicted the experimental capacity, some equations predicting the shear capacities underpredicted the capacity while others overpredicted the capacity. Also, some of the equations underpredicted the capacity for one case and overpredicted the capacity for the other case. This inconsistency would indicate that these equations require further refinement. Excluding Hawkins' equation, the ACI 349-85 equation resulted in the largest variation for the two anchor tests - overpredicting the capacity by 40% for the anchor with an edge distance of 254 mm (10 in.) and underpredicting the capacity by 45% for the anchor with an edge distance of 50.8 mm (2 in.) for the case with headed studs. The CEB and CCD equations yielded more consistent ratios of V_u / V_{exp} for the three cases than did the other did equations. These ratios are conservative but this consistency would lend itself to the development of a rational safety factor.

Of the seven equations in Table 4.1, Hawkins' equation (Eq. 4-14) does not account for the effect of edge distance and this is reflected by the high capacities predicted for the anchors with the 101.6 (4 in.) and 50.8 mm (2 in.) edge distances.

Table 4.1 Predicted Shear Capacities.

Predictive Equation	Expansion Anchor		Headed Stud			
	102 mm (4 in.) Edge Distance		254 mm (10 in.) Edge Distance		51 mm (2 in.) Edge Distance	
	Predicted Shear Capacity, V_u kN (k)	V_u / V_{exp}^\ddagger	Predicted Shear Capacity, V_u kN (k)	V_u / V_{exp}^\ddagger	Predicted Shear Capacity, V_u kN (k)	$V_u / V_{exp}^{\ddagger\ddagger}$
1. CEB Design Guide (Eq. 4-16)	22.8 (5.1)	0.68	77.3 (17.4)	0.61	9.0 (2.0)	0.61
2. ACI 349-85 (Eq. 4-6)	29.0 (6.5)	0.87	178.1 (40.0)	1.40	7.8 (1.8)	0.55
3. CCD (Eq. 4-8)	27.5 (6.2)	0.83	90.4 (20.3)	0.71	10.5 (2.3)	0.70
4. AISC(Eq. 4-13)	NA ^{††}	---	118.8 (26.7)	0.93	NA ^{††}	--
5. Eligehausen & Fuchs (Eq. 4-2)	36.7 (8.2)	1.09	131.8 (29.6)	1.03	13.0 (2.9)	0.88
6. Hawkins (Eq. 4-14)	89.2 (20.2)	2.69	158.9 (35.9)	1.25	100.0 (22.5)	6.8
7. McMackin (Eq. 4-20)	--- ^{†††}	---	106.5 (23.9)	0.84	19.0 (4.3)	1.3

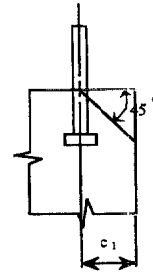
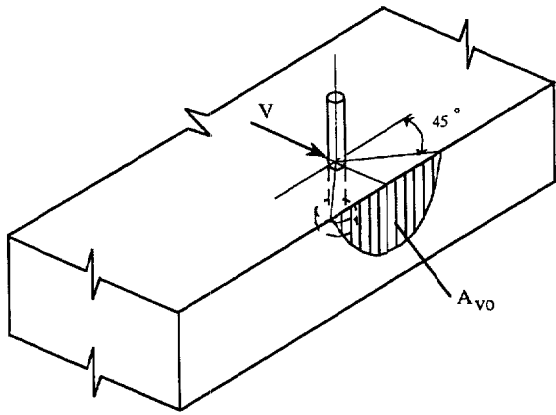
[‡] Experimental shear capacity = 33.3 kN (7.5 k) from Hallowell (1996).

[†] Experimental shear capacity = 127.2 kN (28.6 k) from McMackin et al. (1973).

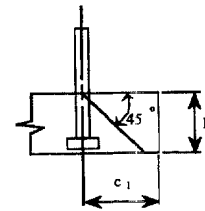
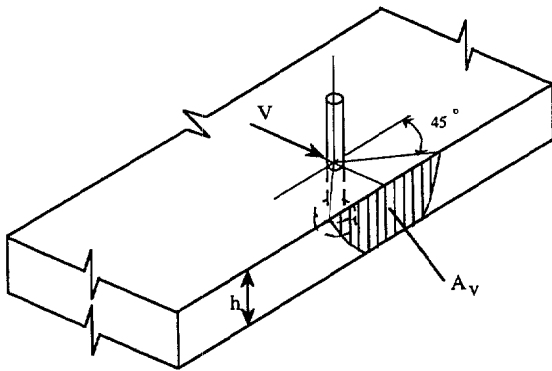
^{‡‡} Experimental shear capacity = 14.7 kN (3.3 k)

^{††} Not applicable since the restriction on the edge distance is not met. See Appendix B.

^{†††} Not all information available for the use of the predictive equation.

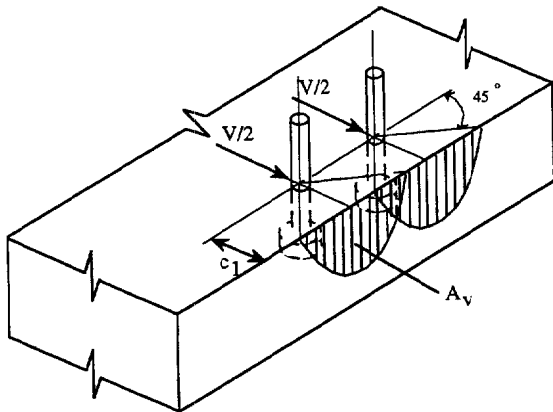


$$A_{vo} = \frac{\pi}{2} c_1^2$$



$$A_v = \left(\pi - \frac{\pi \theta}{180} + \sin \theta \right) \frac{c_1^2}{2}$$

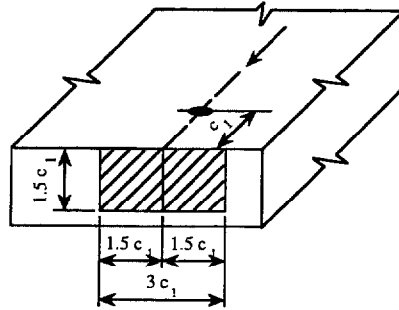
$$\theta = 2 \arccos \frac{h}{c_1}$$



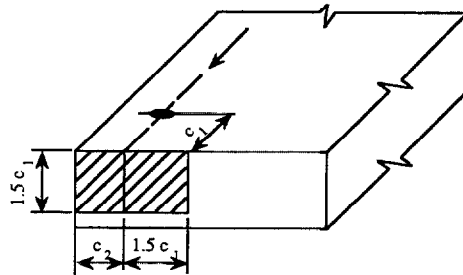
$$A_v = \left(\pi - \frac{\pi / 2 * \theta}{180} + \sin \theta \right) c_1^2$$

$$\theta = 2 \arccos \frac{s_1}{2c_1}$$

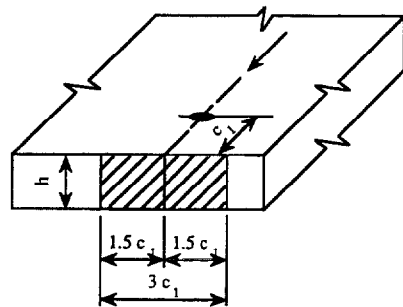
Figure 4.1 Projected Areas for ACI 349-85 Method taken from Fuchs et al. (1995).



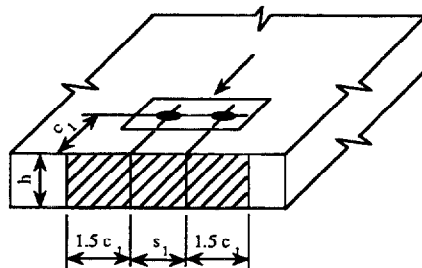
$$\begin{aligned}
 A_v &= A_{v0} \\
 &= 1.5c_1 (2 * 1.5c_1) \\
 &= 4.5c_1^2
 \end{aligned}$$



$$\begin{aligned}
 A_v &= 1.5c_1 (1.5c_1 + c_2) \\
 \text{if: } &c_2 < 1.5c_1
 \end{aligned}$$



$$\begin{aligned}
 A_v &= (2 * 1.5c_1) h \\
 \text{if: } &h \leq 1.5c_1
 \end{aligned}$$



$$\begin{aligned}
 A_v &= (2 * 1.5c_1 + s_1) h \\
 \text{if: } &h \leq 1.5c_1 \\
 &s_1 \leq 1.5c_1
 \end{aligned}$$

Figure 4.2. Projected Areas for CCD Method taken from Fuchs et al. (1995).

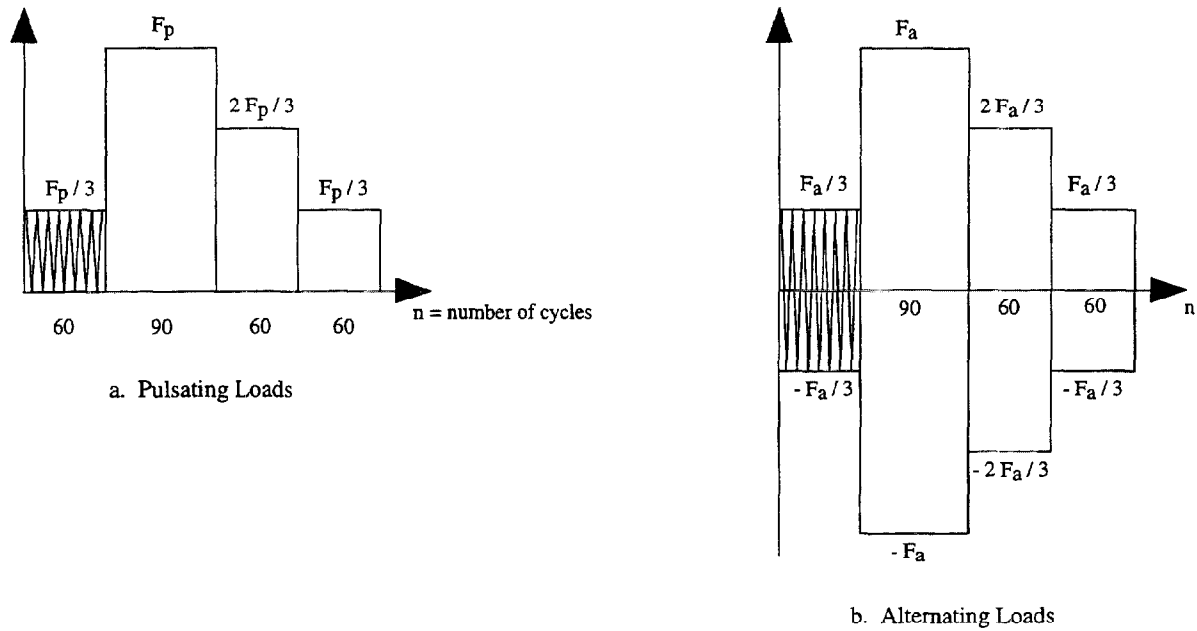


Figure 4.3 Loading Sequences for Cyclic Tests.
Taken from Ammann (1992).

BLANK PAGE

5.0 ANCHORS SUBJECTED TO COMBINED TENSION AND SHEAR LOADS

5.1 Study by the Cannon, Burdette, and Funk

One hundred and eighty-six anchor tests were conducted by Cannon et al. (1975) at the Tennessee Valley Authority. The test program consisted of three phases: Phase I - tension, Phase II - shear, Phase III - combined tension and shear. The variables in the test program included the number of anchors, type of anchor, and anchor size, embedment depth, edge distance, angle of the load, and spacing between multiple anchors.

In the combined shear and tension tests, all tests were on groups of 4 bolts. Four of the tests were with 19 mm (3/4 in.) diameter ASTM A307, A325, and A490 bolts at a load angle of 60°; seven tests were with 19 mm (3/4 in.) diameter A307 bolts at a load angle of 30°; three tests were with 16 mm (5/8 in.) diameter A307 bolts at a load angle of 60°, and five tests were with expansion anchors at a load angle of 30°. The bolts were grouted with an expansive grout. Embedment depths varied from 89 mm (3 1/2 in.) to 241 mm (9 1/2 in.).

It was found that the load causing slip was higher for combined loading than it was for shear alone (Fig. 5.1). The effects of combined loading for the various anchor types are shown in Fig. 5.2. The proposed relationship between the failure load and the tension/shear ratio is given by:

$$P_u = \frac{N_u V_u}{V_u \sin \theta + N_u \cos \theta} \quad (5-1)$$

where,

P_u = Failure load under combined shear and tension

N_u = Tensile capacity

V_u = Shear capacity

θ = Angle of applied load as measured from the horizontal axis.

The stiffnesses of the connections were found to be reduced as a result of the combined loading.

5.2 Study by Eligehausen and Fuchs

For uncracked concrete, Eligehausen and Fuchs (1988) proposed a tri-linear relationship for headed studs subjected to combined shear and tension loading:

$$\frac{N}{N_u} \leq 1 \quad (5-2a)$$

$$\frac{V}{V_u} \leq 1 \quad (5-2b)$$

$$\frac{N}{N_u} + \frac{V}{V_u} \leq 1.2 \quad (5-2c)$$

where

- N = Applied tensile load
- V = Applied shear load
- N_u = Failure load in tension
- V_u = Failure load in shear

Equations 5-2a-c were based on a few tests with single anchors and a few tests with 4 anchors grouped in a square arrangement. These equations may also be applicable to anchor bolts. No research has been conducted for anchors in cracked concrete but Equations 5-2a-c may be used if N_u and V_u were computed for cracked concrete.

5.3 Study by McMackin, Slutter, and Fisher

Included in McMackin's et al. (1973) study on headed anchors were tests of anchors subjected to combined shear and tension loading. Variables in the tests included type of concrete (normal or lightweight), embedment length, angle of loading (30° and 60°, 90° = pure tension¹), and distance to free edge. The anchor diameter was 19 mm (3/4 in.) for all tests except for three where the anchor diameter was 22 mm (7/8 in.). The tensile capacity, f_u , of the anchor studs was 441 MPa (64 ksi). The concrete strength was approximately 35 MPa (5000 psi).

McMackin et al. (1973) developed the following equation for headed anchors subjected to combined tension and shear loads with full embedment and placed in normal weight concrete:

$$\left(\frac{N}{N_u} \right)^{5/3} + \left(\frac{V}{V_u} \right)^{5/3} \leq 1 \quad (5-3)$$

- A_s = Area of anchor, in²
- f_c = Compressive strength of concrete, MPa (ksi)

¹ The convention of 90° = pure tension is different from that used in the researchers' paper. This convention is used in this paper for uniformity in the discussion.

$$\begin{aligned}
E_c &= \text{Concrete modulus of elasticity, MPa (ksi)} \\
N &= \text{Applied tension load} \\
V &= \text{Applied shear load} \\
N_u &= \text{Tensile capacity of anchor} = f_u A_s \\
V_u &= \text{Shear capacity of the anchor} \\
&= 1.827 A_s f_c'^{0.3} E_c^{0.44} \leq N_u \quad (\text{N}) \\
&= 1.106 A_s f_c'^{0.3} E_c^{0.44} \leq N_u \quad (\text{k})
\end{aligned}$$

As compared with the smaller diameter anchors, the larger diameter anchor showed a slight increase in the tensile and shear forces under combined loading. The results for anchors with full embedment and placed in lightweight concrete had more variability. The shear strength of the anchors in lightweight concrete was less than that for anchors in normal weight concrete. By applying a safety factor of 0.9 to N_u and V_u in Eq. 5-3, the above equation may be used for normal and lightweight concrete.

For anchors with partial embedment and placed in normal weight concrete, the following equation was proposed:

$$\left(\frac{N}{N_{cu}} \right)^{5/3} + \left(\frac{V}{V_u} \right)^{5/3} = 1 \quad (5-4)$$

where

$$\begin{aligned}
N_{cu} &= 4 (f_c')^{1/2} A_c \\
&= 1.47 C (h_e + d_h) h_e \sqrt{f_c'} \leq f_u A_s \quad (\text{N, mm, MPa}) \\
&= 0.56 C (h_e + d_h) h_e \sqrt{f_c'} \leq f_u A_s \quad (\text{kips, in, ksi}) \\
C &= 0.75 \text{ for "all lightweight concrete"} \\
&= 0.85 \text{ for sanded lightweight concrete} \\
&= 1.0 \text{ for normal weight concrete}
\end{aligned}$$

Again, a safety factor may be applied to N_{cu} and V_u . Results from tension tests of anchor studs with partial embedment show that the equation for N_{cu} is valid for direct tension.

The proposed equations gave reasonable estimates for combined loading. The margin of safety for pure tension and the 30° combined loading case was less than for the case of pure shear and the 60° combined loading.

5.4 Study by Johnson and Lew

An experimental study of 24 - 25 mm (1 in.) wedge-type expansion anchors were conducted by Johnson and Lew (1990). The anchors were not preloaded and were tested in uncracked concrete. Variables in the study included concrete strength [31 MPa (4.5 ksi) and 41

MPa (6.0 ksi)], embedment length [76 mm (3 in.) to 152 mm (6 in.)], and angle of load, ϕ , (0° - pure shear, 22.5° , 45° , 60° , 70° , 80° , 90° - pure tension). The effects of edge distance were not studied.

A summary of the results follows:

1. The behavior of anchors subjected to pure shear was variable [$f_{u, exp} = 3.4$ kN (15 k) and 7.6 kN (34 k)] for $h_e = 102$ mm (4 in.)). Anchor behavior in terms of capacity, failure mode, and stiffness was not significantly affected by the concrete strength and the embedment length [102 mm (4 in.) and 133 mm (5.25 in.)].
2. For $\phi = 45^\circ$, increased embedment depth increased anchor capacity and changed the mode of failure from fracture at the reduced section to fracture of the anchor shank. Increased embedment depth also increased the point at which the load-deformation plot became nonlinear.
3. For $\phi \leq 60^\circ$, anchors failed in shear due to steel fracture. The ultimate strength was not significantly affected by the concrete strength but by the properties of steel and the magnitude of the bending stress present.
4. For $\phi > 60^\circ$, the failure changed to tension failure mode - steel fracture or concrete cone around the anchor. Although the effects of embedment depth and concrete strength were not isolated, it was postulated that the anchor capacity would increase with increased concrete strength and embedment length with limits on both beyond which fracture of the anchor or anchor pullout would control. For the type of anchor tested, an embedment depth of 152 mm (6 in. or $6d$) was found to be the limit beyond which no increase in anchor capacity was expected.
5. As the embedment depth increased, the depth of spalling around the anchor decreased which reduced the bending stress in the anchor. This reduction in bending stress resulted in an increase in anchor capacity.
6. The load angle did not significantly affect the anchor strength.
7. A straight line was proposed to determine the lower bound anchor capacity for combined loading (See Eq. 5-7).

5.5 Study by Lindquist

The effects of preload on the ultimate strength of 19 mm (3/4 in.) diameter expansion anchors, wedge and shell types, were studied by Lindquist (1982). The test parameters included the amount of preload (full, half, none), type of loading [static (8 total) - tension and shear or dynamic (36 total) - tension, shear, combined shear and tension]. In the dynamic tests, the anchors were cycled 40 times at each load level with the initial load level equal to 0.2 times the static capacity and the levels thereafter increased by increments of 0.2 times the static capacity.

In the combined shear and tension tests, the tension to shear ratio was 1.732 (load angle of 60°, 90° = pure tension).

Some of the findings from Lindquist's experiments were:

1. The ultimate capacities from dynamic tests were not significantly lower than those from static tests.
2. The ultimate capacities of anchors subjected to dynamic loading were not affected by the preload level.
3. The anchor stiffness in dynamic tests was less than in static tests.
4. If failure was defined based on deflection, the wedge anchor under tension and the shell anchor under shear exhibit slight effect of preload under dynamic loading.
5. Under dynamic loading, no difference in displacements were noted for anchors with full and half preload. However, the displacements were greater for anchors with no preload.

5.6 Studies Reported in the CEB Bulletin D'Information

5.6.1 Static Load

The CEB Bulletin also included discussions on the behavior of anchors subjected to static combined tension and shear. For steel failure of headed and undercut anchors under combined loading, an equation based on the shear friction theory ACI 349-85 with a strength reduction factor of 1 was presented:

$$N + \frac{V}{\mu} \leq A_s f_y \quad (5-5)$$

where

$$\begin{aligned} \mu &= \text{coefficient of friction} \approx 0.55 - 0.9 \\ A_s &= \text{area of threaded anchors} \end{aligned}$$

A second equation not based on shear friction theory was proposed and the elliptical interaction curve had the following form similar to Eq. 5-3:

$$\left(\frac{N}{N_u} \right)^\alpha + \left(\frac{V}{V_u} \right)^\alpha \leq 1.0 \quad (5-6)$$

where α ranges from 5/3 to 2.

For concrete failure under combined loading, three interaction curves were proposed:

1. Straight line per Johnson and Lew (1990).

$$\frac{N}{N_u} + \frac{V}{V_u} = 1.0 \quad (5-7)$$

where

N, V = Applied tension and compression load, respectively
 N_u, V_u = Ultimate tension and compression load, respectively

2. Tri-linear curve with the form of Eq. 5-2.
3. Elliptical curve with the form as in Equation 5-6.

The tri-linear curve (Eq. 5-2) is recommended by the CEB Design Guide (1997) and is conservative. More realistic values may be obtained using Eq. 5-6. Recommended values of $\alpha = 2$ for steel failure mode, $\alpha = 1.5$ for all other failure modes and $\alpha = 1$ for simplification.

For undercut and adhesive anchors, failure of the anchors due to concrete failure occurred for load angles less than 75° (as measured from the concrete surface) and to steel failure for load angles greater than 45° .

Two equations to predict the shear strength for multiple headed anchors dominated by shear were proposed by Cook and Klinger (1989) and were:

$$V = \gamma \sqrt{N_u^2 - N^2} \quad (5-8a)$$

$$V = \gamma (N_u - N) \quad (5-8b)$$

where

V = Shear strength of anchor subjected to combined shear and tension.
 γ = Ratio of shear strength of anchor to tensile strength of anchor, V_u/N_u .
 = 0.5 for CIP adhesive anchors
 = 0.6 for undercut anchors

Equations 5-8a and 5-8b are the same as Eq. 5-6 for $\alpha = 2$ and 1, respectively. Equation 5-8b, straight line, yields more conservative results than Eq. 5-8a, parabolic curve, which fits the data better.

For torque-controlled expansion anchors in cracked concrete, Dieterle et al. (1990) found that concrete failures occurred for load angles up to 60° (as measured from the concrete surface) and steel failures for angles greater than 60° . Similarly, it was found that a load angle of 25° was the change over point for drop-in anchors. Equations 5-6 and 5-2 could be used for the anchor capacity predictions. However, for bolt-type torque-controlled anchors, it was found that these equations were not applicable.

5.6.2 Seismic Load

Studies on anchors subjected to reversed cyclic combined shear and tension loads are presented in the CEB Bulletin (1991). One such study was carried out by Usami et al. (1980, 1981a, 1981b). The tests were of multiple headed anchors [number of anchors = 2 and 8, $d=19$ mm (3/4 in.), $f_t = 480$ MPa (70 ksi), $h_e = 8.4d$] and bonded anchors (epoxy resin and polyester resin) in uncracked concrete. The tests were load controlled. The tension/shear (T/V) ratio varied from 0.25 and 4.0. For paired anchors, steel failure occurred for $T/V \leq 1.0$ (load angle $\leq 45^\circ$, $0^\circ =$ pure shear) with concrete cone failure occurring otherwise. For anchor groups of eight, steel failure occurred for $T/V \leq 0.5$ (load angle $\leq 27^\circ$) with concrete cone failure occurring otherwise. Similar results were obtained for bonded anchors.

Another study conducted by Okada and Seki (1984) concluded that the behavior of the anchors under cyclic "combined tension and shear is very sensitive to the failure mode".

5.7 Report by the ASCE Nuclear Structures and Materials Committee

For headed anchors, cast-in-place inserts, expansion anchors, and grouted anchors, two shear-tension relationships are suggested by the ASCE Nuclear Structures and Materials Committee (1984). One being a straight line interaction similar to Eq. 5-5 and the other being an elliptical interaction similar to Eq. 5-6. A value of 5/3 was suggested for the value of α in Eq. 5-6. However, when the shear exceeded the tension load by 40%, it was suggested that the elliptical equation yielded unconservative results or may not be applicable and the use of the straight line interaction was recommended.

5.8 Report by Teledyne Engineering Services

An extensive test program was conducted by Teledyne Engineering Services (1979) to study the shear-tension behavior of expansion anchors. The test program also examined the effects of cyclic loads on the anchor capacity. There were three types of cyclic tests:

1. Low cycle - Tension only. 1,000 cycles at 3 Hz between $N_u / 8$ and $N_u / 4$.
2. High cycle - Tension only. 1,000,000 cycles at 80 Hz between $N_u / 7.4$ and $N_u / 5$.

3. Shear-tension - 1,000,000 cycles at 80 Hz. Tension loads cycled between $N_u / 7.4$ and $N_u / 5$ with the shear load at $V_u / 16$.

After completion of the cyclic loads, the bolt was subjected to a static tension load to failure.

The shear-tension test variables included type and manufacturer of the expansion bolt, bolt diameter, and different load angles (0° - pure shear, 22° , 45° , 67° , 90°). The cyclic test variables included type and manufacturer of bolts and bolt diameter.

The conclusions drawn from the study were:

For the shear-tension tests -

1. A linear shear-tension interaction was conservative.
2. The presence of a shear force increased the anchor capacity particularly for smaller bolt sizes.
3. For the steel failure mode, the failure was in shear.

For the cyclic load tests -

1. Cyclic loading did not reduce the capacity of expansion bolts.
2. Presence of a constant shear load during cyclic tension load did not reduce the bolt capacity.
3. Bolts did not fail during cyclic loading.
4. Anchor slip occurred in the initial loading.
5. Preload of anchors to the design load was not necessary to develop anchor capacity.

5.9 Discussion

From the previous sections, there seems to be a general consensus that the relationship as given by Eq. 5-2 or Eq. 5-6 could be used to determine the capacity of anchors under combined tension and shear loads. However, these equations were developed based on a limited number of tests and there is little data for adhesive anchors subjected to combined shear and tension.

For purposes of comparing the two equations, four curves were plotted along with some experimental data to determine the accuracy of the equations as shown in Fig. 5.3. Three of the curves plotted in Fig. 5.3 were obtained using Eq. 5-6 with $\alpha = 1$ (linear), $5/3$, and 2 . The fourth curve was obtained using Eq. 5-8 which is a tri-linear curve. The selection of the experimental data was based solely on the availability of all pertinent data in a report or paper - McMackin et al. (1973), Johnson and Lew (1990), and Teledyne (1979). The results from the Teledyne tests (1979) were chosen because the anchors were similar in size and had similar embedment depths to the other tests, and the reported failure mode was anchor pullout. The pullout failure mode was selected to determine if this type of failure mode yielded results that differed from the results

for anchors experiencing concrete or steel failure in McMackin's et al. (1973) and Johnson and Lew's (1990) studies.

For use in the predictive equations, the ultimate tensile capacity, N_u , is assumed to be equal to $f_u A_s$. The ultimate shear capacity, V_u , is assumed to be equal to $1.106 A_s (f_c')^{0.3} E_c^{0.44}$ [McMackin et al. (1973)] and E_c was taken as $57\sqrt{f_c'}$. For experimental data where the material properties were not available in the report, N_u and V_u were obtained from tests where the load was either pure tension or pure shear, respectively.

From Fig. 5.3, it can be seen that there is a lot of scatter in the data as can be expected as the data was obtained from different studies with varying parameters. However, the fit of an interaction curve through the data is, at best, fair. Of the four curves, Eq. 5-6 with $\alpha = 2$ encompasses the majority (approximately 80%) of the experimental data and would therefore yield a better estimate of the actual capacity of an anchor as compared to the other equations. As mentioned in the previous sections of this chapter, the linear equation, Eq. 5-6 with $\alpha = 1$ was conservative and this is seen in Fig. 5.3 where approximately 50% of the data points lie above the linear equation. Thus, the conclusions drawn by other researchers and presented in earlier sections of this chapter are borne out in Fig. 5.3. For anchors with pullout failure as compared with those with concrete or steel failure, no difference was noted in the relationship between the experimental data and the predictive equations.

As mentioned at the beginning of this section, there is a lack of data for adhesive anchors under combined shear and tension. Therefore, more experimental work needs to be conducted to determine the behavior of these anchors. This is necessary as the use of these anchors to connect infill walls to existing concrete frames is common.

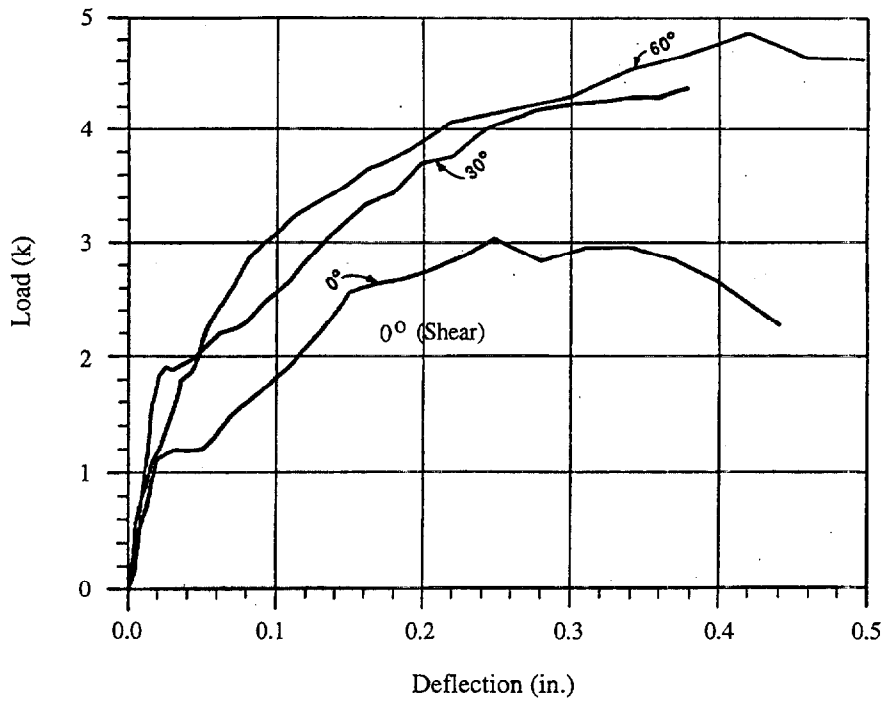


Figure 5.1 Load - Deflection Under Combined Loading.
Taken from TVA (1975).

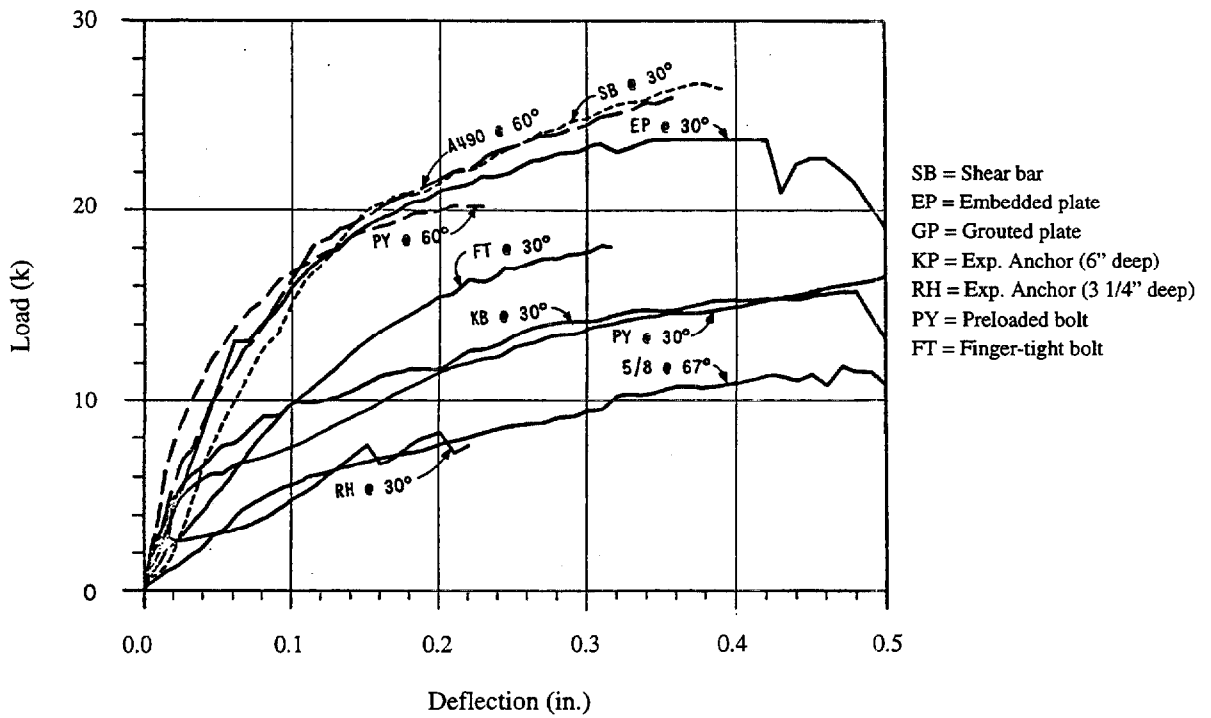


Figure 5.2 Load-Deflection for Various Anchor Types.
Taken from TVA (1975).

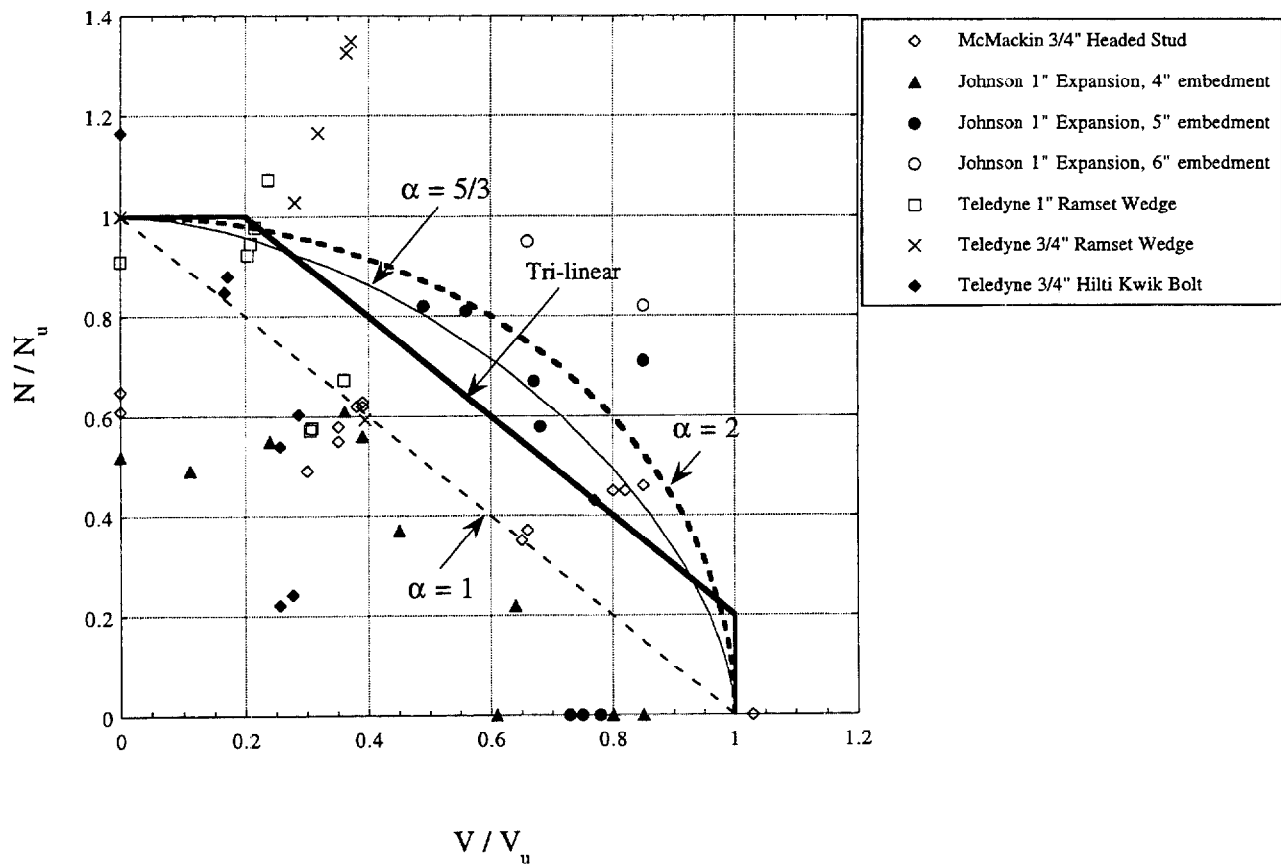


Figure 5.3 Comparison of Eqs. 5-2 and 5-6 with Experimental Data.

BLANK PAGE

6.0 SUMMARY AND CONCLUSIONS

6.1 General

In general, the failure modes for anchors are steel failure, concrete cone failure, bursting failure, splitting failure, anchor pull-out failure, bond failure between anchor and bonding agent, bond failure between concrete and bonding agent, or combinations of two or more of the failure modes. Not all types of anchors will experience all the failure modes listed.

Factors that affect the behavior of anchors include anchor size, anchor strength, edge distance, spacing between anchors, thickness of members, embedment depth, concrete strength, type of loading, eccentricity of loading, anchor preload, anchor installation procedure, and other reinforcement near the anchor.

Substantial research work on anchors has been conducted at the University of Stuttgart, at the University of Texas at Austin, and at the University of Florida, Gainesville. The results from these efforts and from other researchers both in the United States and abroad have contributed to the understanding of anchor behavior as shown in this report. In addition, some recent or ongoing research projects not included in this report are:

1. University of Wisconsin at Milwaukee - Tests to determine the ductility of multiple headed studs have been conducted. The report is currently in preparation.
2. University of Stuttgart - Study the influence of hole cleaning and dampness on bonded anchors, behavior of deformation controlled anchors in cracked concrete, splitting effects near edge, the effects of fire on the anchor steel, on concrete capacity, and on the pullout behavior.
3. University of Texas at Austin - Tests included tensile and shear loading of single anchors in cracked and uncracked concrete, seismic response of multiple anchors near edge, and dynamic loading simulating earthquake forces on anchors.
4. University of Florida, Gainesville - Develop in conjunction with the University of Stuttgart a design model for bonded anchors. The model will be based on 190 tests.

Also, the Electric Power Research Institute has sponsored several studies on anchorage for nuclear power plant equipment, but these studies were not included in this report as this information is proprietary.

As can be seen in the previous three chapters and from the ongoing research presented in the above paragraph, there is sufficient information on the behavior of anchors subjected to tension loads and to shear loads to provide a good understanding of the anchor behavior under these loading conditions. From the research conducted and data available, a design guide for fastening

to concrete is in preparation by ACI Committee 355 - Anchorage to Concrete and changes to the ACI 318 Building Code are being considered. A similar guide, the CEB Design of Fastenings in Concrete: Design Guide (1997), was recently published and is used by the European community. This guide does not currently include provisions for adhesive anchors but these provisions are being prepared and will be included as part of the CEB Design Guide. The behavior of anchors, especially adhesive anchors, under combined tension and shear are based on a limited number of studies. Also, the behavior of anchors subjected to reversed cyclic loads and anchors located in cracked concrete requires further investigation.

6.2 Summary of Findings

6.2.1 Concrete Compressive Strength

Concrete compressive strength is important when the failure mode of the anchor is concrete cone failure. This mode of failure is likely to occur for anchors with shallow embedment depths and low strength concrete. For higher concrete compressive strengths [> 28 MPa (4000 psi)] and other types of failure modes (anchors loaded in shear and steel failure), the concrete strength does not appear to significantly affect the anchor capacity. However, in many of the equations proposed to predict the anchor capacity for concrete cone failure, the capacity is proportional to $\sqrt{f'_c}$. Many of these tests were, however, based on concrete strengths of approximately 28 MPa (4000 psi).

6.2.2 Anchor Preload

A reduction of about 30-40% of the anchor preload may be expected for preloaded expansion anchors due to anchor relaxation. For expansion anchors, preloading the anchor does not increase the anchor capacity, i.e., anchors with and without preload had essentially the same failure capacity. However, preloaded anchors have smaller displacements at failure than anchors which are not preloaded. Another effect of anchor preload is an increase in anchor stiffness and fatigue life. However, when the applied forces are greater than the anchor preload, loss of anchor stiffness was found to be significant. Also, a preloaded anchor subjected to reversed cyclic loads will experience monotonic cyclic loads only, which is a less severe loading condition, until the preload is exceeded.

6.2.3 Cyclic Loading

Some studies have reported the capacities of anchors subjected to cyclic tension loads to be similar to those subjected to static loads while others have reported a capacity reduction of about 20%. Some studies have found that cyclic loading at levels of about 60-75% of the maximum tension or shear capacity as obtained under static loads did not significantly reduce the capacity or displacement at failure under cyclic loading. Reversed cyclic loading is more severe than cyclic loading and displacements at failure are reduced due to the reversed cyclic loading.

For anchor bolts, the capacity reduction was about 50% of the monotonic shear capacity for anchors subjected to reversed cyclic shear (load sequence included cycles at about 75% of maximum shear capacity of anchor).

The stiffnesses of expansion anchors were reduced when subjected to cyclic loads while the stiffnesses of undercut, adhesive, and grouted anchors with sufficient embedment depths were not affected by cyclic loading. Also, the energy dissipation of the anchors is reduced when subjected to cyclic loads.

6.2.4 Embedment Depth

Increased embedment depths increased the anchor tensile capacity and it was recommended that the capacity be reduced for shorter embedment depths (embedment depths less than recommended by the anchor manufacturer or design provisions). The anchor tensile capacity in many of the proposed capacity equations was proportional to either $h_e^{1.5}$ or h_e^2 . It was found that for CIP anchors, the anchor stiffness decreased for increased embedment depths. The embedment depth has less influence on an anchor's shear capacity than on its tensile capacity.

6.2.5 Cracked Concrete

As with concrete strength, anchors experiencing steel failures are not affected by the presence of cracks. The presence of cracks reduced the capacity of anchors by approximately 30%-50% for CIP, headed, and expansion anchors subjected to tension loads. The capacity reduction for adhesive anchors was larger, about 40-80%. The drop-off of the capacity was greatest between crack widths of 0 - 0.4 mm. For crack widths between 0.4 mm and about 1 mm, no further reduction in capacity occurred. However, for anchors with deeper embedment depths and with concrete cone failure, the effect of cracks on the anchor capacity may be less significant. Also, the effect of cracks on anchor capacity is more significant on smaller diameter anchors than on larger diameter anchors.

The scatter of test results for anchors in cracked concrete is larger than that for results for anchors in uncracked concrete, i.e., the behavior of anchors in cracked concrete is more variable and would thus require a larger safety factor. The presence of cracks would also cause the loss of preload in expansion anchors which would increase the anchor displacement at failure.

6.2.6 Anchor Capacity

Attempts to determine the robustness of some of the proposed predictive equations were made at the end of each of the previous chapters. Robustness was defined as the ability of an equation to yield accurate and consistent results for anchors with a given set of conditions. Comparisons were made between the predicted values and a few experimental values.

In general, the capacity of an anchor subjected to either tension or shear load and experiencing steel failure can be easily computed with good reliability. Also, it appears that the shear capacity of an anchor is more difficult to predict and the tensile capacity of the anchor as there is a greater variability in the predicted shear values. Although there is a consensus on the equations to determine the combined shear-tension relationship of anchors, these equations are based on a limited number of tests and as seen in Fig. 5-3, there is a lot of scatter in the test results.

6.2.6.1 Tension Loading

The tensile capacity of anchors experiencing steel failure may be calculated using Eq. 3-15. The CCD method or the method presented in the CEB Design Guide (1997) or the ACI 349R-90 method may be used to calculate the anchor capacity for anchors with concrete failures.

6.2.6.2 Shear Loading

There is more variability in the predicted shear capacities than in the predicted tensile capacities. The shear capacities of anchors experiencing steel failure are less than their tensile capacity and may be determined using Eq. 4-1. Common values for α in Eq. 4-1 range from 0.6 to 0.75. Again, the CCD method or the method presented in the CEB Design Guide (1997) method may be used to compute the anchor capacity if the failure mode of the anchor is concrete failure.

6.2.6.3 Combined Loading

It was found that expansion anchors failed in a tension failure mode for load angles greater than $60^\circ - 75^\circ$ ($0^\circ = \text{shear}$) and 45° for adhesive, undercut, and headed anchors.

The predicted capacity of anchors subjected to combined shear and tension loads may be calculated using the relationship given by Eq. 5-6 or the tri-linear relationship given by Eq. 5-2.

A more conservative approach using a linear interaction as given by Eq. 5-7 may also be used. However, these equations are based on a limited number of experimental tests unlike the equations for predicting the tensile or for predicting the shear capacities.

6.2.7 Transverse Reinforcement

Transverse reinforcement around the anchor was found to increase the capacity and ductility of anchor under shear load especially in situations where insufficient edge distance is provided. The transverse reinforcement used in the studies was hairpin type and it was recommended that this reinforcement be placed near the concrete surface and against the anchor.

6.3 Conclusions

Based on the literature survey conducted, there is insufficient data available to develop a reliable load-displacement relationship for anchors, especially adhesive anchors, subjected to combined shear and tension loads. Therefore, it is proposed that an experimental program to study the behavior of anchors subjected to combined shear and tension loads be conducted to add to the existing database.

The program will investigate anchors that are typically used for connections between concrete infill walls and LRC frames. For this situation, some factors that need to be considered include edge distances parallel and perpendicular to the direction of loading, anchor spacing, and multiple anchors. The imposed loading sequence would be reversed cyclic loads to simulate seismic loading. The test plan will call for tests of identical specimens to try to reduce, if possible, the scatter as seen in Fig. 5.3. The selection of only a few anchor types and sizes will also help reduce the scatter in the test results. Also, when fabricating the test specimens, the number of concrete pours will be minimized to reduce the effect of varying concrete strengths.

BLANK PAGE

REFERENCES

- ACI Committee 349 [1985], *ACI Manual of Concrete Practice: Code Requirements for Nuclear Safety Related Concrete Structures (ACI 349-85)*, Part 4, American Concrete Institute, Detroit, MI, 1985.
- ACI Committee 349 [1996], *ACI Manual of Concrete Practice: Code Requirements for Nuclear Safety Related Concrete Structures (ACI 349R-90)*, Part 4, American Concrete Institute, Detroit, MI, 1996.
- ACI Committee 355 [1993], "*State-of-the-Art Report on Anchorage to Concrete*," ACI 355.1R-91, American Concrete Institute, Detroit, MI, August, 1993.
- ASCE Nuclear Structures and Materials Committee [1984], "*State-of-the-Art Report on Steel Embedments*," *Structural Engineering in Nuclear Facilities*, Vol. 2, American Society of Civil Engineers, 1984, pp. 1080-1218.
- Akiyama, T., Yamamoto, Y., Hirosawa, M., Matsuzaki, Y., and Imai, K. [1992], "*A Study on Shear Capacity of Post-Installed Bonded Anchors*," *Proceedings of the Tenth World Conference on Earthquake Engineering*, July 19-24, Madrid, Spain, Vol. 9, 1992, pp. 5253-5256.
- American Institute of Steel Construction (AISC) [1978], "*Specification for the Design, Fabrication, and Erection of Structural Steel Buildings, with Commentary*," New York, 1978, 235 pp.
- Ammann, W. [1992], "*Fastening Systems Under Seismic Loading Conditions*," *Proceedings of the Tenth World Conference on Earthquake Engineering*, July 19-24, Madrid, Spain, Vol. 9, 1992, pp. 5247-5252.
- Bass, R. A., Carrasquillo, R. L., and Jirsa, J. O. [1989], "*Shear Transfer Across New and Existing Concrete Interfaces*," *ACI Structural Journal*, Vol. 86, No. 4, July-August, 1989, pp. 383-393.
- Bode, H. and Hanenkamp (1985), "*Zur Tragfähigkeit von Kopfbolzen bei Zugbeanspruchung (Bearing Capacity of Headed Studs Under Tension)*," In: *Bauingenieur*, 60, 1985, pp. 361-367.
- Bode, H. and Roik, K. (1988), "*Headed Studs - Embedded in Concrete and Loaded in Tension*," *Anchorage to Concrete*, ACI SP-103, American Concrete Institute, 1988, pp. 61-89.
- Burdette, E., Perry, T., and Funk, R. (1988), "*Tests of Undercut Anchors*," *Anchorage to Concrete*, ACI SP-103, American Concrete Institute, 1988, pp. 133-152.

- CEB Bulletin d'Information [1991], "*Fastenings to Reinforced Concrete and Masonry Structures: State of the Art Report*", Part 1, No. 206, Comité Euro-International Du Béton, Aug., 1991.
- CEB [1997], "*Design of Fastenings in Concrete: Design Guide*," Comité Euro-International Du Béton, Thomas Telford Services Ltd., 1997.
- Cannon, R. W., Burdette, E. G., and Funk, R. R. [1975], "*Anchorage to Concrete*," Report No. CEB 75-32, Tennessee Valley Authority, Division of Engineering Design Thermal Power Engineering, Civil Engineering Branch Research and Development Staff, Dec., 1975.
- Cheok, Geraldine. S., ed. (1995), "*Proceedings, Workshop on the Seismic Rehabilitation of Lightly Reinforced Concrete Frames*," June 12-13, NISTIR 5741, National Institute of Standards and Technology, Gaithersburg, MD, 1995.
- Conard, R. [1969], "*Tests of Grouted Anchor Bolts*," Journal of the American Concrete Institute, Vol. 66, No. 9, Detroit, Sept., 1969, pp.725-728.
- Cook, R. A. [1993], "*Behavior of Chemically Bonded Anchors*," Journal of Structural Engineering, Vol. 119, No. 9, ASCE, Sept., 1993.
- Cook, R. A., Fagundo, F. E., Biller, M. H., and Richardson, D. E., [1991], "*Tensile Behavior and Design of Single Adhesive Anchors*," Structures and Materials Research Report No. 91-3, University of Florida, Gainesville, Fla., 1991.
- Cook, R. A., Collins, D. M., Klingner, R. E., and Polyzois [1992], "*Load-Deflection Behavior of Cast-in-Place and Retrofit Concrete Anchors*," ACI Structural Journal, Vol. 89, No. 6, American Concrete Institute, Detroit, November-December, 1992.
- Cook, R. A. and Klingner, R. E. (1989), "*Behavior and Design of Ductile Multiple-Anchor Steel-to-Concrete Connections*," Research Report CTR 1126-3, Center of Transportation Research, University of Texas at Austin, 1989.
- Collins, D. M, Klingner, R. E., and D. Polyzois [1989], "*Load-Deflection Behavior of Cast-in-Place and Retrofit Concrete Anchors Subjected to Static, Fatigue, and Impact Tensile Loads*," Research Report 1126-1, Center for Transportation Research, University of Texas at Austin, February, 242 p. ** This is the same as ref. 8.
- Dieterle, H. and Opitz, V. [1989], "*Tragverhalten von nicht generell zugzonentauglichen Dübeln; Teil 2: Verhalten im ungerissenen Beton und im bewegten Parallelriß (Bearing Behavior of Anchors Designed for use in Uncracked Concrete; Part 2: Behavior in Uncracked Concrete and in Opened and Closed Line of Cracks - In German)*," Unpublished report

No. 1/36-89/1, Institut für Werkstoffe im Bauwesen, Universität Stuttgart, 1989.

- Doerr, G. T. and Klingner, R. E. [1989], *"Adhesive Anchors: Behavior and Spacing Requirements,"* Research Report 1126-2, Center for Transportation Research, University of Texas, Austin, March, 1989.
- Eligehausen, R. [1988a], *"Gutachtliche Stellungnahme zur Eignung des Setzbolzen-Befestigungssysteme,"* M8H-15-37 P8 DX Kwik der Hilti AG für die Befestigung leichter Unterdecken an Stahlbetondecken, Universität Stuttgart, 1988.
- Eligehausen, R. [1988b], "Anchorage to Concrete by Metallic Expansion Anchors," Anchorage to Concrete, ACI SP-103, American Concrete Institute, Detroit, MI, 1988, pp. 181-201.
- Eligehausen, R., and Fuchs, W. [1988], *"Load-bearing Behavior of Anchor Fastenings under Shear, Combined Tension and Shear or Flexural Loading,"* Betonwerk + Fertigteil - Technik, Vol. 2, Feb, 1988, pp. 48-56.
- Eligehausen, R., Mallee, R., and Rehm, G., [1984a] *"Fixings Formed with Resin Anchors,"* Betonwerk + Fertigteil, October, 1984, pp. 686-692.
- Eligehausen, R., Mallee, R., and Rehm, G., [1984b] *"Fixings Formed with Resin Anchors, Part 2,"* Betonwerk + Fertigteil, November, 1984, pp. 781-785.
- Endo, T., and Shimizu, Y. [1985], *"Behavior of Expansion Anchor Bolts,"* Memoirs of Faculty of Tokyo Metropolitan University, No. 35, Tokyo, 1985, pp. 3607-3620.
- Faoro, M. [1988], *"Zur Bestimmung der Umsetzung des Anziehdrehmomentes M_p in Vorspannkraften, Spreiz- und Spaltkräfte bei Metallspreizdübeln (Determination of the Relationship Between Tightening Torque into Prestress, Expansion and Splitting Forces of Expansion Anchors) in German,"* Report Nr.: 3/7 - 88/9, Universität Stuttgart, 1988.
- Farrow, C. B. and Klingner, R. E. (1995), *"Tensile Capacity of Anchors with Partial or Overlapping Failure Surfaces: Evaluation of Existing Formulas on an LRFD Basis,"* ACI Structural Journal, Vol. 92, No. 6, American Concrete Institute, Detroit, MI, November-December, 1995, pp. 698-710
- Fuchs, W. [1984], *"Tragverhalten von Befestigungsmitteln bei Querkraftbeanspruchung (Bearing Behavior of Fastening Elements Under Shear Loading - In German),"* Werkstoffe und Konstruktion, Institut für Werkstoffe im Bauwesen der Universität Stuttgart, 1984, pp. 37-46.
- Fuchs, W., Eligehausen, R., and Breen, J. [1995], *"Concrete Capacity Design (CCD) Approach for Fastening to Concrete,"* ACI Structural Journal, Vol. 92, No. 1, American Concrete

- Institute, Detroit, January-February, 1995, pp. 73-94.
- Furche, J. [1988], "*Einfluß der Hinterschnittform auf das Last-Verschiebungsverhalten bei zentrischem Zug. Verankerungen im ungerissenen Beton (Influence of the Undercut Shape on the Load-Displacement Behavior Under Axial Tension. Anchors in Uncracked Concrete)*," Unpublished report No. 9/6-88/19, Institut für Werkstoffe im Bauwesen, Universität Stuttgart, 1988.
- Furche, J. and Eligehausen, R. [1990], "*Lateral Blow-out Failure of Headed Studs Near the Free Edge*," ACI Convention, Toronto, 1990.
- Hawkins, N. [1987], "Strength in Shear and Tension of Cast-in-Place Anchor Bolts", Anchorage to Concrete, SP-103, American Concrete Institute, Detroit, MI, 1987.
- Higashi, Y., Endo, T., Shimizu, Y., and Tomatsuri, H. [1983], "*Shear Strength of Expansion Anchor Bolts*," Transaction of the Japan Concrete Institute, Vol. 5, 1983, pp. 473-480.
- Hosokawa, Y. [1993], "*Post-Installed Anchor Bolts Subjected to Tension*," Earthquake Resistance of Reinforced Concrete Structures: A Volume Honoring Hiroyuki Aoyama, November, 1993, pp. 455-466.
- Johnson, M. K. and Lew, H. S. [1990], "*Experimental Study of Post-Installed Anchors Under Combined Shear and Tension Loading*," NISTIR 90-4274, National Institute of Standards and Technology, Gaithersburg, MD, March, 1990, 73 pp.
- Keintzel, F. [1990], "*Dübel Unter Dynamischer Beanspruchung (anchor under dynamic Loading)*," In: Beiträge zum 24. Forschungskolloquium in Karlsruhe, 1990.
- Klingner, R. and Mendonca, J. [1982], "*Shear Capacity of Short Anchor Bolts and Welded Studs: A Literature Review*," ACI Journal, Vol. 79, No. 5, Sept.-Oct., 1982, pp. 339-349.
- Liberum, K., (1985), "*Dübelverankerungen in Bereichen maximaler Moment und erhöhter Hauptzugspannungen (Anchors in Regions of Maximum Moments and Augmented Principal Tensile Stresses - in German)*," In: Proceedings 3, Internationales Darmstädter Kolloquium "Vernakern mit Dübeln," 1985.
- McMackin, P. J., Slutter, R. G., and Fisher, J. W., [1973], "*Headed Steel Anchor Under Combined Loading*," AISC Engineering Journal, Vol. 10, No. 2, April, 1973, pp. 43-52.
- Federal Emergency Management Agency (FEMA) [1992], "NEHRP Handbook for Seismic Rehabilitation of Existing Buildings," FEMA-172, Washington, DC, 1992.

- Okada, T. and Seki, M. [1984], "*Nonlinear Earthquake Response of Equipment System Anchored on Reinforced Building Floor*," Proceedings of the Eighth World Conference on Earthquake Engineering, San Francisco, 1984, pp. 1151-1158.
- Paschen, H. and Schönhoff, T. (1983), "*Untersuchungen über in Beton eingelassene Schwerbolzen aus Betonstahl (Investigation of Steel Shear Lugs Anchored in Concrete)*," Deutscher Ausschuß für Stahlbeton, Heft 346, Berlin, 1983.
- Rehm, G., Eligehausen, R., and Mallée, R. (1988), "*Befestigungstechnik*," In: Betonkalender, Vol. 2, Berlin, 1988, pp. 564-663.
- Rodriguez, M. (1995), "*Behavior of Anchors in Uncracked Concrete Under Static and Dynamic Tensile Loading*," Master Thesis, University of Texas at Austin, August, 1995.
- Shaik, A. and Whayong, Y. (1985), "*In-place Strength of Welded Headed Studs*," Journal of the Prestressed Concrete Institute, 1985, pp. 56-81.
- Spieth, H. -P. (1961), "*Das Verhalten von Beton hoher örtlicher Pressung (Behavior of Concrete Under High Local Pressure)*," In: Beton- und Stahlbetonbau, Heft 11, 1961, pp. 257-263.
- Teledyne Engineering Services [1979], "*Summary Report. Generic Response to USNRC I&E Bulletin Number 79-02 Base Plate/Concrete Expansion Anchor Bolts*," Technical Report 3501-2, August, 1979.
- Usami, S., Abe, Y., and Matsuzaki, Y. [1980], "*Experimental Study on the Strength of Headed Anchor Bolts Under Alternate Shear Load and Combined Shear Load*," Proceedings of the Annual Meeting of the Annual Meeting of Kantou Branch of Architectural Institute of Japan, 1980.
- Usami, S., Abe, Y., and Matsuzaki, Y. [1981a], "*Experimental Research on Tensile Fatigue Strength of 19 mm Headed Studs*," Proceedings of the Annual Meeting of the Annual Meeting of Kantou Branch of Architectural Institute of Japan, 1981.
- Usami, S., Abe, Y., and Matsuzaki, Y. [1981b], "*Experimental Study on the Strength of Bonded Anchors Under Alternate Shear Load and Combined Shear Load*," Proceedings of the Annual Meeting of the Annual Meeting of Kantou Branch of Architectural Institute of Japan, 1981.
- Vintzelou, E. and Eligehausen, R. [1990], "*Behavior of fasteners Under Monotonic or Cyclic Shear Displacements*," Presented at the ACI-Symposium on Anchorage to Concrete, Toronto, 1990.

Ward, D. [1993], "*Chemical Anchors*," Concrete Repair Digest, December, 1993.

Wagner-Grey, U. [1977], "*Einflüsse auf die Tragfähigkeit von Speizdübeln im Beton (Influences on the Bearing Capacity of Expansion Anchors in Concrete) in German*,"
Verbindungstechnik, Heft 4, 1977, pp. 27-30.

APPENDIX A - TENSILE CAPACITY

A.1 CONCRETE FAILURE - EXPANSION ANCHOR

Sample calculations of the tensile anchor capacity is presented in this appendix. An expansion anchor, Specimen 24, as taken from Johnson's and Lew's (1990) study will be used in the following sample calculations. The expansion anchor had a 25.4 mm (1 in.) diameter shank. The concrete compressive strength was 32.2 MPa (4670 psi) and the ultimate tensile strength of the anchor was 546.1 MPa (79.2 ksi). The embedment depth (h_e) was 101.6 mm (4 in.) and the edge distance (c_1) was 381 mm (15 in.). The failure mode of Specimen 24 was concrete cone failure and the experimental failure load, N_u , was 110.8 kN (24.9 k). The tensile capacity of specimen was:

$$\begin{aligned} N_n &= f_{ut} A_s \\ &= 79.2 (0.61) \\ &= 48.3 \text{ kips } (213.4 \text{ kN}) \end{aligned}$$

where A_s was the tensile area of a threaded anchor and was calculated using:
 $A_{net} = \pi/4 [d - (0.9743 / n)]^2$ with $d=1$, n = number of threads per inch = 8.

CEB Design Guide (Eq. 3-19)

$$\begin{aligned} \Psi_{A,N} &= 1 && \text{since } A_{c,N} = A_{c,NO} \\ \Psi_{s,N} &= 1 && \text{since } c_1 \geq 1.5 h_e = 1.5 (101.6) = 152.4 \text{ mm} \\ \Psi_{ec,N} &= 1 && \text{since no eccentricity} \\ \Psi_{re,N} &= 1 && \text{since } h_e = 101.6 \text{ mm} > 100 \text{ mm} \\ \Psi_{ucr,N} &= 1.4 && \text{for uncracked concrete} \\ k_1 &= 7.5 && \text{for expansion anchors} \end{aligned}$$

$$\begin{aligned} N_u &= N_{uo} \Psi_{A,N} \Psi_{s,N} \Psi_{ec,N} \Psi_{re,N} \Psi_{ucr,N} \\ &= k_1 \sqrt{f'_c} h_e^{1.5} \Psi_{A,N} \Psi_{s,N} \Psi_{ec,N} \Psi_{re,N} \Psi_{ucr,N} \\ &= 7.5 \sqrt{32.2} (101.6)^{1.5} (1)(1)(1)(1)(1.4) \\ &= 61,018 \text{ N } (13,718 \text{ lbs}) \\ &= 61.7 \text{ kN } (13.7 \text{ kips}) \end{aligned}$$

ACI 349-85 Method (Eq. 3-6a)

$$d = d_h$$

$$\begin{aligned} N_{uo} &= 4 \sqrt{f'_c} \pi h_e^2 \left(1 + \frac{d_h}{h_e} \right) \\ &= 4 \sqrt{4670} \pi (4)^2 \left(1 + \frac{1}{4} \right) \\ &= 17,175 \text{ lbs } (76,394 \text{ N}) \\ &= 17.2 \text{ kips } (76.4 \text{ kN}) \end{aligned}$$

Concrete Capacity Design (CCD) Method (Eq. 3-8)

$$\begin{aligned} k_{nc} &= 13.5 \text{ for post-installed anchors} \\ f_{cc} &= 1.18 f'_c \end{aligned}$$

$$\begin{aligned} N_{uo} &= k_{nc} \sqrt{f_{cc}} h_e^{1.5} \\ &= 13.5 \sqrt{1.18 (32.2)} (101.6)^{1.5} \\ &= 85,220 \text{ N } (19,159 \text{ lbs}) \\ &= 85.2 \text{ kN } (19.2 \text{ kips}) \end{aligned}$$

Variable Angle Cone (VAC) Method (Eq. 3-12)

$$\begin{aligned} A_N &= A_{NO} \text{ no edge influence} \\ f_{cc} &= 1.18 f'_c \\ \theta &= 28^\circ + (0.1336 h_e)^\circ \quad \text{for } h_e < 127 \text{ mm (5 in.)} \\ &= 28^\circ + (0.1336 \times 101.6)^\circ \\ &= 41.6^\circ \end{aligned}$$

$$\begin{aligned}
N_{uo} &= \frac{A_N}{A_{NO}} 0.96 \sqrt{f_{cc}} \left(\frac{h_e}{\tan \theta} \right) \left(\frac{h_e}{\tan \theta} + d \right) \\
&= (1) 0.96 \sqrt{1.18 (32.2)} \left(\frac{101.6}{\tan 41.6} \right) \left(\frac{101.6}{\tan 41.6} + 25.4 \right) \\
&= 94,692 \text{ N } (21,289 \text{ lbs}) \\
&= 94.7 \text{ kN } (21.3 \text{ kips})
\end{aligned}$$

A.2 CONCRETE FAILURE - UNDERCUT ANCHOR

An undercut anchor, Specimen 1sml5726, as taken from Johnson's and Lew's (1990) study will be used in the following sample calculations. The undercut anchor had a diameter of 19.0 mm (0.75 in.). The concrete compressive strength was 29.2 MPa (4240 psi). The embedment depth (h_e) was 101.6 mm (4 in.) and the edge distance (c_1) was 502 mm (19.75 in.). The failure mode of the specimen was concrete cone failure and the experimental failure load, N_u , was 97.1 kN (21.8 k).

CEB Design Guide (Eq. 3-19)

$$\begin{aligned}
\psi_{A,N} &= 1 && \text{since } A_{c,N} = A_{c,NO} \\
\psi_{s,N} &= 1 && \text{since } c_1 \geq 1.5 h_e = 1.5 (101.6) = 152.4 \text{ mm} \\
\psi_{ec,N} &= 1 && \text{since no eccentricity} \\
\psi_{re,N} &= 1 && \text{since } h_e = 101.6 \text{ mm} > 100 \text{ mm} \\
\psi_{ucr,N} &= 1.4 && \text{for uncracked concrete} \\
k_1 &= 7.5 && \text{for expansion anchors}
\end{aligned}$$

$$\begin{aligned}
N_u &= N_{uo} \psi_{A,N} \psi_{s,N} \psi_{ec,N} \psi_{re,N} \psi_{ucr,N} \\
&= k_1 \sqrt{f'_c} h_e^{1.5} \psi_{A,N} \psi_{s,N} \psi_{ec,N} \psi_{re,N} \psi_{ucr,N} \\
&= 7.5 \sqrt{29.2} (101.6)^{1.5} (1)(1)(1)(1)(1.4) \\
&= 58,106 \text{ N } (13,063 \text{ lbs}) \\
&= 58.1 \text{ kN } (13.1 \text{ kips})
\end{aligned}$$

ACI 349-85 Method (Eq. 3-6a)

$$d_h = d = 0.75 \text{ in.}$$

$$\begin{aligned} N_{uo} &= 4 \sqrt{f'_c} \pi h_e^2 \left(1 + \frac{d_h}{h_e} \right) \\ &= 4 \sqrt{4240} \pi (4)^2 \left(1 + 0. \frac{75}{4} \right) \\ &= 15,547 \text{ lbs } (69,153 \text{ N}) \\ &= 15.5 \text{ kips } (69.2 \text{ kN}) \end{aligned}$$

Concrete Capacity Design (CCD) Method (Eq. 3-8)

$$\begin{aligned} k_{nc} &= 13.5 \text{ for post-installed anchors} \\ f_{cc} &= 1.18 f'_c \end{aligned}$$

$$\begin{aligned} N_{uo} &= k_{nc} \sqrt{f_{cc}} h_e^{1.5} \\ &= 13.5 \sqrt{1.18 (29.2)} (101.6)^{1.5} \\ &= 81,153 \text{ N } (18,245 \text{ lbs}) \\ &= 81.1 \text{ kN } (18.2 \text{ kips}) \end{aligned}$$

Variable Angle Cone (VAC) Method (Eq. 3-12)

$$\begin{aligned} A_N &= A_{NO} \text{ no edge influence} \\ f_{cc} &= 1.18 f'_c \\ \theta &= 28^\circ + (0.1336 h_e)^\circ \quad \text{for } h_e < 127 \text{ mm (5 in.)} \\ &= 28^\circ + (0.1336 \times 101.6)^\circ \\ &= 41.6^\circ \end{aligned}$$

$$\begin{aligned}
N_{uo} &= \frac{A_N}{A_{NO}} 0.96 \sqrt{f_{cc}} \left(\frac{h_e}{\tan \theta} \right) \left(\frac{h_e}{\tan \theta} + d \right) \\
&= (1) 0.96 \sqrt{1.18 (29.2)} \left(\frac{101.6}{\tan 41.6} \right) \left(\frac{101.6}{\tan 41.6} + 19.0 \right) \\
&= 86,046 \text{ N } (19,345 \text{ lbs}) \\
&= 86.0 \text{ kN } (19.3 \text{ kips})
\end{aligned}$$

A.3. CONCRETE FAILURE - CIP ANCHOR BOLT

A.3.1 No Edge Distance Effect

The results from a 19 mm (0.75 in.) diameter ASTM A307 embedded anchor bolt test taken from the Cannon et al. (1975) study are used in the following sample calculations. The diameter of the anchor head was 28.6 mm (1.125 in.). The embedment depth of the anchor was 88.9 mm (3.5 in.) and the edge distance was 381 mm (15 in.). The concrete compressive strength was 29.8 MPa (4315 psi). The tensile capacity of the anchor bolt was 113.0 kN (25.4 k).

CEB Design Guide (Eq. 3-19)

$$\begin{aligned}
\psi_{A,N} &= 1 && \text{since } A_{c,N} = A_{c,NO} \\
\psi_{s,N} &= 1 && \text{since } c_1 \geq 1.5 h_e = 1.5 (88.9) = 133.3 \text{ mm} \\
\psi_{ec,N} &= 1 && \text{since no eccentricity} \\
\psi_{re,N} &= 1 && \text{no reinforcement present} \Rightarrow s > 100 \text{ mm} \\
\psi_{ucr,N} &= 1.4 && \text{for uncracked concrete} \\
k_1 &= 9.0 && \text{for CIP anchors}
\end{aligned}$$

$$\begin{aligned}
N_u &= N_{uo} \psi_{A,N} \psi_{s,N} \psi_{ec,N} \psi_{re,N} \psi_{ucr,N} \\
&= k_1 \sqrt{f_c} h_e^{1.5} \psi_{A,N} \psi_{s,N} \psi_{ec,N} \psi_{re,N} \psi_{ucr,N} \\
&= 9.0 \sqrt{32.2} (88.9)^{1.5} (1)(1)(1)(1)(1.4) \\
&= 59,930.9 \text{ N } (13,473.7 \text{ lbs}) \\
&= 59.9 \text{ kN } (13.5 \text{ kips})
\end{aligned}$$

ACI 349-85 Method (Eq. 3-6a)

$$\begin{aligned} N_{uo} &= 4 \sqrt{f'_c} \pi h_e^2 \left(1 + \frac{d_h}{h_e} \right) \\ &= 4 \sqrt{4315} \pi (3.5)^2 \left(1 + \frac{1.125}{3.5} \right) \\ &= 13,362.3 \text{ lbs } (59,435.3 \text{ N}) \\ &= 13.4 \text{ kips } (59.4 \text{ kN}) \end{aligned}$$

Concrete Capacity Design (CCD) Method (Eq. 3-8)

$$\begin{aligned} k_{nc} &= 15.5 \text{ for cast-in-place anchors} \\ f_{cc} &= 1.18 f'_c \end{aligned}$$

$$\begin{aligned} N_{uo} &= k_{nc} \sqrt{f'_c} h_e^{1.5} \\ &= 15.5 \sqrt{1.18 (32.2)} (88.9)^{1.5} \\ &= 80,085.4 \text{ N } (18,004.8 \text{ lbs}) \\ &= 80.1 \text{ kN } (18.0 \text{ kips}) \end{aligned}$$

Variable Angle Cone (VAC) Method (Eq. 3-12)

$$\begin{aligned} A_N &= A_{NO} \text{ no edge influence} \\ f_{cc} &= 1.18 f'_c \\ \theta &= 28^\circ + (0.1336 h_e)^\circ \quad \text{for } h_e < 127 \text{ mm (5 in.)} \\ &= 39.9^\circ \end{aligned}$$

$$\begin{aligned} N_{uo} &= \frac{A_N}{A_{NO}} 0.96 \sqrt{f_{cc}} \left(\frac{h_e}{\tan \theta} \right) \left(\frac{h_e}{\tan \theta} + d \right) \\ &= (1) 0.96 \sqrt{1.18 (29.8)} \left(\frac{88.9}{\tan 39.9} \right) \left(\frac{88.9}{\tan 39.9} + 25.4 \right) \\ &= 79,845.4 \text{ N } (17,950.9 \text{ lbs}) \\ &= 79.8 \text{ kN } (18.0 \text{ kips}) \end{aligned}$$

A.3.2 Edge Distance Effect

The results from a 19 mm (0.75 in.) diameter ASTM A307 embedded anchor bolt test taken from the Cannon et al. (1975) study are used in the following sample calculations. The diameter of the anchor head was 28.6 mm (1.125 in.) The embedment depth of the anchor was 88.9 mm (3.5 in.) and the edge distance was 76.2 mm (3 in.). For the given edge distance, the behavior of the anchor was influenced by its proximity to the edge. The concrete compressive strength was 29.8 MPa (4315 psi). The tensile capacity of the anchor bolt was 81.4 kN (18.3 k).

CEB Design Guide (Eq. 3-19)

$$\Psi_{A, N} = A_{c, N} / A_{c, NO} = 0.79$$

$$A_{c, N} = (c_1 + 1.5 h_e) (2 * 1.5 h_e) = [76.2 + 1.5 (88.9)] (2 * 1.5 * 88.9) = 55,887 \text{ mm}^2$$

$$A_{c, NO} = 9 h_e^2 = 9 (88.9)^2 = 71,129 \text{ mm}^2$$

$$\begin{aligned} \Psi_{s, N} &= 0.7 + 0.3 (c_1 / 1.5 h_e) \text{ since } c_1 < 1.5 h_e = 1.5 (88.9) = 133.3 \text{ mm} \\ &= 0.7 + 0.3 [76.2 / 1.5 (88.9)] \\ &= 0.87 \end{aligned}$$

$$\Psi_{ec, N} = 1 \quad \text{since no eccentricity}$$

$$\Psi_{re, N} = 1 \quad \text{no reinforcement present} \Rightarrow s > 100 \text{ mm}$$

$$\Psi_{ucr, N} = 1.4 \quad \text{for uncracked concrete}$$

$$k_f = 9.0 \quad \text{for CIP anchors}$$

$$N_u = N_{uo} \Psi_{A, N} \Psi_{s, N} \Psi_{ec, N} \Psi_{re, N} \Psi_{ucr, N}$$

$$= k_1 \sqrt{f'_c} h_e^{1.5} \Psi_{A, N} \Psi_{s, N} \Psi_{ec, N} \Psi_{re, N} \Psi_{ucr, N}$$

$$= 9.0 \sqrt{32.2} (88.9)^{1.5} (0.79) (0.87) (1) (1) (1.4)$$

$$= 41,190.5 \text{ N } (9,260.5 \text{ lbs})$$

$$= 41.2 \text{ kN } (9.3 \text{ kips})$$

ACI 349-85 Method (Eq. 3-7)

$$A_{no} = \pi h_e^2 (1 + d_h / h_e) = \pi (3.5)^2 (1 + 1.125 / 3.5) = 50.85 \text{ in}^2$$

$$\begin{aligned} A_n &= A_{no} - [(\text{Length of arc def}) r - c x] / 2 \quad \text{Refer to Fig. A.1 for notation.} \\ &= 50.85 - \{ [(\pi r A^\circ) / 180^\circ] r - c x \} / 2 \\ &= 50.85 - \{ [\pi (4.06) (84.8) / 180] 4.06 - 5.48 (3.0) \} / 2 \\ &= 46.86 \text{ in}^2 \quad (30,235.12 \text{ mm}^2) \end{aligned}$$

$$N_{uo} = 13,362.2 \text{ k} \quad (59,435.3 \text{ N}) \quad \text{from Section A.1.2, ACI 349-85 Method using Eq. 3-6a.}$$

$$\begin{aligned} N_u &= \frac{A_n}{A_{no}} N_{uo} \\ &= 13,362.26 \left(\frac{46.86}{50.85} \right) \\ &= 12,313.8 \text{ lbs} \quad (54,771.7 \text{ N}) \\ &= 12.3 \text{ kips} \quad (54.8 \text{ kN}) \end{aligned}$$

Concrete Capacity Design (CCD) Method (Eq. 3-9)

$$\begin{aligned} A_N &= (c_1 + 1.5 h_e) (3 h_e) \quad \text{since } c_1 \leq 1.5 h_e = 1.5 (88.9) = 133.3 \text{ mm} \quad (5.25 \text{ in.}) \\ &= [76.2 + 1.5 (88.9)] [3 (88.9)] \\ &= 55,887.0 \text{ mm}^2 \quad (86.6 \text{ in}^2) \end{aligned}$$

$$\begin{aligned} A_{NO} &= 9 h_e^2 \\ &= 9 (88.9)^2 \\ &= 71,128.9 \text{ mm}^2 \quad (110.3 \text{ in}^2) \end{aligned}$$

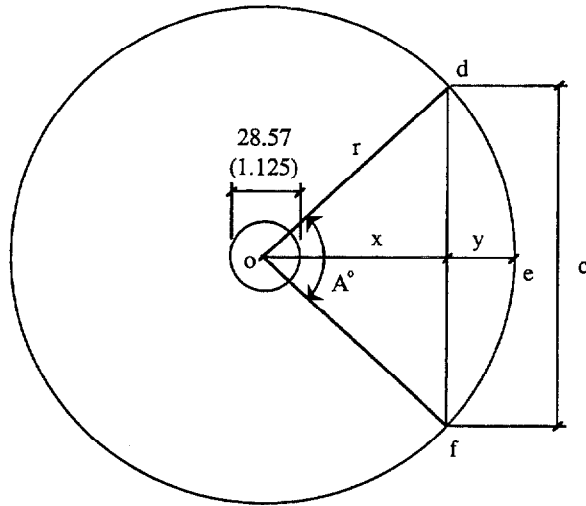
$$\begin{aligned} \psi_2 &= 0.7 + 0.3 (c_1 / 1.5 h_e) \quad \text{since } c_1 \leq 1.5 h_e \\ &= 0.7 + 0.3 [76.2 / (1.5 * 88.9)] \\ &= 0.87 \end{aligned}$$

$$N_{uo} = 80,085.4 \text{ N} \quad (18,004.8 \text{ lbs})$$

$$\begin{aligned} N_u &= \frac{A_N}{A_{NO}} \psi_2 N_{uo} \\ &= \frac{55,887.0}{71,128.9} 0.87 (80,085.4) \\ &= 54,744.1 \text{ N} \quad (12,307.6 \text{ lbs}) \\ &= 54.7 \text{ kN} \quad (12.3 \text{ kips}) \end{aligned}$$

Variable Angle Cone (VAC) Method (Eq. 3-12)

Unable to locate reference to compute the reduced area due to short edge distance. As a result, the predicted load for this method was not calculated.



$$\begin{aligned}
 r &= d_h / 2 + h_{ef} \\
 &= 1.125 / 2 + 3.5 \\
 &= 103.19 \quad (4.06) \\
 x &= 76.20 \quad (3.0) \\
 y &= 26.99 \quad (1.06) \\
 c &= 139.16 \quad (5.48)
 \end{aligned}$$

$$\begin{aligned}
 \tan A/2 &= (c/2) / x \\
 &= 2.7493 \\
 A &= 84.8
 \end{aligned}$$

Figure A.1 Projected Area Calculation for ACI 349-85 Method.

APPENDIX B - SHEAR CAPACITY

B.1 STEEL FAILURE - EXPANSION ANCHOR

Sample calculations are made using the average of the results of Johnson's and Lew's Specimens 12 and 27 which were duplicate specimens. The reason for using the average result is due to the spread in the experimental shear capacities of the two specimens - 68.5 kN (15.4 k) and 151.2 kN (34.0 k) for specimens 12 and 27, respectively. Again, the anchors were 25.4 mm (1 in.) diameter expansion anchors. The embedment depth was 101.6 mm (4 in.), and the edge distance was 381.0 mm (15 in.) . The ultimate tensile strength of the anchor was 546.1 MPa (79.2 ksi) and the average concrete strength was 31.1 MPa (4510 psi). Anchor failure was caused by fracture of the anchor at the reduced section of the anchor and the average shear capacity was 109.9 kN (24.7 k).

Eligehausen and Fuchs (1988), CEB Design Guide (1997) and others (Eq. 4-1):

$$\begin{aligned} A_s &= A_{\text{net}} = \text{Net area of threaded portion anchor} \\ &= 0.61 \text{ in}^2 \end{aligned}$$

$$\begin{aligned} V_{no} &= \alpha A_s f_u \\ &= 0.6 (0.61 \text{ in}^2) (79.2 \text{ ksi}) \\ &= 29.0 \text{ k} \quad (128.9 \text{ kN}) \end{aligned}$$

Since the fracture occurred at the reduced section, the shear capacity using the area of the reduced section [332.5 mm² (0.52 in.²)] would be 109.9 kN (24.7 k).

B.2 CONCRETE FAILURE - EXPANSION ANCHORS

The results from an expansion anchor test in Hallowell's (1996) study on anchors under static loading are used in this sample calculation. The 19 mm (0.75 in.) diameter expansion anchor (Specimen 1SKR5718) had an embedment depth of 87.3 mm (3.44 in.) and with edge distances, c_1 , of 101.6 mm (4 in.) and c_2 of 330.2 mm (13 in.). The concrete test blocks were 355.6 mm (14 in.) deep. A hairpin (U-shaped #6 reinforcing bar) was located 32 mm (1-1/4 in.) from the anchor. The concrete compressive strength was 29.0 MPa (4210 psi). The anchor experienced concrete failure and the experimental capacity was 33.3 kN (7.5 k). The expansion anchor was in uncracked concrete.

CEB Design Guide Method (Eq. 4-16):

$$A_{c,v} = A_{v0} \text{ since } c_2 > 1.5 c_1 = 1.5 (101.6) = 152.4 \text{ mm}$$

$$\begin{aligned}\Psi_{A,v} &= A_{c,v} / A_{v0} \\ &= 1.0\end{aligned}$$

$$\Psi_{h,v} = \left(\frac{1.5 c_1}{h} \right)^{1/3} = \left[\frac{1.5 (101.6)}{355.6} \right]^{1/3} = 0.75 \geq 1$$

$$= 1.0$$

$$\Psi_{s,v} = 1.0 \text{ for } c_2 > 1.5 c_1$$

$$\Psi_{ec,v} = 1 \text{ no eccentricity}$$

$$\Psi_{\alpha,v} = 1 \text{ for } \alpha_v = 0^\circ$$

$$\Psi_{ucr,v} = 1.4 \text{ for uncracked concrete}$$

$$V_u = V_{uo} \Psi_{A,v} \Psi_{h,v} \Psi_{s,v} \Psi_{ec,v} \Psi_{\alpha,v} \Psi_{ucr,v}$$

$$= k_4 \sqrt{d} \left(\frac{\ell_f}{d} \right)^{0.2} \sqrt{f'_c} c_1^{1.5} \Psi_{A,v} \Psi_{h,v} \Psi_{s,v} \Psi_{ec,v} \Psi_{\alpha,v} \Psi_{ucr,v}$$

$$= 0.5 \sqrt{19} \left(\frac{87.3}{19} \right)^{0.2} \sqrt{29.0} (101.6)^{1.5} (1)(1)(1)(1)(1)(1.4)$$

$$= 22,873 \text{ N } (5,132 \text{ lbs})$$

$$= 22.8 \text{ kN } (5.1 \text{ kips})$$

ACI 349-85 Method (Eq. 4-6):

No reduction factor for member thickness applied since $h > c_1$.

$$V_{uo} = 2 \sqrt{f'_c} \pi c_1^2$$

$$= 2 \sqrt{4210} \pi (4.0)^2$$

$$= 6,523 \text{ lbs } (29,014 \text{ N})$$

$$= 6.5 \text{ kips } (29.0 \text{ kN})$$

Concrete Capacity Design (CCD) Method (Eq. 4-8):

$$\begin{aligned}A_v &= A_{v0} \text{ since } c_2 > 1.5 c_1 \\A_{v0} &= 4.5 c_1^2 = 4.5 (10)^2 = 450 \text{ in}^2 \\ \psi_4 &= 1 \text{ No eccentricity} \\ \psi_5 &= 1 \text{ since } c_2 > 1.5 c_1\end{aligned}$$

$$\begin{aligned}V_{uo} &= 13 \left(\frac{1}{d} \right)^{0.2} \sqrt{d f'_c} c_1^{1.5} \\ &= 13 \left(\frac{1}{0.75} \right)^{0.2} \sqrt{0.75 (4210)} (4)^{1.5} \\ &= 6,190 \text{ lbs } (27,533 \text{ N})\end{aligned}$$

$$\begin{aligned}V_u &= \frac{A_v}{A_{v0}} \psi_4 \psi_5 V_{uo} \\ &= (1)(1)(1)(6,190) \\ &= 6,190 \text{ lbs } (27,533 \text{ N}) \\ &= 6.2 \text{ kips } (27.5 \text{ kN})\end{aligned}$$

AISC Method (Eq. 4-13):

Check that

$$\begin{aligned}(c_1 - 1) &\geq 8d \\ 4 - 1 &\geq 8 (0.75) \\ 3 &\geq 6 \quad \text{Not applicable.}\end{aligned}$$

Elgehausen and Fuchs (Eq. 4-2):

$d_o = d + 3.2 \text{ mm (1/8 in.)}$ Hole diameter not given and was assumed for this example.
 $f_{cc} = 1.18 f'_c$
 $h = 355.6 \text{ mm} > 1.4 c_1 = 142.2 \text{ mm} \Rightarrow$ No reduction factor required for member thickness.

$$\begin{aligned} V_{ou} &= 1.3 \sqrt{d_o} \sqrt{f_{cc}} c_1^{1.5} \\ &= 1.3 \sqrt{22.2} \sqrt{1.18 (29.0)} (101.6)^{1.5} \\ &= 36,694 \text{ N (8,250 lbs)} \\ &= 36.7 \text{ kN (8.2 kips)} \end{aligned}$$

Hawkins (Eq. 4-14):

$$\begin{aligned} V_u &= 18.2 d^{0.33} \sqrt{f'_c} (15 + 1.1 h_e + d_w) \\ &= 18.2 (0.75)^{0.33} \sqrt{4210} [15 + 1.1 (3.44) + 0] \\ &= 20,154 \text{ lbs (89,644 N)} \\ &= 20.2 \text{ kips (89.6 kN)} \end{aligned}$$

McMackin et al. (Eq. 4-20):

The information on the ultimate tensile strength of the anchor was not available and therefore, this equation could not be used.

B.3 CONCRETE FAILURE - HEADED STUDS

B.3.1 254 mm (10 in.) Edge Distance

The results from one anchor test in McMackin's et al. (1973) study on headed anchors are used in this sample calculation. The 19 mm (0.75 in.) diameter headed anchor (Specimen B3-7) had an embedment depth of 101.6 mm (4 in.) and with edge distances, c_1 of 254.0 mm (10 in.) and c_2 of 304.8 mm (12 in.). The member thickness was 609.6 mm (24 in.). The concrete compressive strength was 28.0 MPa (4060 psi) and the tensile strength of the anchor was 441 MPa

(64 ksi). The anchor experienced concrete failure and the experimental capacity was 127.2 kN (28.6 k).

CEB Design Guide Method (Eq. 4-16):

$$\begin{aligned}
 A_{c,v} &= 1.5 c_1 (1.5 c_1 + c_2) && \text{since } c_2 < 1.5 c_1 = 1.5 (254) = 381 \text{ mm} \\
 &= 1.5 (254) [1.5 (254) + 304.8] \\
 &= 261,289.8 \text{ mm}^2 \\
 A_{v0} &= 4.5 c_1^2 = 4.5 (254)^2 \\
 &= 290,322.0 \text{ mm}^2 \\
 \Psi_{A,v} &= A_{c,v} / A_{v0} \\
 &= 0.9 \\
 \Psi_{h,v} &= \left(\frac{1.5 c_1}{h} \right)^{1/3} = \left[\frac{1.5 (254)}{609.6} \right]^{1/3} = 0.85 \geq 1 \\
 &= 1.0 \\
 \Psi_{s,v} &= 0.7 + 0.3 (c_2 / 1.5 c_1) = 0.7 + 0.3 [304.8 / 1.5 (254)] = 0.94 \\
 \Psi_{ec,v} &= 1 \text{ no eccentricity} \\
 \Psi_{\alpha,v} &= 1 \text{ for } \alpha_v = 0^\circ \\
 \Psi_{ucr,v} &= 1.4 \text{ for uncracked concrete}
 \end{aligned}$$

$$\begin{aligned}
 V_u &= V_{u0} \Psi_{A,v} \Psi_{h,v} \Psi_{s,v} \Psi_{ec,v} \Psi_{\alpha,v} \Psi_{ucr,v} \\
 &= k_4 \sqrt{d} \left(\frac{\ell_f}{d} \right)^{0.2} \sqrt{f'_c} c_1^{1.5} \Psi_{A,v} \Psi_{h,v} \Psi_{s,v} \Psi_{ec,v} \Psi_{\alpha,v} \Psi_{ucr,v} \\
 &= 0.5 \sqrt{19} \left(\frac{101.6}{19} \right)^{0.2} \sqrt{28.0} (254.0)^{1.5} (0.9)(1.0)(0.94)(1)(1)(1.4) \\
 &= 77,322.0 \text{ N } (17,383.5 \text{ lbs}) \\
 &= 77.3 \text{ kN } (17.4 \text{ kips})
 \end{aligned}$$

ACI 349-85 Method (Eq. 4-6):

No reduction factor for member thickness applied since $h > c_j$.

$$\begin{aligned}
V_{uo} &= 2 \sqrt{f'_c} \pi c_1^2 \\
&= 2 \sqrt{4060} \pi (10)^2 \\
&= 40,035 \text{ lbs } (178,077 \text{ N}) \\
&= 40.0 \text{ kips } (178.1 \text{ kN})
\end{aligned}$$

Concrete Capacity Design (CCD) Method (Eq. 4-8):

$$\begin{aligned}
A_V &= 1.5 c_1 (1.5 c_1 + c_2) = 1.5 (10) [1.5 (10) + 12] && \text{since } c_2 < 1.5 c_1 \\
&= 405 \text{ in}^2 \\
A_{V0} &= 4.5 c_1^2 = 4.5 (10)^2 = 450 \text{ in}^2 \\
\psi_4 &= 1 \text{ No eccentricity} \\
\psi_5 &= 0.7 + 0.3 [c_2 / (1.5 c_1)] = 0.7 + 0.3 [12 / (1.5 * 10)] = 0.94
\end{aligned}$$

$$\begin{aligned}
V_{uo} &= 13 \left(\frac{1}{d} \right)^{0.2} \sqrt{d f'_c} c_1^{1.5} \\
&= 13 \left(\frac{1}{0.75} \right)^{0.2} \sqrt{0.75 (4060)} (10)^{1.5} \\
&= 24,028 \text{ lbs } (106,878 \text{ N})
\end{aligned}$$

$$\begin{aligned}
V_u &= \frac{A_V}{A_{V0}} \psi_4 \psi_5 V_{uo} \\
&= \frac{405}{450} (1) (0.94) (24,028) \\
&= 20,328 \text{ lbs } (90,418 \text{ N}) \\
&= 20.3 \text{ kips } (90.4 \text{ kN})
\end{aligned}$$

AISC Method (Eq. 4-13):

$$\begin{aligned}
\text{Check that } (c_1 - 1) &\geq 8d \\
10 - 1 &\geq 8 (0.75) \\
9 &\geq 6 \quad \text{OK}
\end{aligned}$$

$$\begin{aligned}
V_u &= 0.5 A_s \sqrt{f'_c E_c} \\
&= 0.5 A_s \sqrt{f'_c [57 (f'_c)^{0.5}]} \\
&= 0.5 (0.44) \sqrt{4.06 (57) (4060)^{0.5}} \\
&= 26.7 \text{ kips } (118.8 \text{ kN})
\end{aligned}$$

Eligehausen and Fuchs (Eq. 4-2):

d_o = d concrete cast-in-place, i.e., no holes drilled.

f_{cc} = $1.18 f'_c$

$h = 609.6 \text{ mm} > 1.4 c_1 = 355.6 \text{ mm} \Rightarrow$ No reduction factor required for member thickness.

$$\begin{aligned}
V_{ou} &= 1.3 \sqrt{d_o} \sqrt{f_{cc}} c_1^{1.5} \\
&= 1.3 \sqrt{19} \sqrt{1.18 (28.0)} (254)^{1.5} \\
&= 131,838 \text{ N } (29,640 \text{ lbs}) \\
&= 131.8 \text{ kN } (29.6 \text{ kips})
\end{aligned}$$

Hawkins (Eq. 4-14):

$$\begin{aligned}
V_u &= 18.2 d^{0.33} \sqrt{f'_c} (15 + 1.1 h_e + d_w) \\
&= 18.2 (0.75)^{0.33} \sqrt{4060} [15 + 1.1 (4) + 0] \\
&= 35,713 \text{ lbs } (158,850 \text{ N}) \\
&= 35.7 \text{ kips } (158.9 \text{ kN})
\end{aligned}$$

McMackin et al. (Eq. 4-20):

$$\begin{aligned}
 V_u &= V_{uo} \left(\frac{c_1 - 1}{8d} \right) \leq 0.85 f_u A_s \\
 &= 0.94 A_s f_c'^{0.3} E_c^{0.44} \left(\frac{c_1 - 1}{8d} \right) \leq 0.85 f_u A_s \\
 &= 0.94 (0.44) (4.06)^{0.3} (57 \sqrt{4060})^{0.44} \left[\frac{10 - 1}{8(0.75)} \right] \leq 0.85 (64) (0.44) \\
 &= 34.8 \text{ kips} \leq 23.9 \text{ kips} \quad \text{controls} \\
 &= 23.9 \text{ kips} \quad [106.5 \text{ kN}]
 \end{aligned}$$

B.3.2 51 mm (2 in.) Edge Distance

The results from another anchor test in McMackin's et al. (1973) study on headed anchors are used in the following sample calculations but the edge distance, c_1 , was 50.8 mm (2 in.) for this anchor. Similar to the previous anchor test, the 19 mm (0.75 in.) diameter headed anchor (Specimen C3-6) had an embedment depth of 101.6 mm (4 in.) and with an edge distance, c_2 , of 304.8 mm (12 in.). The member thickness was 609.6 mm (24 in.). The concrete compressive strength was 33.9 MPa (4910 psi) and the tensile strength of the anchor was 441 MPa (64 ksi). The anchor experienced concrete failure and the experimental capacity was 14.7 kN (3.3 k).

CEB Design Guide Method (Eq. 4-16):

$$\begin{aligned}
 \Psi_{A, v} &= A_{c, v} / A_{v0} \\
 &= 1.0 \\
 \Psi_{h, v} &= \left(\frac{1.5 c_1}{h} \right)^{1/3} = \left[\frac{1.5 (50.8)}{609.6} \right]^{1/3} = 0.5 \geq 1 \\
 &= 1.0 \\
 \Psi_{s, v} &= 0.7 + 0.3 (c_2 / 1.5 c_1) = 0.7 + 0.3 [304.8 / 1.5 (50.8)] = 1.9 \leq 1.0 \\
 &= 1.0 \\
 \Psi_{ec, v} &= 1 \text{ no eccentricity} \\
 \Psi_{\alpha, v} &= 1 \text{ for } \alpha_v = 0^\circ \\
 \Psi_{ucr, v} &= 1.4 \text{ for uncracked concrete}
 \end{aligned}$$

$$\begin{aligned}
V_u &= V_{uo} \psi_{A,v} \psi_{h,v} \psi_{s,v} \psi_{ec,v} \psi_{\alpha,v} \psi_{ucr,v} \\
&= k_4 \sqrt{d} \left(\frac{\ell_f}{d} \right)^{0.2} \sqrt{f'_c} c_1^{1.5} \psi_{A,v} \psi_{h,v} \psi_{s,v} \psi_{ec,v} \psi_{\alpha,v} \psi_{ucr,v} \\
&= 0.5 \sqrt{19} \left(\frac{101.6}{19} \right)^{0.2} \sqrt{33.9} (50.8)^{1.5} (1.0)(1.0)(1.0)(1)(1)(1.4) \\
&= 8,994.9 \text{ N } (2,022.2 \text{ lbs}) \\
&= 9.0 \text{ kN } (2.0 \text{ kips})
\end{aligned}$$

ACI 349-85 Method (Eq. 4-6):

No reduction factor for member thickness applied since $h > c_j$.

$$\begin{aligned}
V_{uo} &= 2 \sqrt{f'_c} \pi c_1^2 \\
&= 2 \sqrt{4910} \pi (2)^2 \\
&= 1,761.1 \text{ lbs } (7,833.3 \text{ N}) \\
&= 1.8 \text{ kips } (7.8 \text{ kN})
\end{aligned}$$

Concrete Capacity Design (CCD) Method (Eq. 4-8):

$$\begin{aligned}
A_v &= A_{vo} \\
\psi_4 &= 1 \quad \text{No eccentricity} \\
\psi_5 &= 1 \quad \text{Since } c_2 \geq 1.5 c_1
\end{aligned}$$

$$\begin{aligned}
V_{uo} &= 13 \left(\frac{1}{d} \right)^{0.2} \sqrt{d f'_c} c_1^{1.5} \\
&= 13 \left(\frac{1}{0.75} \right)^{0.2} \sqrt{0.75 (4910)} (2)^{1.5} \\
&= 2,363.5 \text{ lbs} \quad (10,512.7 \text{ N})
\end{aligned}$$

$$\begin{aligned}
V_u &= \frac{A_v}{A_{v0}} \psi_4 \psi_5 V_{uo} \\
&= 1.0 (1.0) (1.0) (2,363.5) \\
&= 2,363.5 \text{ lbs} \quad (10,512.7 \text{ N}) \\
&= 2.3 \text{ kips} \quad (10.5 \text{ kN})
\end{aligned}$$

AISC Method (Eq. 4-13):

Check that

$$\begin{aligned}
(c_1 - 1) &\geq 8d \\
2 - 1 &\geq 8(0.75) \\
1 &\leq 6 \quad \text{No good. Cannot use equation.}
\end{aligned}$$

Eligehausen and Fuchs (Eq. 4-2):

$d_o = d$ concrete cast-in-place, i.e., no holes drilled.
 $f_{cc} = 1.18 f'_c$
 $h = 609.6 \text{ mm} > 1.4 c_1 = 71.1 \text{ mm} \Rightarrow$ No reduction factor required for member thickness.

$$\begin{aligned}
V_{ou} &= 1.3 \sqrt{d_o} \sqrt{f_{cc}} c_1^{1.5} \\
&= 1.3 \sqrt{19} \sqrt{1.18 (33.9)} (50.8)^{1.5} \\
&= 12,976.5 \text{ N} \quad (2,917.3 \text{ lbs}) \\
&= 13.0 \text{ kN} \quad (2.9 \text{ kips})
\end{aligned}$$

Hawkins (Eq. 4-14):

$$\begin{aligned}V_u &= 18.2 d^{0.33} \sqrt{f'_c} (15 + 1.1 h_e + d_w) \\&= 18.2 (0.75)^{0.33} \sqrt{4910} [15 + 1.1(4) + 0] \\&= 22,478.5 \text{ lbs} \quad (99,984.4 \text{ N}) \\&= 22.5 \text{ kips} \quad (100.0 \text{ kN})\end{aligned}$$

McMackin et al. (Eq. 4-20):

$$\begin{aligned}V_u &= V_{uo} \left(\frac{c_1 - 1}{8d} \right) \leq 0.85 f_u A_s \\&= 0.94 A_s f_c'^{0.3} E_c^{0.44} \left(\frac{c_1 - 1}{8d} \right) \leq 0.85 f_u A_s \\&= 0.94 (0.44) (4.91)^{0.3} (57 \sqrt{4910})^{0.44} \left[\frac{2 - 1}{8(0.75)} \right] \leq 0.85 (64) (0.44) \\&= 4.3 \text{ kips} \leq 23.9 \text{ kips} \\&= 4.3 \text{ kips} \quad [19.0 \text{ kN}]\end{aligned}$$